UNIVERSITY OF NAPLES FEDERICO II

DEPARTMENT OF PHARMACY

SCHOOL OF MEDICINE

Ph.D. in Pharmaceutical Sciences: XXXII cycle

Ph.D. Thesis

Role of sphingolipids in inflammatory respiratory diseases

MARIA ANTONIETTA RIEMMA

TUTOR: PROF. GIUSEPPE CIRINO

COORDINATOR: PROF. MARIA V. D'AURIA

A.Y. 2017/2020

TABLE OF CONTENTS

LIST OF ABBREVIATIONS

BP: Blood Pressure

EC: Endothelial cells

α-SMA: smooth muscle actin

SL: Sphingolipids

SPT: Serine Palmitoyl Transferase

S1P: Sphingosine-1-Phosphate

GPCR: G-protein-coupled receptor

ABC: transporters ATP-binding cassette transporters

ApoM: apolipoprotein M

ASM cells: airway smooth muscle cells

BAL: Bronchoalveolar lavage

ERK: extracellular-signal-regulated kinase

FCεRII: "high-affinity" IgE receptor

IgE: immunoglobulin E

LDL: low-density lipoprotein

LPS: Lipopolysaccharide

NO: nitric oxide

NOS: nitric oxide synthase

OVA: ovalbumin

SM: sphingomyelins

GSL: glycosphingolipids

TLR4: Toll-like receptor 4

PGE2: prostaglandin E2

VCAM-1: vascular cell adhesion molecule-1

VEGF: vascular endothelial growth factor

SphK: sphingosine kinase

TGF-β: transforming growth factor-β

PLC: phospholipase C

Sph: Sphingosine

Cer: Ceramide

SPPase: S1P phosphatase

SPL: sphingosine lyase

SPTN2: S1P transporter spinster

IgE: immunoglobulin E

IL-13: Interleukin-13

IL-4: Interleukin-4

ApoE: Apolipoprotein E

PEA: Palmitoylethanolamide

MSc: mast cells

LT: leukotriene

EMT: epithelial-mesenchymal transition

CS: cigarette smoke

COPD: Chronic obstructive pulmonary disease

DSCG: Disodium cromoglycate

MΦNgKO-ApoE$^{-/-}$: LysmCre+ Nogo knockout mice

LDL: low-density lipoprotein

ORMDL: ORosoMucoiD-Like protein

NOGO: Neurite OutGrowth inhibitor

ABSTRACT

Ssphingolipid synthesis represents a novel metabolic pathway influencing airway function. Systemic administration of sphingosine-1-phosphate (S1P), the final product of sphingolipid metabolism, without additional adjuvant factors, induces in the mouse a disease closely mimicking the cardinal features of severe asthma in humans such as airway hyperreactivity and pulmonary inflammation. Here, I have investigated the molecular and cellular mechanisms underlying the S1P effects on the airway during a pulmonary inflammatory disease. For this purpose, I have used different in vivo and in vitro experimental models such as asthma-like disease and a model of mild COPD. The results obtained showed a concentrated participation of TLR4, epithelium and mast cells in S1P-induced airway hyperreactivity and lung inflammation following exposure to the allergen. In addition, it has been also demonstrated that airway S1P effects are also triggered by other stimuli such as cigarette smoke. Indeed, exposure of mice to cigarette smoke induces an S1P-mediated AHR in a time-dependent manner. Furthermore, I have evaluated the potential contribution of sphingolipids in coronary artery diseases (CAD) in ApoE-/- mice following pressure overload (TAC), a novel animal model of heart failure. The data obtained demonstrate the protective role of de novo sphingolipid biosynthesis in the development of coronary atherosclerosis in ApoE-/- mice post-TAC. In conclusion, this study demonstrates that S1P is a common denominator of inflammatory based diseases and proposes S1P as a potential new therapeutic target for the attenuation of symptoms of lung diseases and in vascular dysfunction associated with atherosclerosis.

CHAPTER 1 - INTRODUCTION

1.1Sphingolipids: Overview

1.1.1 Structure and chemical features

Sphingolipids (SLs) are fundamental structural components of eukaryotic cell membranes. The origin of the root term “sphingosine” was given by J.L.W. Thudichum in his publication *“Chemical Constitution of the Brain”* in 1884[1]. Sphingolipids are composed of a sphingoid base backbone, similar to sphingosine which is also called D-erythro-sphingosine. The convenient abbreviation for this compound is d18:1 with the first number reflecting the number of carbon atoms, the second the number of double bonds, and “d” referring to the two (di-) hydroxyl groups. This kind of lipids are amphipathic: they are composed of a polar head group attached to a nonpolar long-chain sphingoid backbone, sphingosine, amino alcohol linked different fatty acid. More complex sphingolipids derived from a modification of the basic structure.

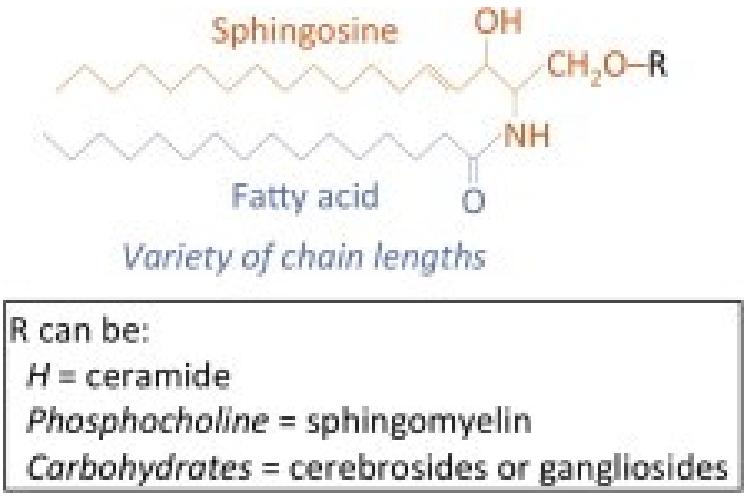

Figure 1: Basic structure of sphingolipids

Reproduced from Abou-Ghali and Jonny Stiban[2] with permission from Elsevier under the CC BY-NC-ND license.

The biophysical properties of these compounds are related to their hydrophobic and hydrophilic chemical elements, their subcellular localization and their biological functions. Most of complex sphingolipids, glycosphingolipids (GSL) and sphingomyelins (SM), called also “bilayer stabilizing” for non-polar properties, are located on the leaflet of the plasma membrane which interact with amino group that can exist in both cationic and neutral form depending on the pKa (between 7 and 8) or can interact through strong van de Waals interactions[3]. Together with cholesterol, they are the major lipid components of the eukaryotic plasma membrane that represents a separation barrier between the extracellular environment and intracellular cytosol. In contrast to these functions, sphingosine-1-phosphate (S1P) is relatively water-soluble to move rapidly between membranes, released from cells and binding with extracellular S1P receptors. This represents the reason why the biological functions of S1P depend on its interaction with extracellular S1P receptors. Two ATP-binding cassette transporter (ABCA1, ABCC1) belong to the ABC transporters superfamily as well as the Spinster2 (Spns-2), a member of a family of non-ATP-dependent organic ion transporters, are involved in the influx and efflux movement of S1P across the bilayer[4,5]. The characteristic and dynamic movements of sphingolipids combined with cholesterol, called lipid raft as well as the assemblies of protein/glycoprotein through the two leaflets of the bilayer create a fluid mosaic with restraining lateral motility in order to preserve the physiological functions of cells[6].

1.1.2 Sphingolipids: biosynthesis, metabolism, and transport

For a long time, sphingolipids have been considered the main structural elements of cell membranes and lipoproteins involved in maintaining cellular structural integrity. Recently, highly sphingolipids metabolites such as Sphingosine (Sph), Ceramide (Cer) and Sphingosine-1-phosphate (S1P) are known to be bioactive lipid mediators which can act by modulating cell survival, migration, differentiation, calcium homeostasis and numerous cellular responses to stress[7]. Among sphingolipids, ceramide is considered the central scaffold which can be generated by three different pathways: 1- *De novo* biosynthesis in the ER membrane, 2- sphingomyelin catabolism in the plasma membrane, 3- lysosome salvage pathway[8]. The most interesting and recognized SLs biosynthetic pathway is the *"De novo"* synthesis. Sphingolipid *de novo* biosynthesis starts at the cytosolic leaflet of the smooth endoplasmic reticulum (ER) where Serine Palmitoyltransferase (SPT), using pyridoxal 5'-phosphate as a cofactor, catalyzes the condensation of L-serine and palmitoyl-CoA to produce 3-ketosphinganine, the first and rate-limiting step. 3-ketosphinganine rapidly reduces to sphinganine (dihydrosphingosine) through NADPH-dependent reductase. SPT enzyme belongs to the oxoamine synthases family, it is a membrane-bound heterodimer composed of two subunits, first purified by chromatography as Lcb1/Lcb2 at a 1:1 ratio in yeast[9–11]. The identification of corresponding homologs in mammalian cells followed soon: there is ~40% identity between yeast and mammalian. In mammalian, SPT protein is composed with a single Lcb1 homolog, Serine PalmitoylTransferase Long Chain subunit 1 (SPTLC1) and two homologs of Lcb2, SPTLC2 and SPTLC3 (SPTLC1/LCB1 and SPTLC2/LCB2 genes, respectively)[12,13]. The active site of SPT is at the interface between each subunit contributing to each other to preserve SPT activity. Mutations in the

human SPTLC1 gene cause hereditary sensory neuropathy type I and mice global knockout for SPTLC1 or SPTLC2 are embryonically lethal[14]. However, the treatment with myriocin, an inhibitor of SPT activity, reduce the area of the atherosclerotic lesions in Apo-E deficient mice providing the strongest link between sphingolipid metabolism and atherosclerosis[15]. Clearly, SPT involved in critical cell functions and disease suggests the importance of its catalytic activity, resulting from the interaction of Spltc1 with Sptlc2 or Sptlc3, depending on the tissue where SPT subunits are expressed and on the cellular sphingolipid requirement[16]. The mechanisms underlying the regulation of cell sphingolipid homeostasis via de novo synthesis are poorly understood. Triola et al (2004), showed the feedback inhibition of SPT activity by accumulation of sphingosine-1- phosphate and dihydrosphingosine-1-phosphate with a dihydroceramide desaturase inhibitor GT11[17] or with myriocin, an inhibitor of SPT activity which could reflect completely disruption of sphingolipid *de novo* synthesis[18].

Besides, ORosoMucoiD-Like proteins (ORMDL) and Neurite OutGrowth inhibitor (NOGO-B), ER membrane proteins, regulate negatively SPT activity meanwhile the SPT small subunits a and b (ssSPTa and ssSPTb) are its independent activators[19,20]. ORMDL-dependent interaction with SPT is involved in childhood asthma and inflammation as a negative regulator of SL biosynthesis via the inhibition of ceramide levels[21,22]. NOGO belongs to Reticulon4 family proteins situated in the endoplasmic reticulum (ER). There are three different isoforms: NOGO-A and NOGO-C are localized in the central nervous system and skeletal muscle, NOGO-B is highly expressed in endothelial cells regulating the local sphingolipid production with direct effects on vascular function and blood pressure through S1P-S1P1-eNOS axis. Indeed, mice lacking NOGO-B in endothelial cells (ECs) show an increase of

SPT activity and SL intake compare to wild type mice while the protein re-expression mediated by the lentivirus vector restores the homeostatic activity of SPT in blood vessels. Additionally, the pharmacological treatment with myriocin inhibits SL biosynthesis and increases blood pressure (BP) in AngiotensinII-treated NOGO-B knock-out mice giving a foundation in a protective role of *de novo* sphingolipid biosynthesis during hypertension[23,24]. Following the sphingolipid biosynthetic pathway, dihydroceramide synthase converts sphinganine into dihydroceramide and then it is N-acylated to produce dihydroceramide. The enzyme dihydroceramide desaturase (DES) reduces dihydroceramide to ceramide.

Ceramide is considered the central metabolite that can be either generated from *de novo* synthesis in the membrane of the endoplasmic reticulum (ER) or released from sphingomyelin by sphingomyelinase. Ceramide serves as a substrate to the subsequent production of other sphingolipid intermediates: structural modifications convert ceramide into more complex sphingolipids as glycosphingolipids (GSL) and sphingomyelin (SM) or it can be hydrolyzed to sphingosine by ceramidase.Three different ceramidases at different pH as neutral ceramidase in the ER, alkaline ceramidase in the plasma membrane and acid ceramidase in the lysosome can carry out the hydrolysis reaction[24].

Once produced, Ceramide must be travel from ER to the Golgi with the action of a ceramide transfer protein CERT. Here, the sphingomyelin synthase (SMS) enzyme catalyzes the reaction among phosphorylcholine groups with ceramide to form SM and release of diacylglycerol (DAG)[25]. Turning back to this reversible reaction is possible to generate ceramide from SM by sphingomyelinase (SMase) enzyme, neutral and alkaline at the plasma membrane or acid at the lysosome. Moreover, through the action of membrane-

bound glucosylceramide synthase (GCS) enzyme, ceramide can be transformed into complex GLS.

Complex sphingolipids (SM and GLS) moving up from the cytosol until the plasma membrane by vesicular trafficking, can be a substrate of ceramide production by sphingomyelinase and then converted in sphingosine by ceramidase.

In addition to *de novo* sphingolipid synthesis, the “salvage pathway” is a partially overlapping pathway of sphingolipid turnover in lysosomes to modulate sphingolipid levels[26].

These two synthetic pathways, localized in different organelles of eukaryotic cells and associated with the “recycling pathway” of complex SL in the lysosome, are highly regulated by selective intracellular trafficking to preserve physiological sphingolipids levels in order to maintain the structure and biological functions of cells.

Sphingosine-1-phosphate (S1P), a high bioactive lipid, is produced from the phosphorylation of sphingosine by two isoforms of the same kinase, the sphingosine kinase I and II (Sphk1 and Sphk2). These enzymes catalyze the phosphorylation of the -OH of sphingosine[27].

S1P regulates many important biological functions as a ligand for its extracellular receptors and as an intracellular second messenger. S1P levels are finely regulated by the balance between its synthesis, catalyzed by two sphingosine kinase isoenzymes, Sphk1 and Sphk2 and its degradation by S1P lyase and S1P phosphatases. Different substrate, functions and subcellular localization are linked with these two enzyme isoforms encoded by separate genes and showing divergent antithetic properties[28].

Sphk1 is a cytosolic enzyme and its activation is required for the biological effect of S1P. Spkh1 can be activated by different stimuli including growth factors as EGF and VEGF, cytokines and lipopolysaccharide (LPS). Trough ERK-dependent phosphorylation on Serine225 or Thr54, Sphk1 can be translocated to membranes where its substrate, sphingosine, is formed[29]. On the contrary, the SphK2 enzyme is mainly localized to the nucleus where it acts as an epigenetic regulator binding to HDACs and inhibiting histone acetylate to regulate the memory, one of the neurodegenerative disorders. Also, with nuclear export after phosphorylation on Ser351 and Thr578 by PKC activator, Sphk2 may protome platelet aggregation and subsequent thrombosis, the proliferation of cancer cells and inflammation progression [30,31].

Ceramide, sphingosine, and sphingosine-1-phosphate are three inter-convertible compounds. All of them often have opposite signaling functions: ceramide and sphingosine typically are pro-apoptotic signals and inhibit cell growth meanwhile S1P stimulates cell growth and inhibits apoptotic. This event has been called ‘‘cellular rheostat’’, where cells utilize this hemodynamic balance between ceramide/sphingosine-1- phosphate with opposite effects to determine growth arrest/ apoptosis versus proliferation/ survival[32].

Sphingosine-1-phosphate signaling ends in different ways: it may be dephosphorylated by S1P phosphatase (SPPase) into sphingosine or irreversibly degraded by sphingosine -1-phosphate lyase (SPL) with the formation of two products, ethanolamine phosphate + hexadecenal. Also, S1P can be transported out of the cell and regulate multiple signaling pathways by binding a family of five S1P receptors, $S1P_{1-5}$. These are G protein-coupled receptors with different heterotrimeric G protein called also endothelial

differentiation gene- Edg- receptors: S1P1-(Edg-1), S1P2-(Edg-5), S1P3(Edg-3), S1P4 (Edg-6) and S1P5 (Edg-8).

These receptors have different cell and tissue distribution triggers, multiple signaling pathways and mediate different biological functions.[33–35]

S1P1, S1P2 and S1P3 are the best characterized. S1P1 mainly activate Gi and both S1P2 -S1P3 are linked to Gi, Gq and G12/13. They are widely expressed meanwhile S1P4 is located to cells in the immune system and S1P5 to cells of the nervous system.

1.1.3 Sphingosine-1-phosphate (S1P): source and receptors

Sphingosine-1-phosphate (S1P) is a high bioactive lipid generated from sphingomyelin on the cell membrane. S1P levels are finely regulated by the balance between sphingosine kinase enzymes for the synthesis and S1P lyase enzymes responsible for its degradation[23,36,37]. S1P is produced inside of plasma membrane but is noting that it needs to be transported out of cells for its biological function through its interaction with S1PRs receptors. Different transporters have been recognized: ABCA1, ABCC1 and the recent discovery about another S1P transporter specifically in endothelial cells, Spinster2 (Spns-2)[38–40]. Once outside of the cell, S1P bound to apolipoprotein M (ApoM) on HDL (65%) and albumin (35%). Erythrocytes, endothelial cells, and platelets represent the best source of S1P in the plasma[41,42]. Thus, the concentration of S1P in plasma is between 0.1 and 0.6 mM and the amounts of S1P in the tissues are very low. The different concentration gradient of S1P “inside-outside the cells” is precisely organized preserving and driving its biological functions.

S1P can bind and act through a family of five S1P receptors, $S1P_{1-5}$. These are G protein-coupled receptors with different heterotrimeric G protein expressed in the whole body. These receptors are associated to different G proteins: Gi, Gq, $G_{12/13,}$ activating small signal molecules such as Rho, Rac, and Ras and the final downstream effectors are adenylyl cyclase, PI3K, PLC, PKC, and intracellular CA^{2+} regulating different biological actions such as suppression of apoptosis and cellular growth. About its binding with S1P1, S1P can regulate the immune cell trafficking[43], the vascular tone, and permeability as well[44]. Both S1P2 -S1P3 receptors are linked to Gi, Gq, and G12/13 and activate phospholipase C (PLC) and Rho[45]. S1P4 is involved in neutrophil cell movement[46] and S1P5 is mainly expressed in the nervous system. S1P signaling in the vasculature is mostly mediated by S1P1- S1P2- S1P3 and their localization appears different between smooth muscle cells and endothelial cells. In particular, S1P2 and S1P3 are GPCR coupled with different α subunits. S1P3 is associated with a Gq thus, after activation, increases the intracellular intake/influx of Ca^{2+} leading to a vasoconstriction response while S1P2 is linked to $G_{12/13}$ with RhoA/Rho pathway activation and lead to the same response, the constriction of smooth muscle cells[47]. Conversely, S1P1 is paired to Gi and its activation is associated with the interaction of PI3K/Akt pathway which would increase phosphorylation of eNOS in endothelial cells promoting vasodilation. Basically, S1P/S1P1 acts via eNOS/NO pathway in endothelial cells by supporting the dilatation of vessels. All these receptors contribute to maintaining over time the vasculature tone[48].

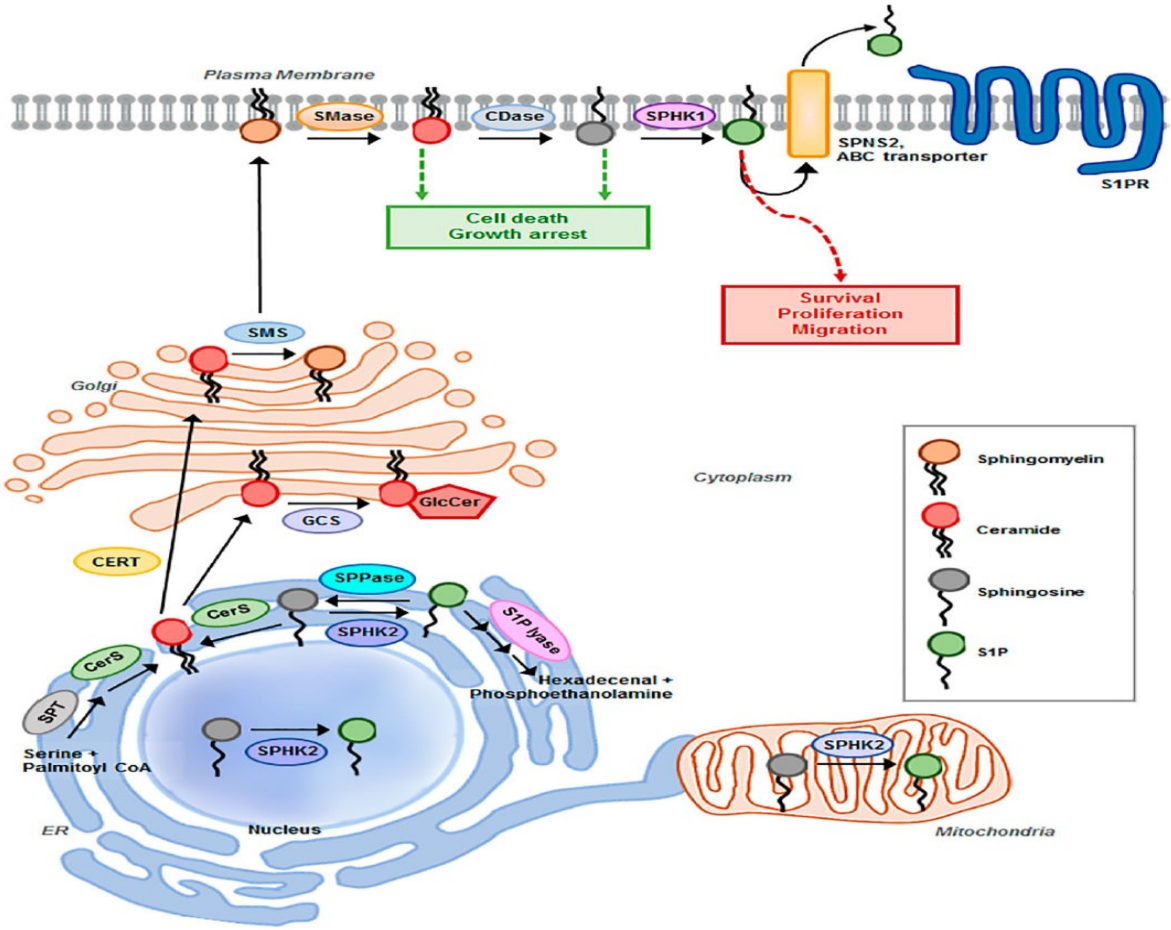

Figure 2: Sphingolipid metabolism

Reprinted from elly M. Kreitzburg and Karina J. Yoon[49] with permission from Cancer Drug Resist under a Creative Commons Attribution 4.0 International License.

1.2 Role of sphingolipids in inflammatory lung disease

1.2.1 S1P and inflammation

Sphingosine-1-phosphate is a bioactive lipid intracellularly generated from the phosphorylation of sphingosine by two isoforms of the same kinase, SPHK1, and SPHK2. Once produced, S1P acts by interacting with its intracellular targets or is transported out of the cells in autocrine/paracrine manner as a ligand for S1P1-S1P5, a family of five G-protein coupled receptors. S1P activity is stopped trough its dephosphorylation by phosphatases to sphingosine or can be irreversibly cleaved by S1P lyase. The amount of S1P is very low in the tissue probably due to the high activity of S1P lyase. Conversely, the erythrocytes and platelets are the main sources of S1P and contain a high level of S1P in the blood (~1μM). In plasma circulation S1P bounds to albumin (30%) and high-density lipoproteins (HDL, 60 %). This different gradient between the level of S1P in the blood and tissue plays a crucial role in driving S1P functions correlated to the trafficking of immune cells[50]. It has been well characterized by the S1P-S1PR signaling in immune cells trafficking and activation in the innate and adaptive immune system, regulating most of the biological events in physiological state and disease[43,51]. Clinical relevance of S1P/ S1Pr has shown to be an important point in the immunological system. Recent studies using pharmacological treatment with Fingolimod (FTY720), a functional antagonist of the S1P1 receptor, showed the arrest of lymphocytes egress from the thymus to secondary lymphoid organs, resulting in a global lymphopenia[52]. FTY720 now is approved by the Food and Drug Administration (FDA) in the treatment of multiple sclerosis (MS) and other immune diseases, preventing lymphocyte migration trough phosphorylation and internalization of S1P1 receptor[53].

In addition to their functions in controlling leukocyte migration, S1P and its receptors have important roles in regulating allergic responses including endothelial barrier integrity, cytokine and adhesion molecule expression. The “inside-out signaling” of S1P has important implications for many functions of S1P in inflammation such as mast cell degranulation, the main player in the initiation of anaphylaxis. For example, mast cell activation and degranulation are promoted, at least in part, by upregulation of SPHK1[54] leading to S1P production after crosslinking of high-affinity IgE receptors on mast cells[55]. S1P is then exported out of cells by ATP-binding cassette (ABC) [39] transporter or by the newly identified S1P transporter spinster (SPNS2). S1P carries out its actions binding its receptors: S1PR1 and S1PR2.

Interestingly, modification of the S1PR1 gene was recently associated with asthma susceptibility and severity[56] meanwhile IgE-mediated allergic responses are attenuated by an S1PR2 antagonist and, of course, in S1PR2-deficient mice. In addition, inhalation of SPHK1 inhibitors could attenuate lungs and BAL fluid inflammation in ovalbumin OVA-challenged, a mouse model of asthma [57]. S1P regulates mast cell migration via S1P1 and S1P2 receptors[58].

S1P, when injected locally to rat-paw, causes edema accompanied by eosinophilic infiltration and strongly up-regulation of CCR3, the main receptors involved in eosinophils functions [59]. Moreover, during severe inflammatory response, vascular barrier integrity is compromised: capillary leakage with subsequent fluid retention and formation of exudate are serious complications in infectious disease to contribute a diffuse airways obstruction[60].

Some studies have tried to demonstrate how S1P is involved in the control of vascular permeability during inflammation. Lipopolysaccharide (LPS) induced barrier permeability is mediated, at least in part, by activation of S1PR2 and

S1PR3 that downstream regulate Rho-dependent cytoskeletal rearrangements with totally breakdown adherens junctions[61]. By contrast, the SPHK1-S1P-S1PR1 axis is a negative feedback mechanism that limits the increase in endothelial-cells permeability by inducting RAC-dependent cytoskeletal rearrangements and promotes adherens junctions cell-cell[62,63].

Any pathogen is recognized by our immune system through the TLR receptor. Among this, TLR4 recognizes bacterial lipopeptides and LPS from Gram-negative bacteria and successively activated immune innate cells (monocytes, macrophages, and DCs). In this context, two elegant studies highlighted the participation of SPHK1 and S1P production in the TLR4 downstream pathway. SPHK1 activation induces S1P production that binds with nuclear factor-kappa (NF-kb) activation. The deletion of SPHK1 or partially inhibition of SPHK1 prevent sepsis in a mouse model of LPS challenge[64]. Definitely, S1P could be a pro or anti-inflammatory signal depending on the source where S1P is produced and the context of inflammation[65].

1.2.2 S1P in inflammatory respiratory disease

Sphingosine-1-phosphate (S1P) is a potent lipid mediator that can regulate most of the cell signaling pathways during inflammation, including migration of mast cells, the proliferation of smooth muscle cells, lymphocyte egress and endothelial barrier function [66].S1P is produced from sphingosine when ceramide is degraded by ceramidase. The phosphorylation of sphingosine by SPHKI and SPHK2 yields S1P. Levels of S1P are regulated by recycling S1P back to sphingosine by dephosphorylation or irreversible S1P degradation by S1P lyase to form phosphoethanolamine and hexadecenal.

S1P acts through a family of G-protein coupled receptors and most of the immune cells express S1P family receptors according to cell type and differentiation state. it has been clearly established that the S1P-S1P receptor axis is dominant regulatory for immune cell trafficking. Among respiratory inflammatory diseases, asthma is a chronic inflammatory respiratory disease which is estimated by more than 300 million affected individuals with a prevalence in children more than adults, females more than males[67]. Repeated episodes of wheezing, shortness of breath, chest tightness and dyspnea are typical symptoms in asthma. These symptoms are associated with reversible limitation of airflow, bronchoconstriction, and overproduction of mucus, where the patients have difficulty moving air in and out of the lungs over time varying in intensity and frequency. All these factors perfectly reflect the physiopathology of this inflammatory disease: airway hyperresponsiveness (AHR) and activation of both, innate and adaptive immune systems[68]. Especially, AHR is an exaggerated response of the airways to non-specific stimuli and the progressive airflow obstruction is the result of two different mechanisms: the increase in mucus production and the airway remodeling due to smooth muscle hyperplasia, collagen deposition and destruction of epithelium and cartilage layers. Allergic asthma is mediated by TH2 phenotype with eosinophilia, IgE-producing B cells, basophils, eosinophils, mast cells and their major cytokines such as IL-4, IL-5, and IL-13[69]. IL-4 is a cytokine that induces differentiation of naïve T cells; IL-5 induces eosinophil recruitment and their maturation, IL-4 and IL-13 stimulate the IgE production from B cells which binds to mast cells releasing proinflammatory mediators such as histamine, eicosanoids (leukotrienes) to induce contraction of smooth muscle, mucus production, and vasodilation. The inflammatory reaction TH2-mediated in allergic asthma requires two consecutive steps including the first contact or “sensitization” to

different environmental allergens and the manifestations of allergic response after the second exposure[70]. Allergen-specific TH2 response starts when an inhaled allergen taken up by dendritic cells (DCs), binds to the FCεRI, the “high affinity” receptor on IgE, which can help antigen-presentation by DCs and the complex is then presented to memory TH2 cells: mast cells, basophils, eosinophils are rapidly activated. For this reason, Immunoglobulin E is responsible for the “early phase” of allergic response via a high-affinity receptor (FCεRI) and are correlated with TH2 total number cells. IgE directly activates airway smooth muscle cells following their contraction and proliferation. Furthermore, the activated cells rapidly release proinflammatory mediators such as histamine, eicosanoids (in particular leukotrienes), and ROS that induce contraction of smooth muscle, mucus production, and vasodilation. Mast cells may have effects on smooth muscle contraction, mucus production and it is the best source of PGD2 meanwhile eosinophils and its degranulation are the principal effectors of innate immune response by increasing AHR and releasing LTs and TGF-beta.

In addition to be the first line of defense against pathogens and prevents the organism from infections, airway epithelium is actively involved in the inflammatory process. Airway epithelial leakage following exposure to environmental factors causes inflammation. Barrier functions of the lung epithelium is mainly provided by adherens junctions. When the epithelial barrier is damaged, epithelial bronchial cells release significantly greater amounts of IL8, GM-CSF, RANTES, and sICAM-1- VCAM in asthmatic patients than in nonallergic controls[71–73]. Another important feature in chronic asthmatic response is the airway remodeling[50]. It is a phenomenon characterized by changes in the airway structures following the abnormal deposition of inflammatory cells such as fibroblast, extracellular matrix protein like collagen,

smooth muscle cell proliferation, vascular membrane modification, and mucus hyperplasia. All together contribute to the irreversible obstruction of airway and limitation of airflow.

Recently, S1P has been shown to play an important role in the pathogenesis of asthma. The first finding came from clinical observations: S1P levels were increased in the bronchoalveolar lavage (BAL) of asthmatic patients 24h after segmental allergen challenge but not in control subjects[74]. High S1P levels in BAL of asthmatic patients are directly correlated with the degree of inflammation such as the number of eosinophils and the number of protein influx, confirming the hypothesis that S1P is an important marker of airway inflammation after exposure of allergen[74]. Moreover, S1P causes intracellular Ca^{2+} increase and airway smooth muscle cell contraction (ASM), the primary effectors in the modulation of bronchial tone[74]. Indeed, the inhibition of SPHK1 using DHS (D,L-threo-dihydrosphingosine) and DMS (N,N-dimethylsphingosine), reduces significantly the contraction of peripheral airways by acetylcholine-mediated contraction via muscarinic M2 and M3 subtypes receptors. Cholinergic hypersensitivity is linked in Asthma bronco-occlusion and these pieces of evidence suggest the involvement of the SphK/S1P signaling pathway in cholinergic constriction of murine peripheral airways[75].

Airway smooth muscle is implicated in both acute inflammatory response and the chronic processes correlated to airway remodeling. One of the mechanisms is through the inhibition of myosin phosphatase and stimulation of myosin light chain phosphorylation mediated by S1P in RhoA-kinase-dependent manner [76] or directly on increase intracellular calcium by SPHK1 activation dependent on muscarinic receptors [75].

Roviezzo et al. hypothesized the role of S1P as a direct modulator of the bronchial tone. They evaluated the effects of exogenous S1P administration on isolated bronchi and whole lungs harvested from BALBC/c mice sensitized to ovalbumin (OVA) by the functional study on bronchial reactivity and lung resistance. They found that exogenous administration of S1P in isolated bronchi from OVA-sensitised but not in control mice caused airway hyperresponsiveness in a dose-dependent manner and increased in lung resistance. Indeed, BML-241 that interferes with S1P3 signaling and DL-threo-Dihydrosphingosine (DTD), significantly inhibits the S1P-induced contraction, indicating an involvement of S1P and especially, sphingosine kinases and S1P2-S1P3 receptors, in airway hyperreactivity[77]. Later on, the same research group demonstrated the molecular mechanisms underlying the effects of S1P on the lungs. The subcutaneous administration of S1P without allergen-sensitization induces airway hyperresponsiveness correlated with an increase in lung TH2 cytokines, IL-4 and IL-13 and circulating IgE in a time and dose-dependent manner reaching a maximal effect 21 days after S1P administration[78,79].

Another hallmark in allergic asthma is represented by mast cells. They act by releasing vasoactive mediators, pro-inflammatory cytokines, chemokine, and leukotrienes. All together contribute to vascular permeability, bronchoconstriction, and recruitment of leukocytes. The number of activated mast cells is directly correlated to bronchial hyperreactivity[80].Crosslinking of the FcεRI on IgE also induces SPHK1 activation and consecutively the production of S1P. Also, mast cell production and their degranulation are mediated by S1PR1 and S1PR2 activation[58].

1.2.3 S1P and airway hyperreactivity (AHR)

Asthma and other pulmonary inflammatory disease are mainly characterized by inflammation, airway wall remodeling and airway hyperreactivity (AHR). One of the distinctive features of asthma is AHR. During allergic inflammation mast cells play an important role in smooth muscle contraction, mucus production and it is the best source of PGD2 meanwhile eosinophils and its degranulation are the principal effectors of innate immune response by increasing airway hyperreactivity (AHR) and releasing LTs and TGF-β. All this mediator contributing to AHR during allergic sensitization[81]. The result of this pathological condition is progressive and irreversible obstruction of airflow as well as the capacity to eject air out of the lungs ending in emphysema, permanent enlargement of alveolar walls. These symptoms increase during acute exacerbation of inflammatory respiratory disease until the loss of lung functions and their elasticity too. The development is associated with lung failure with hypoventilation, hypoxia and respiratory acidosis. These persistent and diffuse inflammatory processes go on and lead to airway fibrosis, mediated by activation of fibroblast by distinct mediators such as TGF-β, connective tissue growth factors, and endothelin. In this context, airway smooth muscle cells overtime contribute to bronchial hyperresponsiveness releasing many inflammatory mediators such as chemokines, cytokines and growth factors[82]. Airway hyperresponsiveness (AHR) is the key feature of many pulmonary diseases. In asthma, AHR is an exaggerated bronchoconstrictor response that results in airway bronchoconstriction. AHR develops after various provocative agents, not only to allergens in which the subjects are sensitized but also to various non-specific stimuli like methacholine, histamine, and cold air[83]. AHR as well the degree of obstruction is measured by various methacholine tests or spirometry which are used to identify individuals with high risk to develop

asthma or other similar pathological conditions. The results of methacholine test are usually expressed as a percentage of decrease in forced expiratory volume over 1s (FEV1) and three parameters are examined: 1- the concentration of an agonist that induces a fixed decrease in lung function (ie a 20% decrease in FEV1), 2- the dose-response curve,3- the dose of provocative agonist where is possible to reach the plateau[84]. Usually, the response is expressed as either a provocative dose (PD20) or a provocative concentration (PC20). Exist a direct relationship between the inflammatory state correlate to the severity of airway hyper-responsiveness and the contribution of smooth muscle hyperplasia/hypertrophy, collagen deposition, and epithelial fibrosis that stronger involved in the development and maintenance of AHR[85]. All these inflammatory processes are connected to each other, at least in part, by the biological role of chemokines. Chemokines are a large group of low molecular weight proteins belong to four supergene families, classified into groups on the basis of the number and homology structure of amino acid sequences at the N terminus. Two of these families (the CC and CXC chemokine groups) contain over 50 identified ligands and their biological effects are mediated by the interaction with seven-transmembrane G-protein-coupled receptors[86,87]. Their main function is the activation and recruitment of leukocytes at the sites of inflammation by chemotaxis. In particular, CXC chemokines such as interleukin-8 (IL-8) activate predominantly neutrophils, CC chemokines such as RANTES target a variety of cell types including macrophages, eosinophils, and basophils. Moreover, chemokine receptors expression is not unlimited on inflammatory cells: structural cells such as epithelial cells, endothelial cells, smooth muscle cells, and fibroblasts also express chemokine receptors[88,89]. In this way, they actively contribute to the inflammatory process. All these effects, including recruitment and activation of leukocytes, smooth muscle proliferation,

regulation of collagen deposition and coordination of fibrosis, may have key individual roles in the activation and maintenance of AHR. It is well known that lung eosinophilia and their infiltration in the airway is a central element of allergic asthma. Eosinophils and their products have been identified in sputum, bronchoalveolar lavage fluid (BALF) and biopsy material of the airways in patients with asthma[90]. Furthermore, the number of these cells and the amount of their products correlate with the severity of airway reactivity (AHR)[91 92]. In addition, preclinical and clinical studies have identified a high level of chemokines and their receptors in BALF and sputum of allergic asthmatics compared to control patients as well in different murine models of allergic asthma[82].Also, chemokine-induced preferentially recruitment of Th2 cells, including monocyte-derived. These cells regulate the persistence and the activation of other cells such as eosinophils or mast cells in the airways of asthmatic patients via both direct contact and through the release of other inflammatory mediators which contribute to increasing the severity of AHR. In addition to eosinophilia, mast cells located in mucosal and peribronchovascular sites are also the main effectors of allergy response[93]. These cells can release a variety of mediators that can cause acute bronchospasm, activate and/or attract other inflammatory cells in the lung, and increase AHR[94]. Indeed, there is a strong direct correlation between amounts of histamine in the airways of allergic asthmatics patients and the sensitivity of the airways to methacholine. Moreover, histologic studies have reported a marked increase in the number of smooth muscle cells in airways from asthmatic subjects; this phenomenon with airway inflammation contributes overtime to AHR and the obstruction of airway[95]. In this chronic and prolonged scenario, fibrosis is an essential component process of tissue repair: clinical studies have demonstrated that the degree of subepithelial fibrosis is correlated with hypersensitivity of the airway

to methacholine. Indeed, the interstitial collagen deposition in the airway basement membrane and subepithelial fibrosis are present in the airways of allergic asthmatics[96]. Infiltrating inflammatory cells such as macrophages, lymphocytes, neutrophils and eosinophils participate in the pathogenesis of lung fibrosis, through the activation of fibroblasts. Recent evidence has shown that MCP-1 enhances collagen deposition by fibroblasts; therefore, increased expression of this chemokine in the lungs of asthmatics might be responsible for the airway remodelling that can exacerbate AHR. It has been demonstrated that sphingosine-1-phosphate (S1P) could interfere with AHR during allergic response through its ability to activate S1PR receptors as well sphingosine kinases directly on smooth muscle cells[97]. Emerging evidence now supports the concept that sphingolipids metabolism may interfere with mechanisms that sustain and promote the increase in the thickness of airway smooth muscle cells (ASM)[96]. Other evidence suggests that high doses of the sphingosine analog FTY720 influence the levels of ceramide that induces apoptosis and chronic inflammation[98,99]. Also, intracellular S1P could interact with smooth muscles cells thickness. Importantly, all these observations are sustained by in vitro experiments that demostrated a cell amplification and/or survival via SphK2-dependent intracellular accumulation of S1P[100].

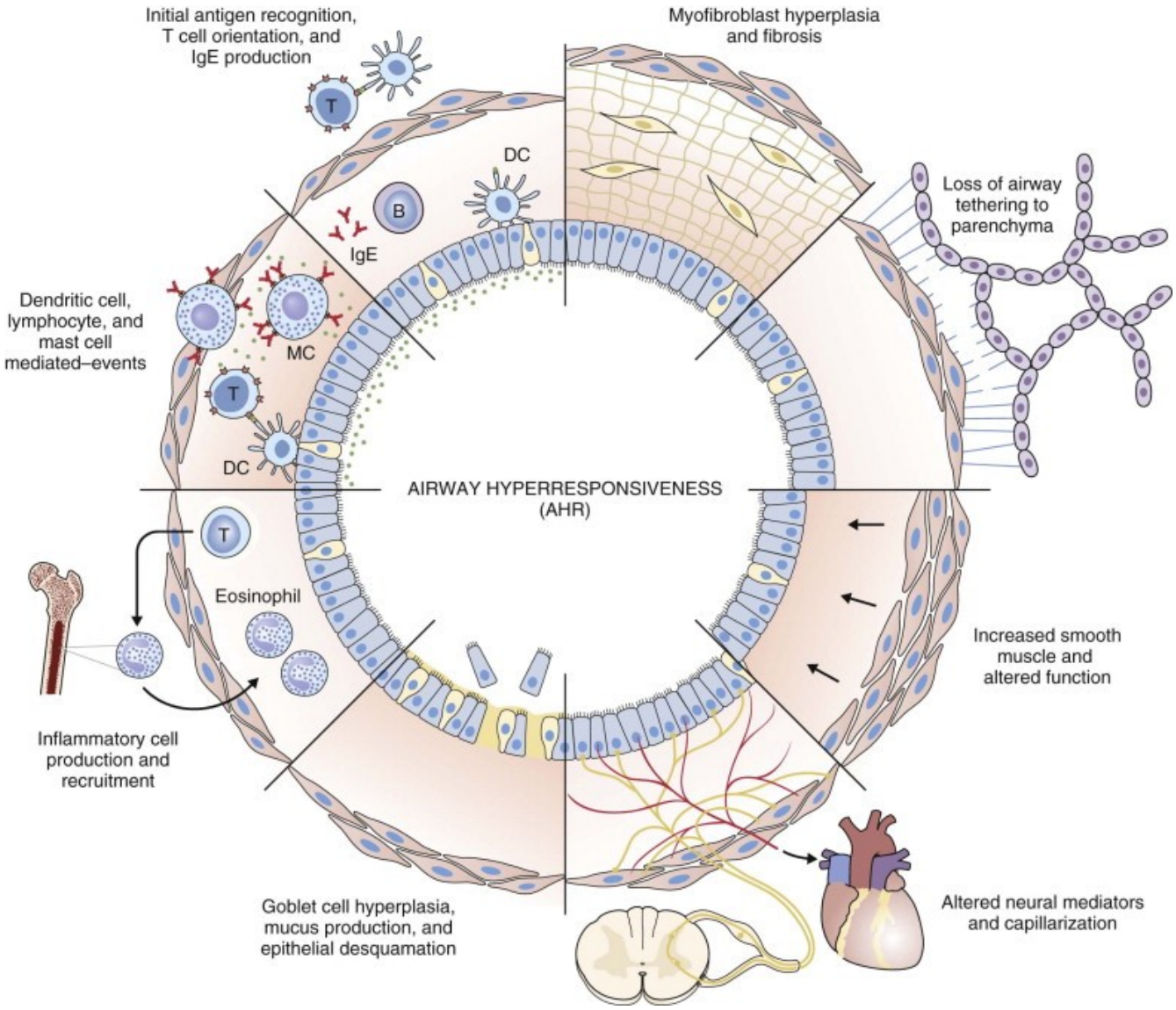

Figure 3: Airway hyperresponsiveness (AHR)

Reproduced from Ian D. Pavord,Ruth H. Green,Pranabashis Haldar[101] with permission from Elsevier

1.3 The relevance of sphingolipids in cardiovascular diseases

1.3.1 Highlights on S1P in Cardiovascular diseases

Cardiovascular diseases (CVD) are the principal cause of death in the world. They represent a group of pathological conditions of heart and blood vessels, including coronary artery disease (CAD) which could lead to myocardial infarction (MI) and cerebrovascular disease could end in a stroke[102]. Overall cardiovascular diseases are primarily caused by atherosclerosis and smoking, abnormal cholesterol levels, high blood pressure, obesity are the principal risk factors [103]. The process of atherosclerosis plaque formation implicates vascular lesions, platelet aggregation and infiltration of inflammatory cells and smooth muscle cells (SMC) in the lumen of blood vessels. Also, the accumulation of lipids inside the endothelial cells is another important factor that increases plaque formation: oxidised-LDL (low-density lipoproteins) and recruitment/infiltration of monocytes which can then differentiate into to macrophages lead to form foam cells[104]. Moreover, activation of immune cells can release pro-inflammatory mediators such as tumor necrosis factor (TNF), interferon-gamma and IL-12, IL-15 interleukins are interfering with an increase in plaque formation that can cause arterial stenosis and contribute overtime to tissue plaque rapture triggering thrombosis, platelet aggregation. This leads to partial or complete occlusion of the lumen arterial vessel resulting in myocardial infarction (MI) or ischaemic stroke if the occlusion of blood vessels occurred respectively in coronary arteries or cerebral arteries[105]. Heart attack or MI occurs when blood flow is blocked resulting in damage to myocardial tissue for the hypoxia process. This can occur following plaque rupture or thrombotic/embolic events in the coronary arteries[106]. In this context, the role of sphingolipids in the cardiovascular system is not well clarified. Sphingolipids

have an important role in the regulation of a multitude of cell functions, including cardiovascular homeostasis. Ceramide, sphingosine, sphingosine-1-phosphate (S1P) are the main protagonists. S1P is formed from sphingosine when ceramide is degraded by ceramidase. The phosphorylation of sphingosine by SPHKI and SPHK2 yields S1P. Levels of S1P are regulated by recycling S1P back to sphingosine by dephosphorylation or irreversible S1P degradation by S1P lyase to form phosphoethanolamine and hexadecenal. Dysfunction in sphingolipids production or altered sphingolipids levels are correlated with cardiovascular diseases and atherosclerosis but specific molecular mechanisms are poorly understood and could represent a possible good approach to overcome the pathological problem[107]. It has been shown that the overproduction of sphingolipids causes severe damage to the cardiac function through the improvement of chronotropic and inotropic action of the heart and hypertrophy process. The pathological state as the ischemic heart shows a decrease of the cardiac contractility and myocardial apoptosis probably due to an increase of TNF alfa production and inhibition of ceramidase and sphingomyelinase which then leads to an increase of sphingolipids levels and cardiac function[108]. Conversely, preclinical and clinical studies reported a reduced level of S1P in patients with coronary artery diseases and it is inversely correlated with the severity of the diseases. The heart is protected from ischemia-reperfusion by exogenous administration of S1P, underlying the cardioprotective role of S1P signaling[109]. The protective role of S1P in the heart was demonstrated by Zhang et al during a cardiac pressure overload through S1P/S1P1r/ eNOS pathway activation. In the heart, NOGO-B, an inhibitor of SPT, is only mainly evident in blood vessels and the cardiomyocytes the atria of the heart. In mice lacking NOGO-B, the endothelium produces higher levels of S1P, which activates S1PR1- S1PR3 inducing NO production and

endothelial barrier integrity, improving overtime vessel compliance to the high pressure and reducing extravasation of plasma proteins and inflammatory cells[110]. This study is in perfect tune with the evidence that S1P plays also an important role in vascular homeostasis through the activation of eNOS/NO endothelial pathway. Recently, the research group of Prof Di Lorenzo discovered a new regulatory mechanism of the sphingolipid de novo pathway. They demonstrated that S1PR1 is a key regulator of blood pressure and flow through endothelial S1P-S1PR1-eNOS. Also, a novel mechanism by which endothelial sphingolipids biosynthesis is identified: NOGO-B[24]. NOGO-B is a membrane protein that negatively inhibits SPT activity and controls the production of sphingolipids, in particular S1P and ceramide, playing and active role in the control of hypertension, vascular inflammation, and heart failure conditions.

AIMS

The role of sphingolipids in inflammatory airway disease initiation is not well defined, however recent literature suggests that it is these early activation events resulting in altered sphingolipid pathways that may be a key aspect of airway dysfunction. Alterations in de novo sphingolipid metabolism have been shown to lead to airway hyperreactivity (AHR), the cardinal feature of asthma, without allergic sensitization or inflammation. Here I investigated how S1P, the final product of sphingolipid metabolism, could contribute to airway dysfunction in inflammatory pulmonary diseases. I also attended as a co-worker in some projects where I tested the pharmacological efficacy of different compounds in experimental models of asthma. During my second part of my Ph.D. project at Weill Cornell Medical College under the supervision of Prof Di Lorenzo, I have focused my attention on the cardioprotective role of *De novo* sphingolipid pathway in a novel mouse model of heart failure.

The main aims of this study are:

1. Role of S1P in airway function
2. Role of mast cells in sensititazion mechanisms
3. Study of *De novo* sphingolipid biosynthesis and its cardioprotective functions in a mouse model of heart failure

Chapter 2

Materials and Methods

CHAPTER 2 - MATERIALS AND METHODS

Animal studies

2.1 Mice

Adult female and male BALB/c and C57BL/6 mice, mast cell-deficient Kit $^{W\text{-}Sh/W\text{-}sh}$ mice[111,112] and CH3/HeJ ($Tlr4^{Lps\text{-}d}$)[113] mice were purchased from Charles River Laboratories (Italy). All mouse strains aged 8-9 weeks; weight male 24-27g and female 18-22g, were housed at 24±2 °C in a controlled environment with a 12-hour light/dark cycle under specific pathogen-free conditions at the Department of Pharmacy (University of Naples, Italy). They were supplied with standard rodent chow diet and water *ad libitum* and acclimatized for 4 days before experiments. All experiments were conducted during daylight according to Italian regulations on the protection of animals used for experimental and other scientific purposes (D.lgs. 26/2014) as well as with the European Economic Community regulations (EU Directive 2010/63/EU). All the studies were conducted under authorizations numbers 2012/0081821, 1092/2015, 186/2015 released by Healthy Italian Ministry.

2.2 Experimental protocols

Exposure to S1P

Female BALB/c mice, mast cell-deficient Kit $^{W\text{-}Sh/W\text{-}sh}$ mice[111,112] , C3H/HeJ ($Tlr4^{Lps\text{-}d}$)[113] mice received subcutaneous injection (s.c.) of 0.1ml of S1P (10ng/µl); Enzo Life Science, Italy) dissolved in sterile saline containing BSA (0,001 %) on days 0 and 7 and sacrificed at different time points: 14 and 21 days after the first administration of S1P. Control mice received only 0.1ml of BSA (0,001%) as a vehicle[78,79].

Part of female BALB/c mice also received 30 min before S1P or vehicle administration, intraperitoneal injection of disodium cromoglycate (DSCG; 50mg/Kg; Sigma Aldrich, Italy) or they were intraperitoneally pretreated with compound 48/80, a mast cell degranulator, every 12h for four days following the template: day1 0.6mg/kg; day2 1.0mg/kg; day3 1.2 mg/kg and day4 2.4mg/kg. After 24h of the last administration of CM48/80 the S1P protocol was made[114].

We already published that the systemic administration of S1P induces in BALB/c mice a disease mimicking the cardinal features of severe asthma in humans sustained by Th2 response with bronchial hyperresponsiveness and pulmonary eosinophil inflammation[78,79].

In another set of experiments, female BALB/c or C3H/HeJ ($Tlr4^{Lps\text{-}d}$) mice received intranasal instillation of lipopolysaccharide (0.1 μg/mouse of LPS from *Escherichia coli* O111:B4; Sigma Aldrich, Italy) or subcutaneous injection of S1P (10ng/μl) or the combination LPS+S1P at days 0 and 7.

In another group of experiments, BALB/c mice were treated with purified rabbit anti-TLR4 (10 μg/mouse; i.p., sc-10741, Santa Cruz) in the same days but 30 min before subcutaneous administration of S1P or vehicle.

The growth factor-beta (TGF-beta) signaling has been implicated in the develop of fibrosis as a result of airway remodeling after persistent inflammation[115]. For this, in another set of experiments, a novel small-molecule inhibitor of the TGF-β receptor I kinase (LY2109761) [116,117] was used in female BALB/c mice at the dose of 50mg/Kg 15 min before S1P is administrated. Again, non-selective sphingosine kinases inhibitor for SKI-SKII was administered at doses of 3mg/Kg before ovalbumin (OVA) sensitization, a common allergen used in a mouse model of allergic asthma[118]. In this procedure, mice were injected

subcutaneously with 0.4 ml of OVA (100 µg/mouse) absorbed to 3.3mg of aluminium hydroxide gel (13 mg/ml Al(OH)3 stock solution) in sterile saline or only vehicle (sterile saline) on days 0 and 7.

Exposure to cigarette smoke

The experimental animal models with smoking mice that better summarises the several features of human COPD were made in collaboration with University of Siena (Italy) [119,120].

Male C57BL/6 mice (4 to 6 weeks old) were exposed to cigarette (CS) smoke (Marlboro Red, 12mg of tar and 0.9mg of nicotine) or room air as control mice.

The experimental design consists of three cigarettes per day, 5 days per week for 9, 10 and 11 months from the start of the experiment.

The mice were housed in groups of two to four in specially designated macrolon cages with a removable filter cover where the air flows out of the cages and to be continuously renovated. The smoke was originated by the combustion of three cigarettes/day/cage and was introduced into the chamber through the airflow generated by a mechanical ventilator (7025 Rodent Ventilator, Ugo Basile, Biological Research Instruments, Comerio, Italy) for a total duration of 90 min.

Exposure to Ovalbumin

Adult male and female BALB/c and C57BL/6 mice were treated subcutaneously (s.c.) with 0.4mL (100μg) of ovalbumin (OVA) complexed to 3.3mg of aluminum hydroxide gel (13 mg/ml Al(OH)3 stock solution) in sterile saline on days 0 and 7, while control mice received an equal volume of vehicle (sterile saline).

In another set of experiments, animals received intraperitoneal administration (i.p.) of montelukast (MS,1mg/kg cys-LT receptor antagonist), 30min before each OVA injection and 3 times per week until day 21. Similarly, mice were treated with zileuton (ZIL, 35mg/kg inhibitor of 5-LOX) and MK886 (MK, 0.1mg/kg FLAP inhibitor) or vehicle (0.5mL DMSO 2%) 30min before each OVA injection and at 14 days.

In another set of experiments, only female BALB/c mice were intraperitoneally (i.p.) treated with Palmitoylethanolamide (PEA 10mg/kg) or vehicle (ETOH and Tween-20, ratio 8:1:1) 15 min before each OVA administration.

In another set of experiments, only female BALB/c received an intraperitoneal injection (i.p.) of Salvinorin A (10mg/kg, diterpene isolated from *Salvia divinorum*) or vehicle (dimethyl sulfoxide 4% in 0.5ml) 30 min before each OVA sensitization.

All treated mice were sacrificed 14 and 21 days after OVA-sensitization and blood, main bronchi and lungs were collected and processed for functional and molecular studies. Each lung was divided into two parts: right lobes were frozen in liquid nitrogen for 2h before storage at -80 °C and successively homogenate for cytokine measurements by ELISA kit, while the left lobes were fixed in 10% formalin buffer for histopathological analysis.

2.3 Bronchial reactivity

Mice were anesthetized by isoflurane and then subjected to euthanasia. A 25G needle was inserted into the heart and blood was extracted and mixed with anticoagulant (sodium citrate 3.8%) in a ratio 1:10. Per mouse was collected approximately 0.5ml of blood. Blood samples were transferred to ice and centrifuged at 12000 rpm for 15 min at 4°C. Once plasma was separated samples were placed into -80 until use for molecular dosage.

Following a vertical middle incision of the thorax to expose the respiratory system, right and left main bronchial tissue was dissected from the lungs out of the mouse and rapidly cleaned from fat and connective tissue. Bronchial rings of 1 to 2 mm length were cut and transferred in organ baths (3 ml) filled with Krebs solution at 37°C (mol/l: NaCl 0.118, KCl 0.0047, MgCl2 0.0012, KH2PO4 0.0012, CaCl2 0.0025, NaHCO3 0.025, and glucose 0.01) and oxygenated with a mix of 95% O_2 and 5% CO_2.

Rings were mounted to isometric force transducers (type 7006; Ugo Basile, Comerio, Italy), and connected to a Powerlab 800 (ADInstruments, Italy).

Rings were initially stretched until a resting tension of 0.5 g was reached and left to equilibrate for at least 30 minutes, during which tension was adjusted to 0.5 g, if necessary, and the bathing solution was periodically changed. During the preliminary study, we found the optimal resting tension corresponding to 0.5 g to develop the perfect response to stimulation with contracting agents. In each experiment, bronchial rings were firstly challenged with carbachol (10μM or 10^{-6} M) until the responses were reproducible. Once reproducible, bronchial reactivity was tested performing a cumulative concentration-response curve to carbachol (10nM-30μM 10^{-9}-3×10^{-6} M or 10nM-30μM) or S1P (10^{-8}-3×10^{-5} M). In another set of experiments, main bronchial tissues were incubated with S1P2

antagonist (TY52156, 10μM, 15min; Tocris Bioscience, UK), S1P3 antagonist (JTE-013, 10μM, 15min) or Sph-K inhibitor (SK-I, 10μM, 30min; Tocris, Bristol, UK). After incubation, bronchial reactivity was assessed as previously described.

Data were expressed as contraction capacity (dine/mg of tissue) compared to increasing concentrations of carbachol or S1P.

2.4 Isolated perfused mouse lung preparation

Lung function was measured using an isolated and perfused mouse lung system in collaboration with the University of Campania Luigi Vanvitelli, Italy.

Pulmonary artery was cannulated, and the lungs were perfused at a constant flow of 1 ml/minute, resulting in a pulmonary artery pressure of 2 to 3 cmH_2O. The perfusion medium used was RPMI1640 lacking phenol red (37°C).

The lungs were ventilated by negative pressure (-3 and -9 cmH2O) with 90 breaths/min and a tidal volume of approximately 200 μl. Hyperinflation (-20 cmH2O) was performed every 5 minutes. Artificial thorax chamber pressure was measured with a differential pressure transducer (Validyne DP 45–24, Validyne Engineering, Los Angeles,CA) and airflow velocity with a pneumotachograph tube connected to a differential pressure transducer (Validyne DP 45–15, Validyne Engineering, Los Angeles,CA). The lungs respired humidified air. The arterial blood pressure was continuously monitored using a pressure transducer (Isotec Healthdyne, Irvine, USA) which related to the cannula ending in the pulmonary artery. All data were transmitted to a computer and analyzed with the Pulmodyn software (Hugo Sachs Elektronik, Germany). The data were analyzed through the following formula: P = V × C-1

+ RL × dV·dt-1, where P is chamber pressure, C pulmonary compliance, V tidal volume, RL airway resistance. Subsequently, the airway resistance value registered was corrected for the resistance of the pneumotachometer and the tracheal cannula of 0.6 cmH_2O s ml^{-1}. Lungs harvested from mice of each group treated as described before were perfused and ventilated for 45 minutes without any treatment to obtain a baseline state. Subsequently, the lungs were challenged with carbachol. Repetitive dose-response curves of carbachol or S1P (10^{-8}-$3x10^{-5}$ M) were administered as 50 µl bolus, followed by intervals of 15 minutes, in which lungs were perfused with buffer only. In another set of experiments, lungs were pretreated with SK-1 inhibitor, TY52156 (S1P2 antagonist) or JTE-013 (S1P3 antagonist) before challenging with carbachol or S1P.

2.5 Histology

Left lung lobes from each treated group mice were collected and processed for morphological, immunohistochemical and immunofluorescence analysis.

Lungs were fixed with formalin (4%) at least for 24h, washed in PBS and then dehydrated. All lungs were then embedded in OCT or paraffin medium. The blocks were cut with a thickness of 7µm per section and stained to evaluate different parameters.

The morphology of the lungs was observed with hematoxylin and eosin (H&E) staining and the fibrotic tissue was determined using a Masson's trichrome stain kit according to the manufacturer's instructions.

The degree of inflammation was scored with Periodic Acid/Alcian blue/Schiff (PAS) staining (Sigma-Aldrich, Italy). PAS staining was performed according to

the manufacturer's instructions. Positive PAS+ cryosections were classified with arbitrary scores 0 to 4 to describe low to severe lung inflammation as follows: 0: <5%; 1: 5–25%; 2: 25–50%; 3: 50–75%; 4: >75% positive staining/total lung area.

For each animal was considered at least five sections and the mean of the positive staining was compared with the total lung area.

For immunohistochemistry analysis, the lung sections were pre-treated with hydrogen peroxide for blocking the endogenous peroxidase. After that, antigen retrieval was made, and sections were put in a microwave for 20 min in 0.01 M pH 6.0 citrate buffer and cool down to room temperature. All sections were incubated with 3% BSA for 30 min at room temperature to block non-specific antibody binding. Next, lung sections were incubated overnight at 4°C with primary antibody: anti-sphkI antibody (1:200, Bioss Cat# bs2652R), anti-sphkII antibody (1:70, Abcam Cat# ab37977), anti-S1P2 antibody (1:150, Biorbyt Cat# orb5558), anti-S1P3 antibody (1:100, Bioss Antibodies, Woburn, US), anti- α-SMA antibody (1:400, Sigma, St. Louis, US), anti-CD23 antibody (eBioscience, San Diego, CA), anti-TLR4 antibody (Santa Cruz, CA, USA), anti-FGF2 (1:250, Santa Cruz Technology, USA), anti-IL-33(1:250, Termofischer, Italy) in 3% BSA. After 3 washes in TBST, secondary antibodies anti-rat IgG (1:200) was added for 30 min at room temperature followed by incubation with peroxidase-anti peroxidase complex. The diamino-benzidinic acid system (DAB) was used to detect complexes as a chromogen (Vector Laboratories, Burlingame, CA).

Mast cell activation was evaluated by toluidine blue (Sigma-Aldrich, Italy) positive staining by immunohistochemistry.

All Positive staining was quantified by means of Image J software (NIH, USA) and expressed as positive staining compared with the total lung area.

Immunohistochemical images were captured under light microscopy at 10X magnification.

To assess lipid deposition was performed Oil red O staining in the coronary arteries. Frozen heart sections were stained with Oil Red O (MilliporeSigma) as previously described. Briefly, heart cryosections were washed in PBS, stained with 0.2% Oil Red O in 60% isopropanol for 20 minutes, and washed with 60% isopropanol. After counterstaining performed with hematoxylin, sections were washed and coverslipped with aqueous mounting medium. Images were acquired by using a Zeiss Axio Observer.Z1 microscope, and the area of Oil Red O staining was calculated by using ImagePro (Media Cybernetics). Coronary stenosis was calculated by measuring the area of the lumen (AL) and the internal elastic lamina (AIEL); the percentage of stenosis was calculated as follows: (AIEL – AL)/AIEL × 100. Oil Red O percentage in the plaque stenosis was calculated as the ratio of positive Oil Red O staining area to the percentage plaque area.

Lung paraffin-sections were also used for immunofluorescence staining.

The lung sections were first permeabilized with 0.5% Triton X-100 in a solution of 5% BSA and followed by blocking with BSA 5% for 45 min at room temperature. Then, the sections were incubated with primary antibodies overnight at 4% and subsequently, conjugated-secondary antibodies were added for 1 hour at room temperature. Lung sections were stained for TLR4-AlexaFluor488 (Invitrogen, CA, USA) or S1P1-AlexaFluor555 (Invitrogen, CA, USA). Nuclei were counterstained with DAPI (Sigma Aldrich, Rome, Italy). Immunofluorescence images of lungs were captured with Carl Zeiss confocal microscopy at 40X magnification.

2.6 Flow cytometry

At 10 or 14 days after S1P challenge, the mice were sacrificed, and lungs were immediately picked up. The composition of lung inflammatory cells was determined by flow cytometry (BD FacsCalibur, Italy) using different antibodies for each cell subtypes and an appropriate isotype control. Lungs were isolated and digested with 1 U/ml collagenase. Cell suspensions were passed through 70 μm cell strainers and red blood cells were lysed. Cell suspensions were used for flow cytometric analysis of different cell subtypes.

2.7 ELISA assay

For each different group mice, blood and lung were collected for biochemical dosage. Blood was collected through intracardiac puncture using 25G needle and sodium citrate 3.8% as anti-coagulant in 1:10 ratio. Per mouse was collected approximately 0.5ml of blood. Blood samples were transferred to ice and centrifuged at 12000 rpm for 15 min at 4°C. Once plasma was separated samples were immediately frozen at -80°C until use for molecular dosage. Moreover, frozen lungs were digested with 1U/ml collagenase (Sigma Aldrich, Milan, Italy). The homogenate is centrifugated at 12000 rpm for 10 min at 4 °C. The levels of IL-13, IL-4 or plasma IgE were measured with commercially available enzyme-linked immunosorbent assay (ELISA) kit according to manufacturer's instructions. Levels of cytokines were expressed as pg/mg tissue.

2.8 Western blotting

Lungs were homogenized in ice-cold lysis buffer (RIPA: 50mM Tris/HCl, pH 7.4, 1% Triton X-100, 0.25%, sodium deoxycholate, 150 mM NaCl, 1 mM EDTA, 1 mM PMSF, 10 µg/ml aprotinin, 20 µM leupeptin, and 50 mM sodium fluoride) containing protease inhibitors added just before use and centrifuged at 14,000 g in a precooled centrifuge for 15 minutes. The total supernatant protein concentration was measured using Bradford's method. The supernatant was collected, added to 6X SDS sample buffer, containing 333 mM Tris-HCL (pH 6.8), 13% SDS, 67% glycerol, 665 mM DL-Dithiothreitol and a pinch of bromophenol blue, to a final concentration of 1X and incubated at 95°C for 5 min. The samples were separated on a 10% SDS-PAGE gel and transferred to a PVDF membrane. After the transfer was complete the nitrocellulose membrane was reversibly stained with Ponceau S to confirm protein transfer. Excess Ponceau S was rinsed off with dH_2O. The nitrocellulose membrane was blocked in 5% fat-free milk power PBS containing 0.1% Tween-20 for 1 h. The membrane was briefly rinsed with PBS and incubated with primary antibody overnight at 4°C under constant agitation. The primary antibodies are: rabbit polyclonal anti-TLR4(1:1000, H-80, sc-10741; Santa Cruz) or rabbit monoclonal ant-S1P1(1:1000, ab125074; Abcam, UK). After the overnight incubation primary antibody was removed and membrane washed 3 x 10 min PBS containing 0.1% Tween-20 and then the membrane was incubated in anti-horseradish peroxidase (HRP)-conjugated secondary antibody prepared in PBS (1:1000) for 2 h at room temperature under constant agitation. After detection with secondary antibody, the nitrocellulose membrane was washed 3 x 10 min in PBS and developed using enhanced chemiluminescence (ECL) to visualize immunoreactive bands. Enhanced chemiluminescence was carried out using

previously prepared detection reagents luminol and coumaric acid stored at -20°C. 50 µl of 3% HRP and 100 µl 68 mM coumaric acid (in DMSO) were added to 10 ml of 1.25 M luminol (in 0.1M Tris-HCl, pH 8.5). Cover the membrane and incubated for 1 min. The band intensity was quantified by densitometric analysis using ImageJ program and normalized with GADPH expression as housekeeping.

2.9 Gene expression analysis by quantitative Real-Time RT-PCR

Mouse bronchi tissue from each treated group mice were immediately stored at -80°C until RT-PCR analysis. Tissues were homogenized in 1.0 ml of TRIZOL (Invitrogen) and RNA was extracted by the use of PureZOL RNA isolation reagent (Bio-Rad, Hercules, CA) following the manufacturer's instructions. Total RNA was purified, quantified, characterized and retrotranscribed. Quantitative real-time PCR was carried out in Biorad system by use of SYBER Green Mix (ThermoFisher Scientific, Monza, Italy). Each sample was amplified simultaneously and GAPDH (glyceraldehyde-3-phosphate dehydrogenase, constitutively expressed proteins) expression was used as the housekeeping gene for PCR efficiency determination. Data were calculated using the 2^-ΔΔCt method.

2.10 Fibroblast culture

Murine lung fibroblasts were isolated from control mice and treated mice. Mice were sacrificed and lungs were removed. Lungs were chopped and incubated with DMEM containing two different digestive enzymes: 0.7 mg/ml of

collagenase type XI (Sigma C9407) and 30 μg/ml DNAse I (Sigma D5025). Then, with 5ml syringe aspirated and released the solution with the pieces of the heart in order to break down gently the lung. The cell suspension was filtered through 150 μm filter and spin down at 1200 rpm 10 min. Isolated fibroblasts were incubated with DMEM containing 15% FCS and cultures were replaced three times a week. Fibroblast proliferation was assessed by the MTT, (3-[4,5- dimethylthiazol-2-yl]-2,5-diphenyl tetrazolium bromide, colorimetric assay. Fibroblast differentiation was tested by incubating cells with mouse monoclonal antibody against α-SMA (SigmaAldrich, Italy) or rabbit polyclonal antibody against vimentin (Santa Cruz, CA). For detection fluorescein-labeled anti-mouse IgG (ABNOVA, Italy) or Texas-Red labeled anti-rabbit IgG (ABNOVA, Italy) were used.

2.11 Cell culture

A549 cells were maintained under standard culture conditions. Cells were harvested at 80% confluence. Morphology of the cells on phase-contrast microscopy was examined and photographed at 20X magnification. In another set of experiments primary murine cells harvested by naive animals were treated *in vitro* with TGF-β (2ng/ml) or S1P (10^{-7}M) for 72h in presence of the vehicle or incubated with LY2109761 (2 μM).

2.12 Statistical analysis

For each experiment, mice were divided into equal groups (n=6 per group). Results are expressed as means ± SEM. Observation in treated groups

compared with controls were analyzed using one-way analysis of variance (ANOVA), followed by Bonferroni's post-test for multiple comparisons, and/or Student's t-test, by using the GraphPad Prism software (USA). Two-way ANOVA was applied where required. p-values less than 0.05 were considered significant.

Chapter 3

Results

CHAPTER 3 - RESULTS

Role of S1P in airway dysfunction

3.1 Effect of Disodium cromoglycate in S1P-induced asthma-like disease in mice.

3.1.1 In-vivo treatment with Disodium cromoglycate (DSCG) and CM 48/80 abrogates bronchial hyperreactivity induced by S1P

Female BALB/c mice received subcutaneous administration (s.c.) of S1P on days 0 and 7 and bronchial reactivity was assessed at 21 days after S1P challenge (Figure 3.1.1A). Systemic administration of S1P in mice induced airway smooth muscle hyperreactivity with maximal effect at 21 days. This effect on airways was associated, at least in part, to pulmonary mast cell recruitment. Intraperitoneal administration of Disodium cromoglycate DSCG (50mg/kg) on the same days but 30 min before S1P challenge (Figure 3.1.1B) or treatment with CM48/80 compound inhibits bronchial hyperreactivity induced by S1P (Figure 3.1.1D). CM48/80, the mast cell degranulation compound dissolved in phosphate-buffered saline (PBS), was injected at 200μl/cavity to mice i.p. every 12h for four days, according to scheme below:0.6 mg/kg day1, 1.0 mg/kg day2, 1.2mg/kg day3, 2.4mg/kg day4. S1P was injected 24h after the last dose of CM48/80 compound. Mice were killed on day 21 and the bronchial reactivity was performed through a cumulative concentration-response to carbachol (10^{-9}-3×10^{-6} M) on bronchial rings in isolated organ baths. The same results have been also observed on lung function via pulmonary resistance (R_L) measurement. DSCG treatment significantly reverts S1P-induced bronchoconstriction (Figure 3.1.1C).

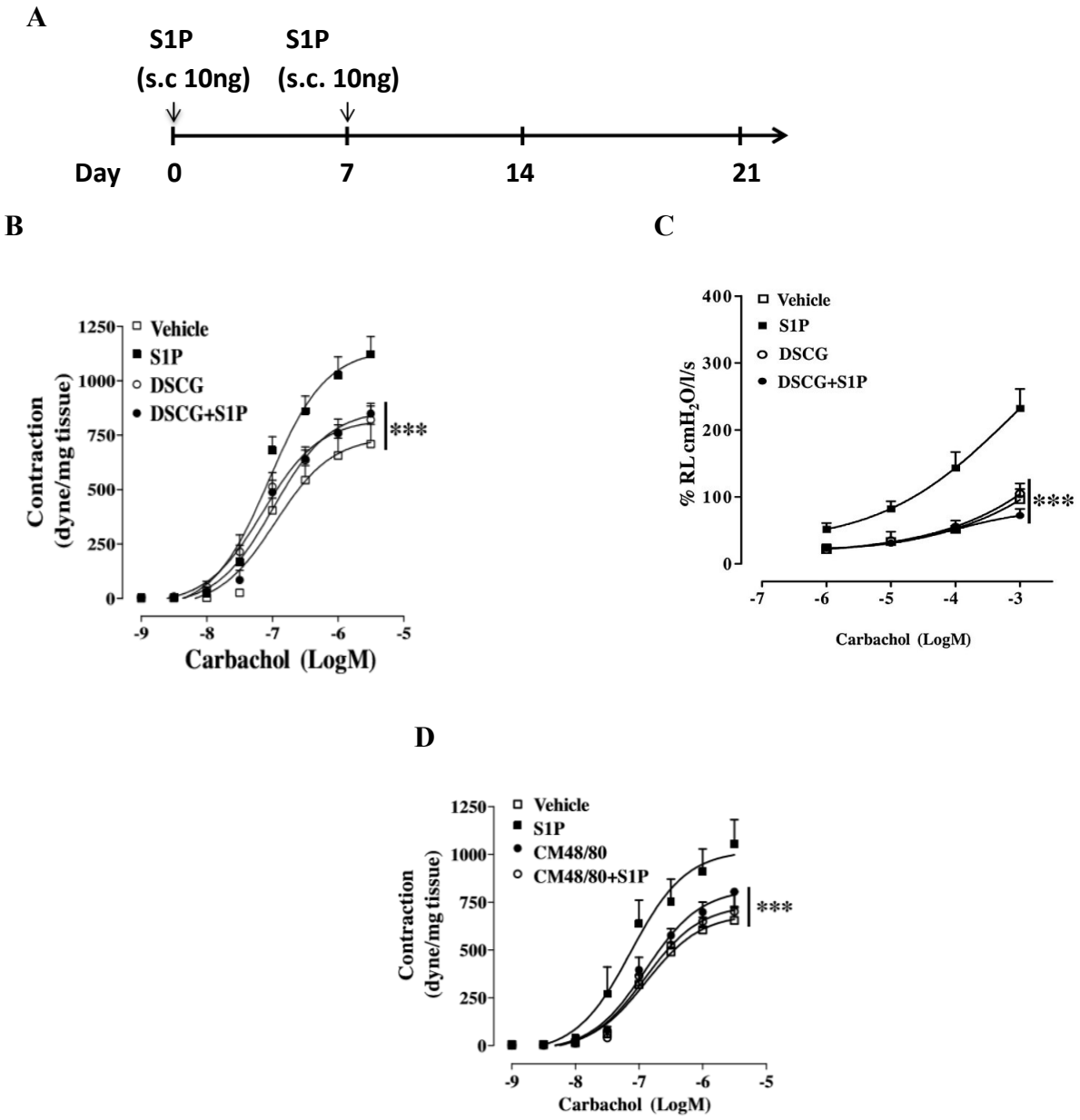

Figure 3.1.1: DSCG and CM48/80 inhibit S1P-induced bronchial hyper-responsiveness.

(A) BALB/c mice received subcutaneous administration of S1P (0.1ng/µl) or vehicle (BSA 0.001%) on days 0 and 7. (B-C) DSCG (50mg/kg) was injected i.p. 30 min before S1P or vehicle on days 0 and 7. Bronchial reactivity and lung resistance to carbachol were evaluated (*** $p<0.001$ vs. S1P, two-way ANOVA with Bonferroni's post-test). (D) Administration of CM48/80 compound dissolved in PBS to mice every 12h for 4 days. S1P was injected 24h after the last dose of CM 48/80. On day 21, bronchial reactivity to carbachol was assessed (*** $p< 0.001$ vs S1P, two-way ANOVA with Bonferroni's post-test). Data are mean ± SEM, n=6 mice in each group.

3.1.2 *DSCG inhibits S1P-induced lung inflammation.*

Inflammatory cytokines and immunoglobulin E were quantified in homogenate lungs and plasma respectively by ELISA assay. A significant reduction was observed in IgE plasma levels (Figure 3.1.2A) and IL-13 pulmonary cytokine (Figure 3.1.2C) after treatment with DSCG in S1P challenged mice but did not show any effect on IL-4 compared with control mice (Figure 3.1.2B). Lung sections were stained with Hematoxylin and eosin (H&E). Lungs from S1P-treated mice displayed an alteration in lung morphology with marked hyperplasia (Figure 3.1.2D) and was associated with an increase in mucus production. Pre-treatment with DSCG significantly reduced goblet cells determined by PAS staining (Figure 3.1.2E).

3.1.3 DSCG treatment interferes with mast cells activity

At 14 days after S1P challenge molecular studies were performed. Flow cytometry analysis on lungs from S1P treated mice showed an increase in the percentage of mast cell recruitment that was significantly reduced after DSCG treatment (Figure 3.1.3B). These beneficial effects well correlate to a drastic reduction in PGD2, a major prostaglandin produced by mast cells and it is critical during the development of allergic disease. PGD2 quantification has been measured in bronchoalveolar lavage (BAL) by specific ELISA Kit (Figure 3.1.3C).

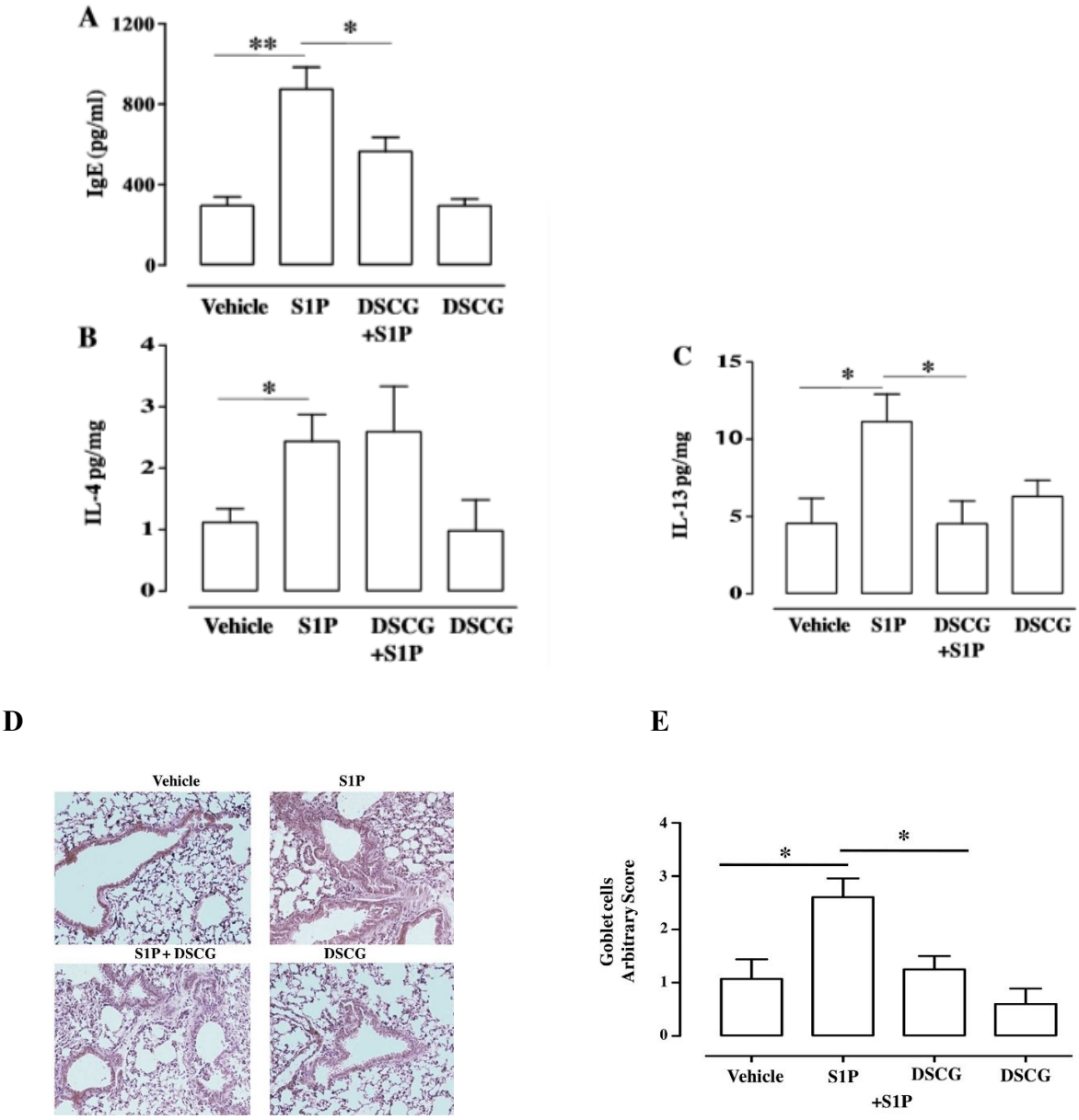

Figure3.1.2: **inhibitory effects of DSCG on S1P-induced lung inflammation.**

(A)Serum was collected and levels of total IgE were determined by using specific ELISA (*p<0.05; **P<0.01 vs S1P, one-way ANOVA with Bonferroni's post-test).(B-C)Right lungs were collected and digested with 1U/mL collagenase.IL-4 and IL-13 levels were detected by using specific ELISA (*p< 0.05 vs S1P, one-way ANOVA with Bonferroni's post-test).(D)Representative images of lung sections stained with H&E. Lung sections were captured under light microscopy at 10X magnification. (E) PAS staining for mucus in airways was quantified with arbitrary scores 0 to 4 to describe low to severe lung inflammation in the following manner: 0:<5%; 1: 5-25%; 2: 25-50%; 3: 50-75%; 4: >75% positive staining/total lung area. (* p<0.05 vs S1P ,Student's t-test).Data are mean ± SEM, n=6 mice in each group.

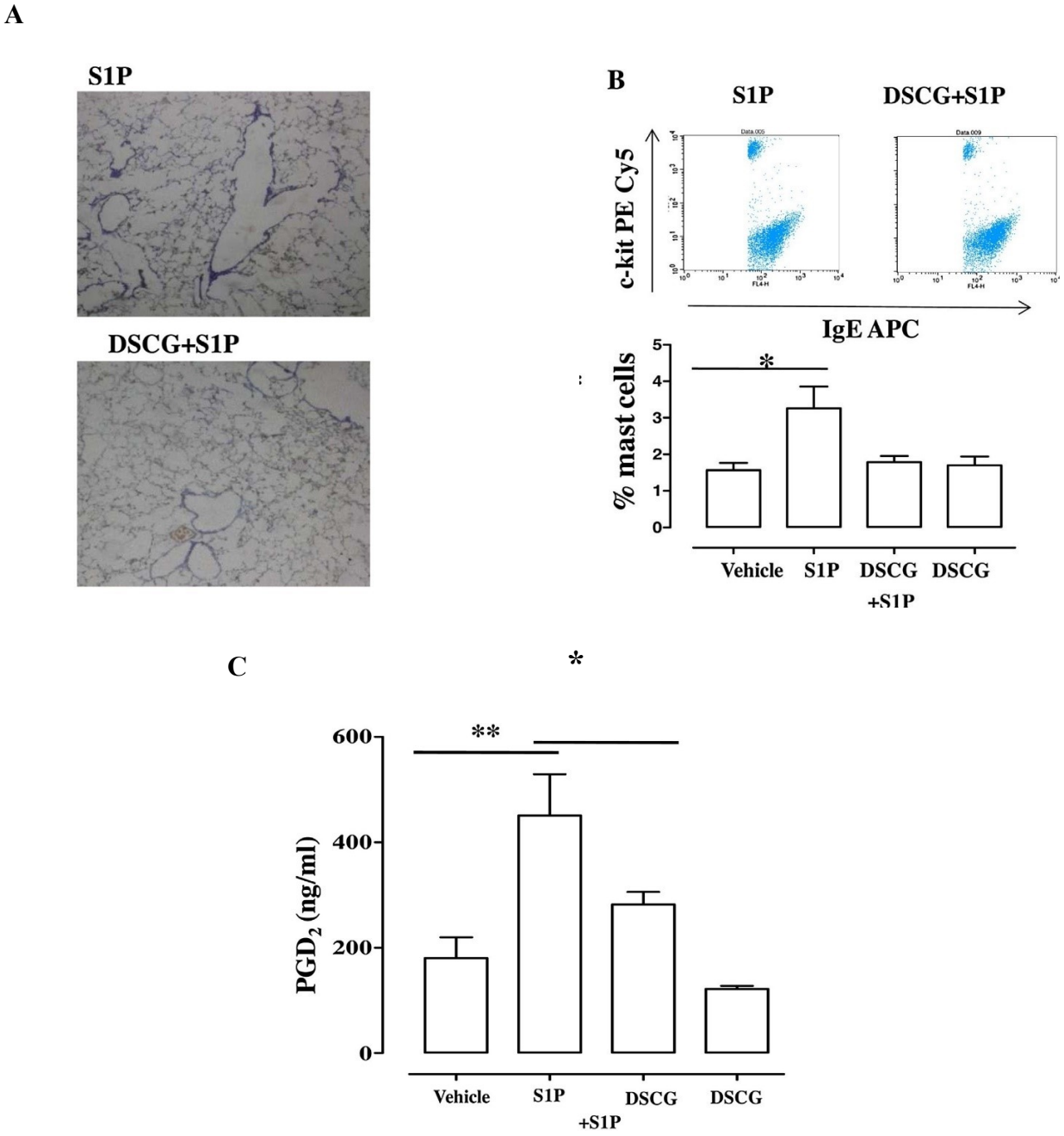

Figure3.1.3: DSCG reverses mast cell recruitment induced by S1P.

(A) Illustrative images of Toluidine blue staining on formalin-embedded lung sections captured under light microscopy at 10X magnification. (B) Quantification of lung mast cells identified as CD11+cKit+IgE+ positive cells by flow cytometry at 14 days following S1P administration, as exposed in dot plot (*p<0.05 vs vehicle, one-way ANOVA with Bonferroni's post-test). (C) At 14 day, bronchoalveolar lavage (BAL) was collected and PGD_2 levels were determined by specific ELISA (**p<0.01 vs vehicle, *p< 0.05 vs S1P one-way ANOVA with Bonferroni's post-test). Data are mean ± SEM, n=6 mice in each group.

3.1.4 Treatment with DSCG reduces CD23 expression in the lung in S1P challenged mice.

CD23 or FcεRII is the "low-affinity" receptor for IgE and it is found on mature B cells. CD23 is known to have an important regulatory role in IgE production. As previously demonstrated in our experimental model, S1P induces smooth muscle bronchial hyperreactivity by engaging mast cell recruitment associated with an increase in plasma IgE levels with an up-regulation of CD23 expression. To support this, pulmonary immunohistochemical detection of CD23 (Figure 3.1.4A) established an up-regulation after S1P exposure and a decrease in DSCG treated mice (Figure 3.1.4B). Again, similar quantification was made by using mast cell-deficient Kit $^{W\text{-}Sh/W\text{-}sh}$ mice. 0 and after 7 days, mast cell-deficient Kit $^{W\text{-}Sh/W\text{-}sh}$ mice received subcutaneous (s.c.) administration of S1P (10ng) or vehicle (BSA 0.001%). Lung harvested from Kit $^{W\text{-}Sh/W\text{-}sh}$ mice did not show any increment in CD23 expression following S1P (Figure 3.1.4C). To better summarized the beneficial action of DSCG, we carried out the flow cytometry analysis on the whole lung at 14 days following the S1P challenge. We observed a total number reduction of CD23 expression on both CD4 and CD8 T cells (Figure 3.1.4D-E) and B cells (Figure 3.1.4F) after pharmacological treatment with DSCG. All this data confirms a direct correlation with mast cells/ IgE/CD23 signaling that driving the effects of S1P in the airways and the beneficial effects of DSCG treatment.

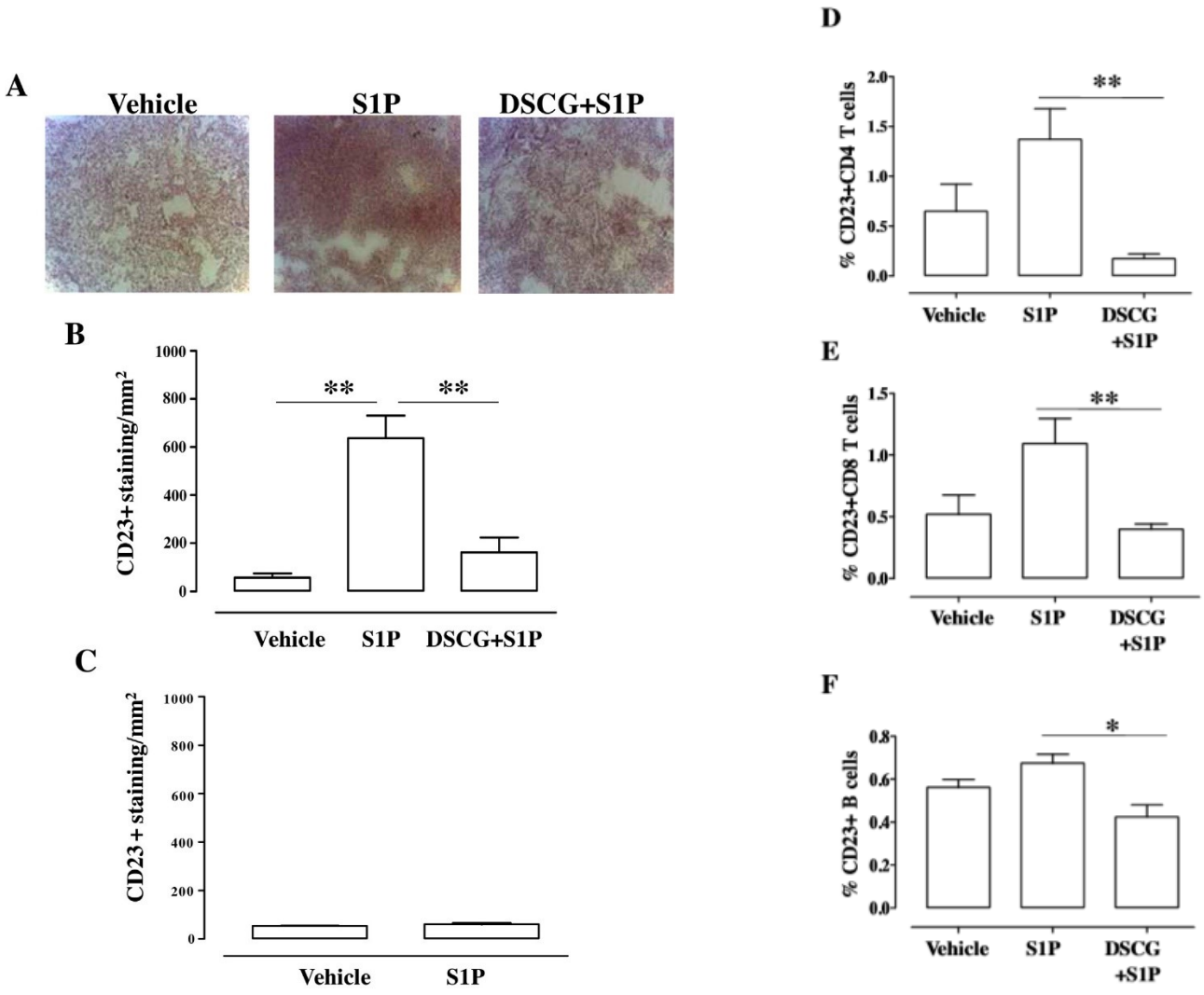

Figure3.1.4: Effect of DSCG on CD23 expression in the lung.

(A)Immunohistochemical detection of CD23 was made on lung sections harvested from mice treated with vehicle, S1P or DSCG+S1P. Lung images were captured under light microscopy at 10X magnification. (B) CD23 positive staining was quantified by comparison with the total area of the lung section. For each animal in each treated group was considered, at least, five sections (**p< 0.01 vs vehicle, **p< 0.01 vs S1P, Student's *t*-test). (C) CD23 quantification on lung sections of mast cell-deficient Kit $^{W\text{-}Sh/W\text{-}sh}$ mice treated with S1P or vehicle. CD23 was detected by using anti-CD23-PE by flow cytometry. CD23 expression was reduced on CD4+ T cells (D), CD8+ T cells (E) and B cells (F) on lung harvested from DSCG+S1P treated mice compared to S1P treated mice (*p< 0.05, **p< 0.01 vs S1P, Student's *t*-test). Data are mean ± SEM, n=6 mice in each group.

3.2 TLR4 contributes to the effects of S1P in airways

3.2.1 Systemic administration of S1P does not induce bronchial hyperreactivity in C3H/HeJ (Tlr4^{Lps-d}) mice.

In order to investigate how and what are the molecular mechanisms underlying the onset of the effects of S1P on the respiratory system, we used a specific animal strain: C3H/HeJ (Tlr4^{Lps-d}) mice. Following exposure to S1P bronchial reactivity was measured in BALB/c mice and C3H/HeJ (Tlr4^{Lps-d}) mice. Subcutaneous administration of S1P in two specific time-point (Figure 3.2.1A) induces bronchial hyperresponsiveness. In bronchi rings carbachol-induced concentration-dependent bronchoconstriction, which reached a maximum value at a concentration of 30 μM in control mice, while this effect was significantly increased after S1P challenged in BALB/c mice shifting the dose-effect curve of carbachol to lower concentrations (Figure 3.2.1E). The development of airway hyperreactivity is associated also with pulmonary inflammation as an increment in the percentage of dendritic cells (DCs) (Figure 3.2.1B) and macrophage into the lung of BALB/c mice (Figure 3.2.1C) and reduction of the percentage of DCs in mediastinal lymph node (Figure 3.2.1D). All these effects were absent when C3H/HeJ (Tlr4^{Lps-d}) mice have undergone the same treatments (Figure 3.2.1E).

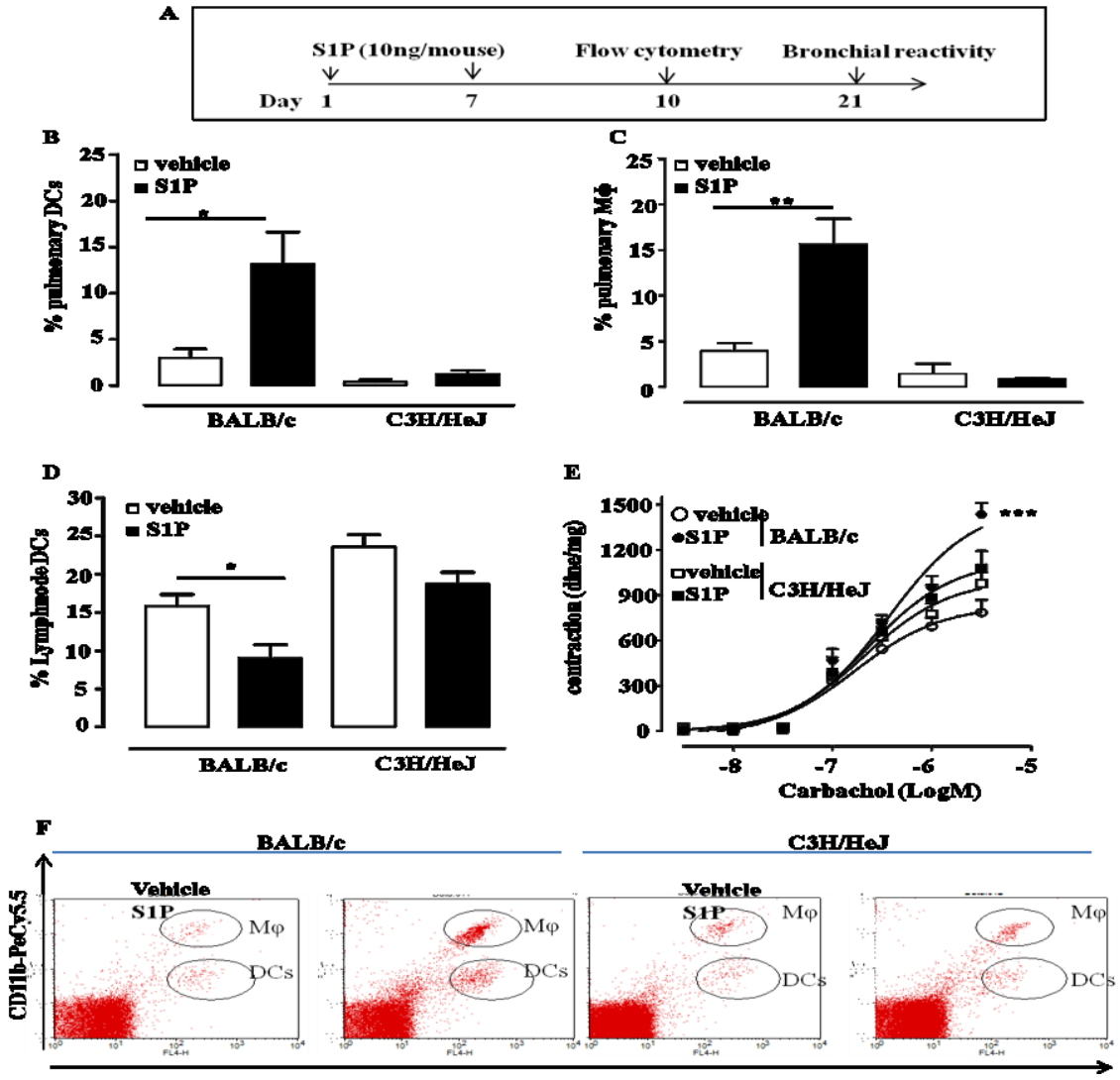

Figure3.2.1: S1P-induced bronchial hyperreactivity is abrogated in C3H/HeJ (Tlr4^{Lps-d}) mice.

(A) Experimental protocol: 0- and 7-days, BALB/c and C3H/HeJ (Tlr4^{Lps-d}) mice received s.c. S1P (10ng) or vehicle (BSA 0.001%). After 10 days flow cytometry analysis was performed: pulmonary and lymph node dendritic cells (DCs) (B-D) were identified as CD11c+CD11^{int} F4/80^{-} cells and macrophage (MΦ) as CD11c+CD11^{int} F4/80^{+} cells (C). macrophage and dendritic cells were quantified after 10 days following S1P administration (*p< 0.05, **p< 0.01 vs vehicle, Student's *t*-test). (E) Assessment of bronchial reactivity to carbachol after 21 days to S1P exposure (*** p< 0.001 vs vehicle, two-way ANOVA with Bonferroni's post-test). Data are mean ± SEM, n=6 mice in each group.

3.2.2 Pharmacological treatment with TLR4 antibody in BALB/c mice inhibits airway hyperreactivity, lung resistance and inflammation by S1P.

In order to investigate the role of TLR4 in S1P-induced airway disfunction, we used a pharmacological treatment with TLR4 neutralizing antibody. Pre-treatment with purified anti-TLR4 to S1P-treated BALB/c mice prevented airway smooth muscle hyperresponsiveness lung resistance (Figure 3.2.2A) as well as mucus production by PAS staining (Figure 3.2.2B).

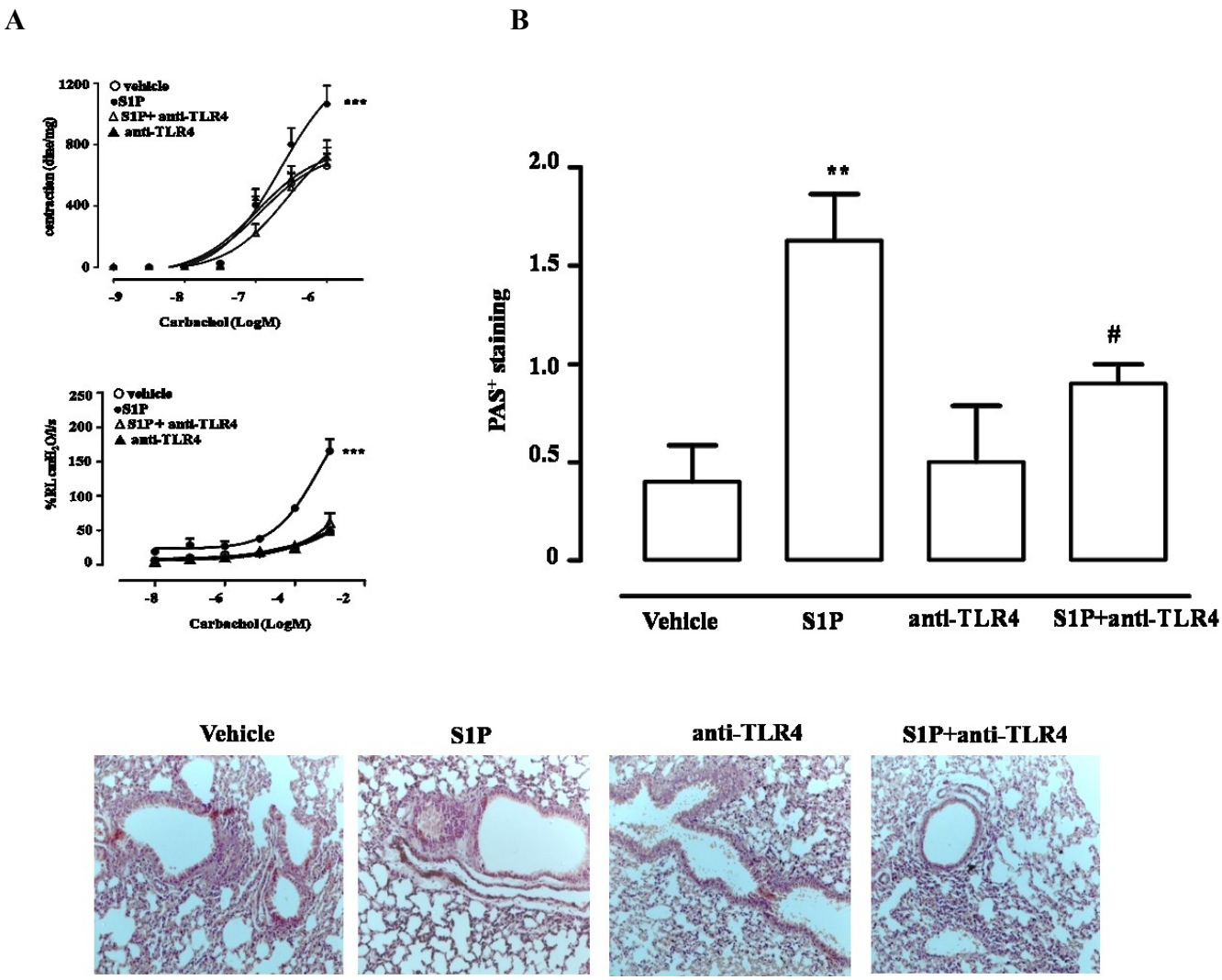

Figure3.2.2: Anti-TLR4 attenuates S1P-mediated effects on the airway.

(A) BALB/c mice received intraperitoneally anti-TLR4 (10µg) 30 minutes before S1P on days 0 and 7. Mice were sacrificed on day 21. Bronchial response and lung resistance to carbachol were evaluated (*** p< 0.001 vs vehicle, two-way ANOVA with Bonferroni's post-test). (B) Periodic acid/Alcian blue/Schiff staining was made on lung sections from mice treated with vehicle, S1P, anti-TLR4 or S1P+anti-TLR4.Quantification of PAS-positive staining with arbitrary scores 0 to 4 to describe low to severe lung inflammation in the following manner: 0:<5%; 1: 5-25%; 2: 25-50%; 3: 50-75%; 4: >75% positive staining/total lung area (**p<0.01 vs vehicle, #p<0.05 vs S1P, Student's t-test). Data are mean ± SEM, n=6 mice in each group.

3.2.3 Intranasal instillation with Lipopolysaccharide (LPS) exacerbates the effects of S1P on airway function.

In order to amplify and elucidate our observations since the role of TLR4 in S1P airway signaling, BALB/c mice and C3H/HeJ ($Tlr4^{Lps\text{-}d}$) mice were treated with intranasal instillation of LPS (0.1μg/mouse) at 0 and after 8 days (Figure 3.2.3A). Administration of LPS induced a significant increase in bronchial reactivity to cumulative concentration-response to carbachol when compared to control mice. In addition, the simultaneous administration of S1P and LPS in BALB/c mice increases, even more, the response to carbachol compared to mice when treated separately with S1P or LPS (Figure 3.2.3B). All these experimental applications did not induce any effect on bronchi harvested from C3H/HeJ ($Tlr4^{Lps\text{-}d}$) mice (Figure 3.2.3C). Ex-vivo bronchial reactivity experimental data are supported by immunohistochemical quantification of mucus production in lung harvested from each treated group mice (data not show). Lungs from BALB/c mice receiving co-administration of S1P+LPS displayed a significantly higher alteration of lung structure than vehicle or mice treated separately with S1P and LPS.

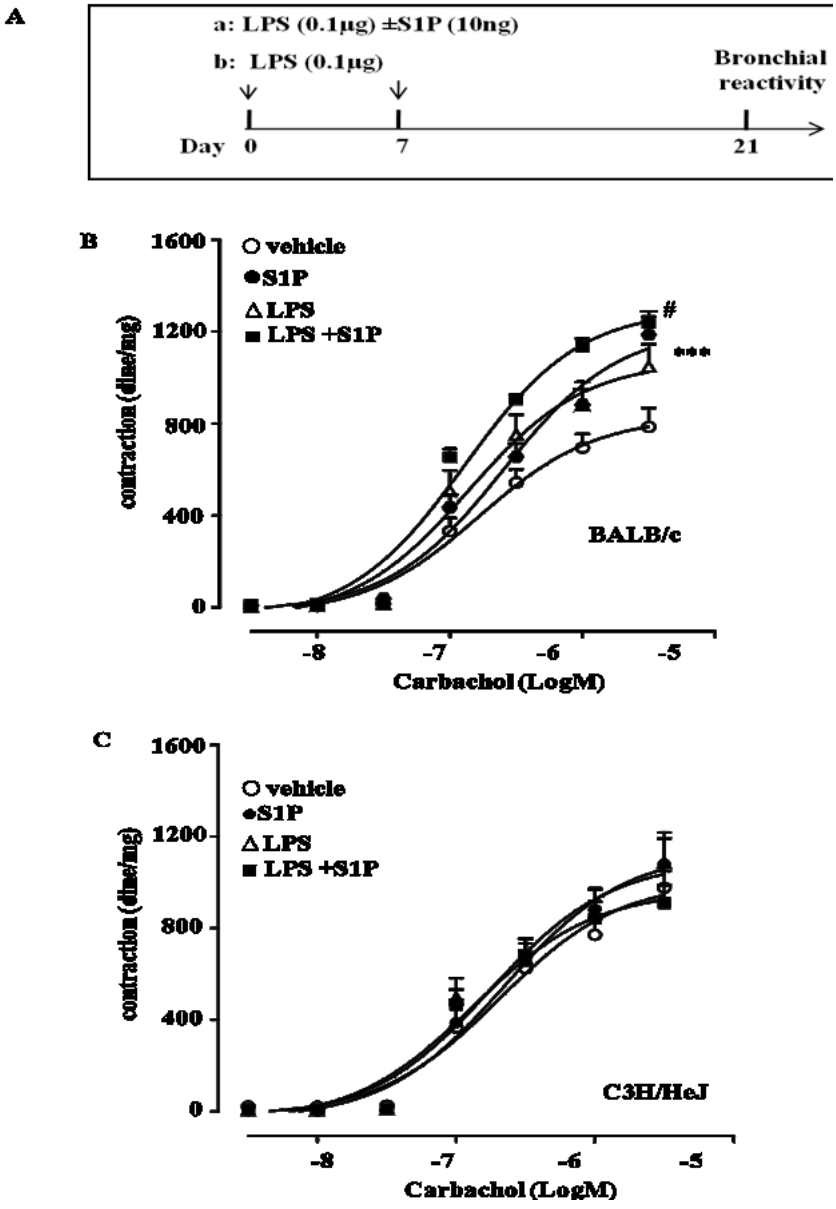

Figure 3.2.3: LPS emphasizes all the effects of S1P on the lung.

(A) An experimental treatment: BALB/c or C3H/HeJ ($Tlr4^{Lps\text{-}d}$) mice received intranasal instillation of LPS (0.1µg/mouse) alone or in association with S1P on days 0 and 7. Bronchial reactivity measurement was evaluated after 21 days of treatment (*** $p< 0.001$ vs vehicle, $^{\#}p<0.05$ vs S1P two-way ANOVA followed Bonferroni's post-test). Data are mean ± SEM, n=6 mice in each group

3.2.4 S1P increases TLR4 but not S1P1 expression in BALB/c mice and promotes S1P1/TLR4 association.

Given that S1P1 receptor is a key regulator of endothelial cell (EC) barrier integrity [121]and considering the role of those cells in the regulation of pulmonary inflammation[122], we tested the hypothesis if there is a correlation between S1P1 and TLR4 following S1P challenge. We have evaluated the expression of TLR4 and S1P1 on homogenized bronchi and lung from S1P or vehicle-treated BALB/c mice. Western blot analysis demonstrated an up-regulation of TLR4 in bronchi harvested from S1P1-treated mice compared to the vehicle but not for the S1P1 receptor (Figure 3.2.4B). In support, immunohistochemical analysis for TLR4 quantification on lung sections confirms a significant increase in TLR4 positive staining in S1P-treated mice compared to vehicle mice (Figure 3.2.4A). Interestingly, immunofluorescence staining on paraffin-embedded lung sections evidenced an increase in the number of TLR4 positive cells on mice received the co-administration LPS+S1P and showing co-localization TLR4/S1P1following exposure to S1P (Figure 3.2.4D). Also, immunoprecipitation for S1P1 confirm the interaction with TLR4 in the lung after S1P exposure (Figure 3.2.4C). These data, taken together, suggest that S1P exerts a positive action on TLR4 signaling in innate immune response as well as in allergy.

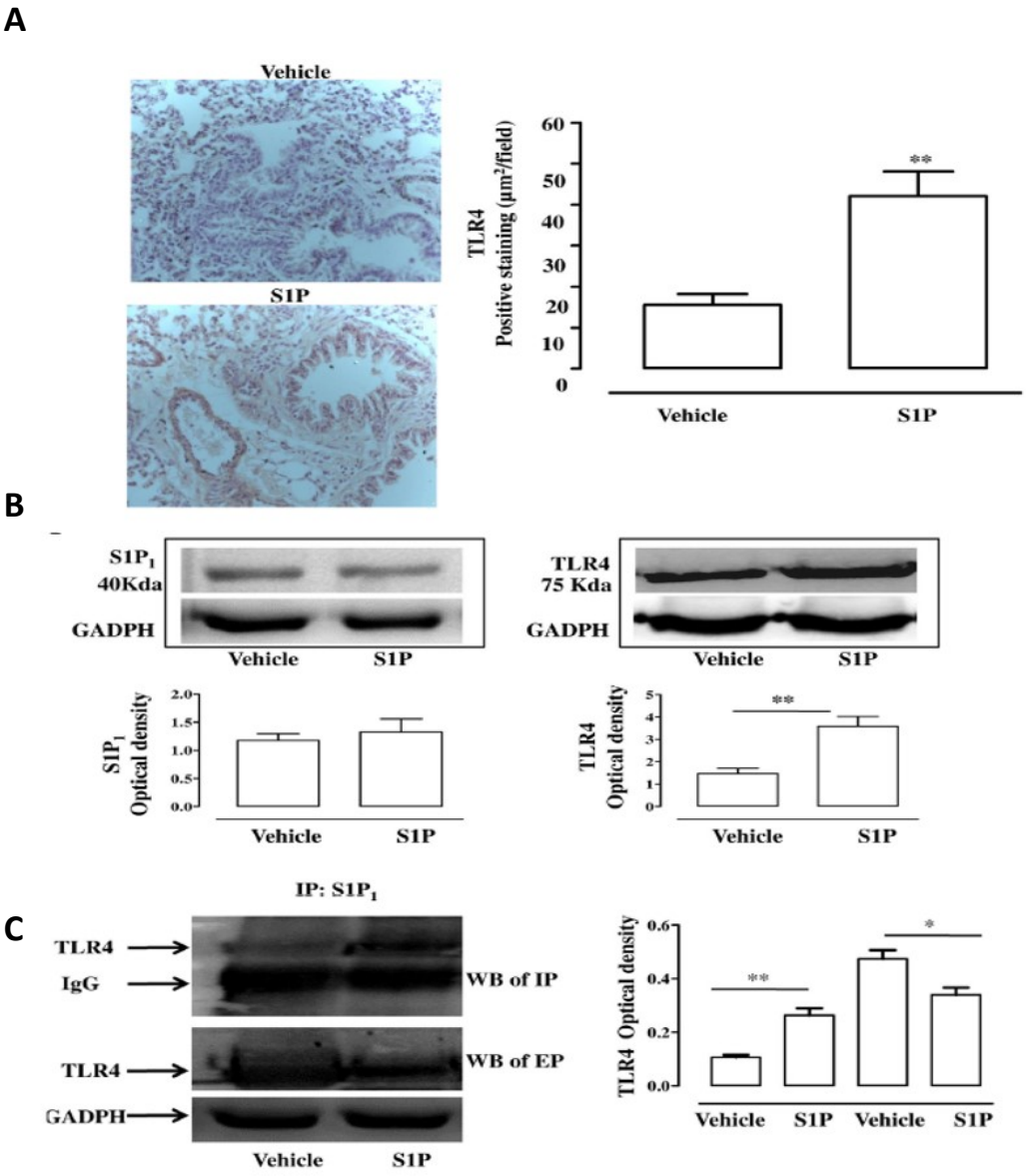

Figure 3.2.4: S1P increases TLR4 expression and promotes S1P1/TLR4 association.

(A) Immunohistochemical quantification for TLR4 in lung sections of S1P or vehicle BALB/C treated mice. Lung images were captured under light microscopy at 40X magnification. (B)Western blot for TLR4 and S1P1 expression on total cell bronchi lysates. Corresponding densitometric quantification normalized to GADPH housekeeping. (C) Western blot of TLR4 in lung lysates cells immunoprecipitated with S1P1 and in the eluted fraction (EP). Densitometric quantification normalized to IgG or GADPH expression respectively for IP and western blot. (*p<0.05; **p<0.01 vs vehicle, Student's t-test).

D

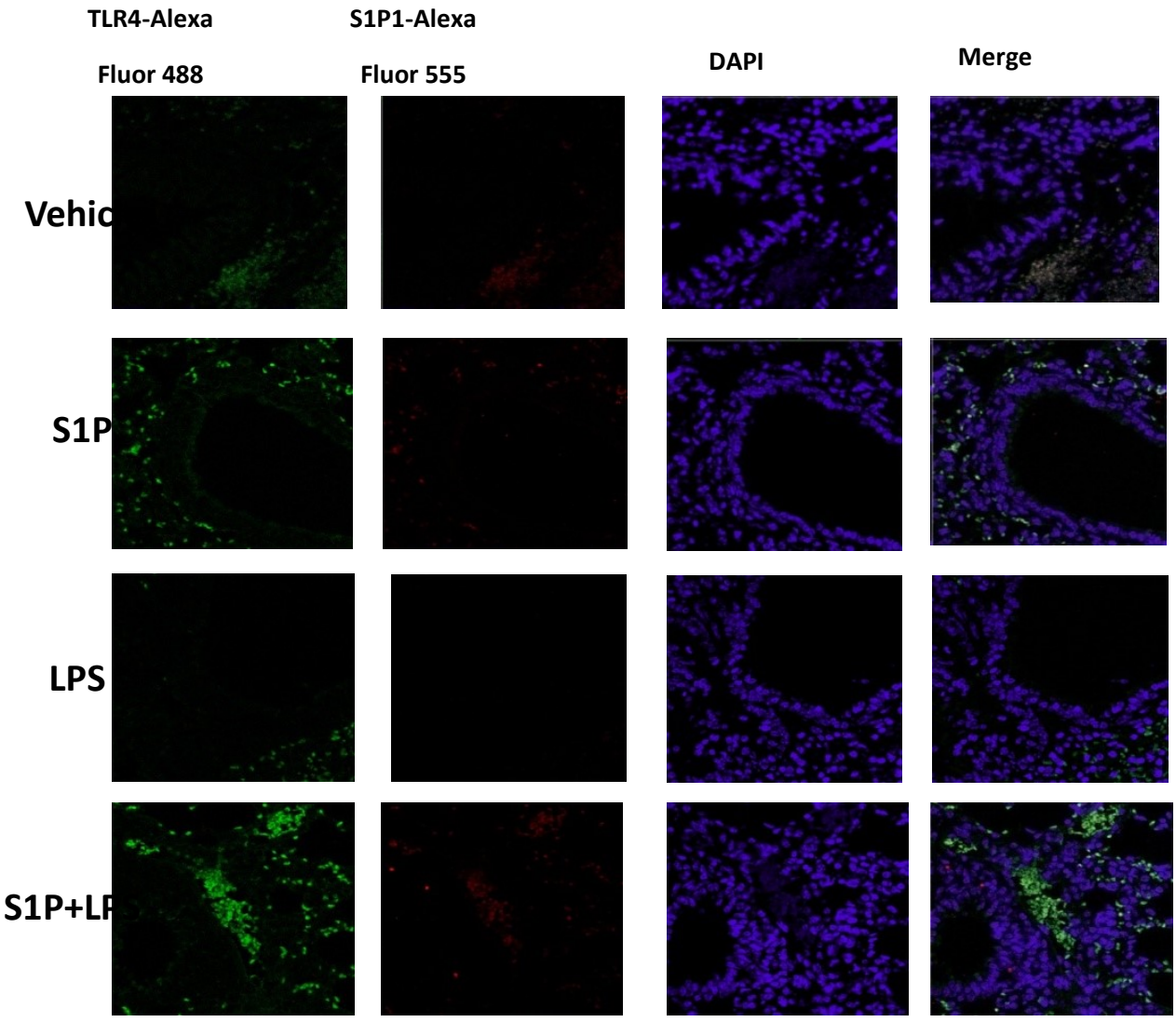

Figure 3.2.4: S1P increases TLR4 expression and promotes the S1P1/TLR4 association.

(D) Representative confocal immunofluorescence images for TLR4-AlexaFluor 488, S1P1-AlexaFluor 555 and DAPI on lung section harvested from BALB/c mice treated with vehicle, S1P, LPS or S1P+LPS association. Lung images were observed and captured with Carl Zeiss confocal microscopy at 40X magnification.

3.3 The contribute of S1P signaling in a mouse model of mild COPD

3.3.1 Smoking mice develop progressive airway disfunction

C57BL/6 mice were exposed to cigarette smoke or room air. Airway function was assessed evaluating both bronchial reactivity and lung resistance after carbachol challenge. Bronchi harvested from mice exposed for 9 months to cigarette smoke showed an increased but not significant in bronchial reactivity to carbachol in comparison to control mice, reaching the maximal effect after 11 months to the same continuous exposure (Figure 3.3.1A). On the other hand, hypersensitivity to carbachol in lung resistance measured in anesthetized, tracheotomized and ventilated mice was already considerable evidence at 9 months relative to the first one (Figure 3.3.1B). Similarly, cumulative administration of S1P (10^{-8}-$3x10^{-5}$ M) on isolated control mouse bronchi does not induce any significant contraction up to 10^{-5} M but only at very high concentrations $3x10^{-5}$ M S1P produces a faint but not significant constriction. Conversely, when mice were exposed to cigarette smoke, S1P caused bronchial contraction was already present at a lower concentration than < 10^{-6}M. Additionally, bronchi harvested from mice exposed to cigarette smoke for 10 and 11 months showed a significant increase in the maximum S1P-induced contraction (Figure 3.3.1C). The same effects were observed in the measurement of lung resistance at the same time-point (Figure 3.3.1D). As we expect, in control mice cumulative concentration-response curve of S1P or carbachol did not change and did not cause any contraction all the time.

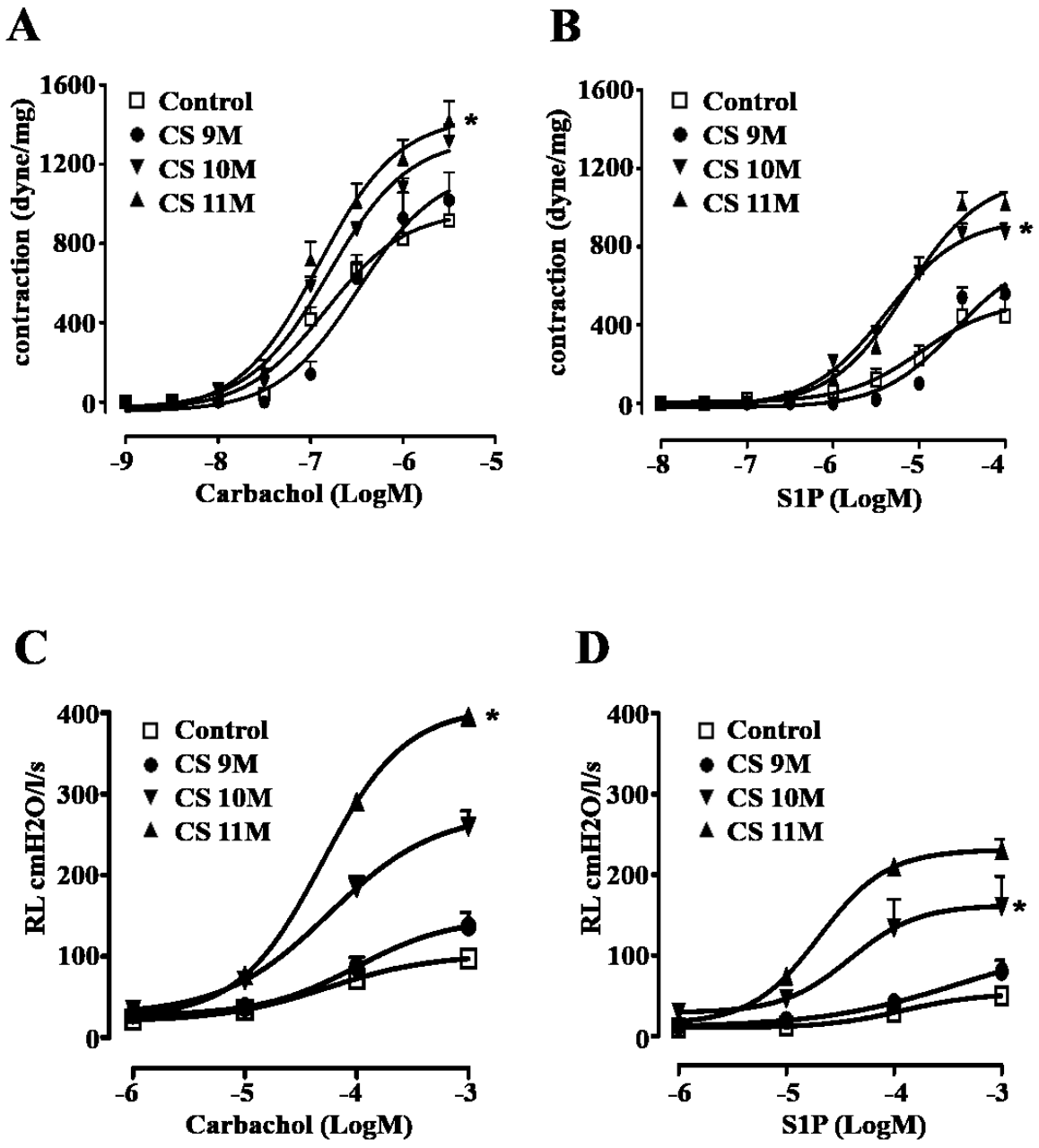

Figure 3.3.1 Cigarette smoke (CS) induces bronchial hyperreactivity and lung dysfunction.

C57BL/6 mice were exposed to cigarette smoke or air room (control) for 9, 10 and 11 months. *Ex-vivo* bronchial reactivity assessment to carbachol (A) or S1P (B). Lung resistances to carbachol (C) or S1P (D) were measured (* $p<0.05$ vs. vehicle, two-way ANOVA with Bonferroni's post-test). Data are mean ± SEM, n=6 mice in each group.

3.3.2 Progressive airway remodeling develops in cigarette smoking mice.

In order to evaluate if cigarette-smoke exposure also produces airway remodeling, immunohistochemical analysis for α smooth muscle actin (α-SMA) (Figure 3.3.2A-B) was assessed on lung paraffin-embedded sections demonstrating a tight layer of α-SMA positive staining in main and distal bronchi of mice chronically exposed to cigarette smoke. In our series, it was evaluated also collagen deposition by Masson's trichrome staining progressively increased during the chronic exposure of cigarette smoke (Figure 3.3.2 C-D).

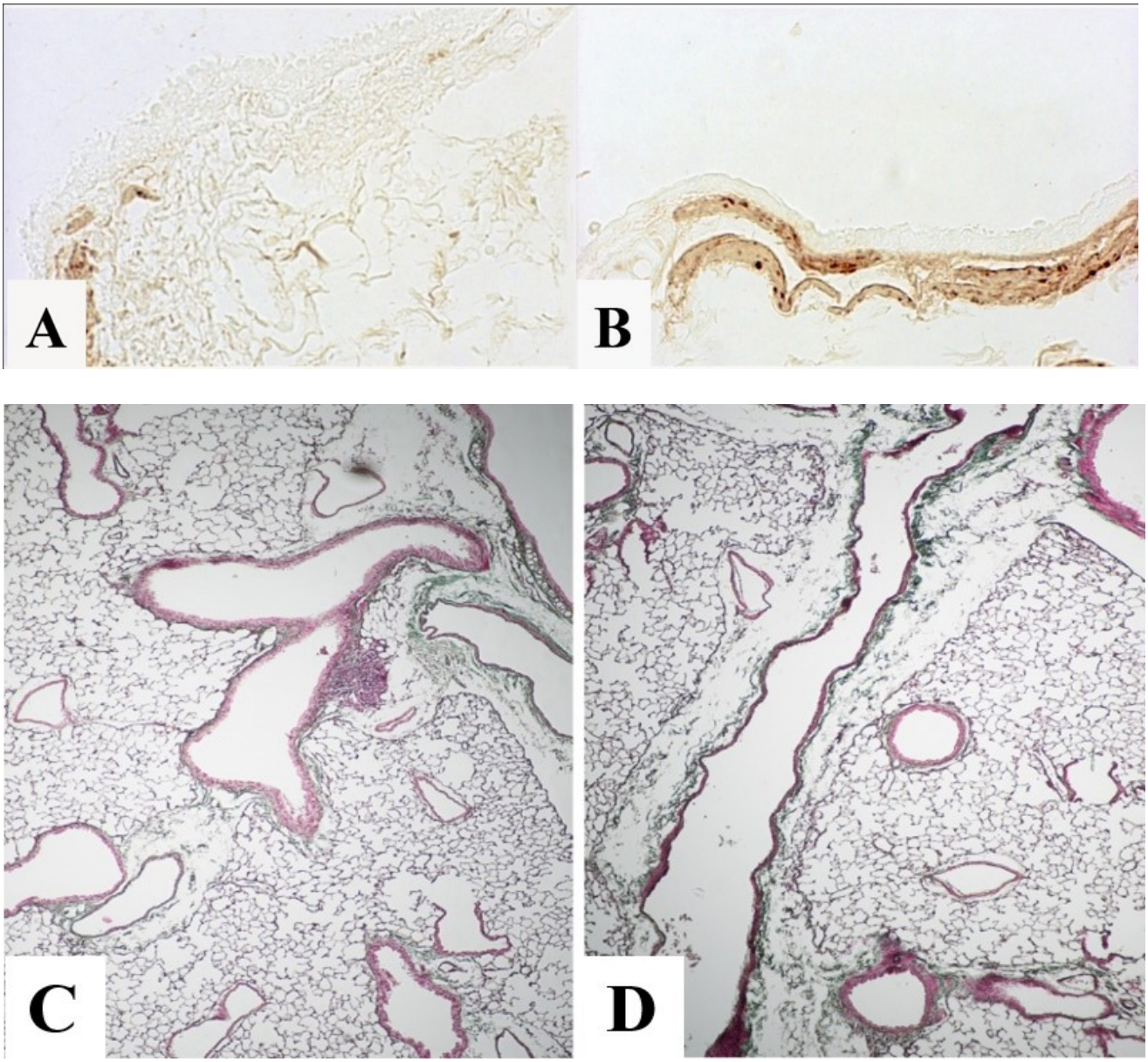

Figure 3.3.2: Cigarette smoke induces pulmonary α-SMA up-regulation and collagen deposition.

Immunohistochemical staining for α-SMA in lung paraffin-embedded sections of control mice(A) and smoking mice after 11 months of od treatment (B). Collagen deposition was determined by using Masson's trichome staining on lung paraffin-embedded sections from mice exposed to cigarette smoke for 10 (C) and 11 (D) months. Collagen deposition is evident around bronchioles and main bronchi. Were used n=6 mice in each group and lung images were captured under light microscopy at 40X magnification.

3.3.3 Role of SPK/S1P in smoking mice

To understand the contribution of S1P signaling in cholinergic bronchoconstriction as well in the control of bronchial tone, bronchial ring preparations were incubated with a selective sphingosine kinase inhibitor, SK-I, and a cumulative concentration-response curve of carbachol was performed. This pre-treatment of bronchial rings harvested from control and smoking mice up to 9 months does not induce any effect on carbachol-induced contraction (Figure 3.3.3A). However, incubation with SK-I inhibitor on bronchi from mice exposed to cigarette smoke for 10 (Figure 3.3.3B) and 11 months (Figure 3.3.3C) prevents the increment of reactivity to carbachol-contraction. All this data was confirmed by measuring the lung resistance in the same experimental condition (Figure 3.3.3 D)

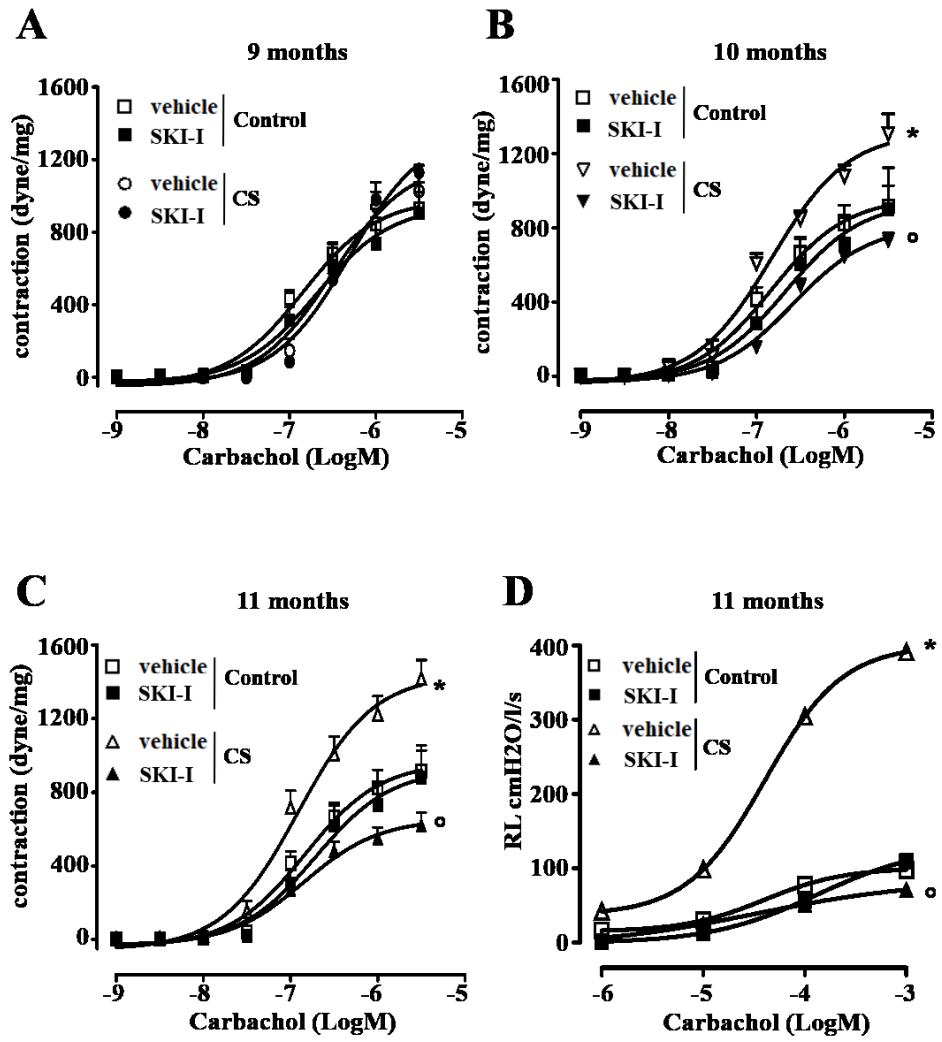

Figure 3.3.3: Pharmacological treatment with sphingosine kinases inhibitor (SK-I) reverts airway hyperreactivity induced by cigarette smoke.

Pre-incubation of sphingosine kinases inhibitor (SK-I; 30min; 10μM) and successive assessment of bronchial reactivity to carbachol in isolated bronchi harvested from control mice and mice exposed to cigarette smoke for 9 (A), 10 (B) and C (11) months. Lung resistance to carbachol was evaluated in control mice or 11 months of cigarette smoke exposure (CS) after administration of SKI-I inhibitor bolus in the pulmonary artery (D). (* $p<0.05$ vs. control vehicle, °$p<0.05$ vs CS vehicle, two-way ANOVA with Bonferroni's post-test). Data are mean ± SEM, n=6 mice in each group.

3.3.4 Modulation of S1P receptors interfering with airway function in smoking mice.

Precedent functional studies suggest an important role for sphingosine kinases in controlling of airway hyperreactivity and lung inflammation in a well-know murine model of COPD. To explore the exact molecular mechanisms of S1P pathway in the control of cigarette smoke-induced airway hyperresponsive, bronchial rings were pre-incubated with S1P2 (JTE-013) or S1P3 (TY52156) receptor antagonists and then exposed to the cumulative concentration-response curve of S1P (10^{-8}-$3x10^{-5}$ M) (Figure 3.3.4A-B). This *in vitro* treatment abrogated S1P-induced contraction on bronchi of smoking mice. Accordingly, the same results were obtained by using a bolus administration of each antagonist in the pulmonary artery ad then evaluated the lung resistance in an isolated and perfused mouse lung preparation (Figure 3.3.4C-D). Immunohistochemical analysis confirms the up-regulation of S1P pathway, showing increased expression of S1P2 and S1P3 in lung sections from smoking mice when compared with control mice (Figure 3.3.4E-F-G). The role of S1P pathway in the development of airway hyperresponsiveness and lung dysfunction in smoking mice, in perfect tune with our molecular and functional studies, was also investigated by measurement of S1P levels using a specific ELISA kit. We found a significant increase in S1P levels in the lung from smoking mice at 11 months when compared to control mice (Figure 3.3.4H).

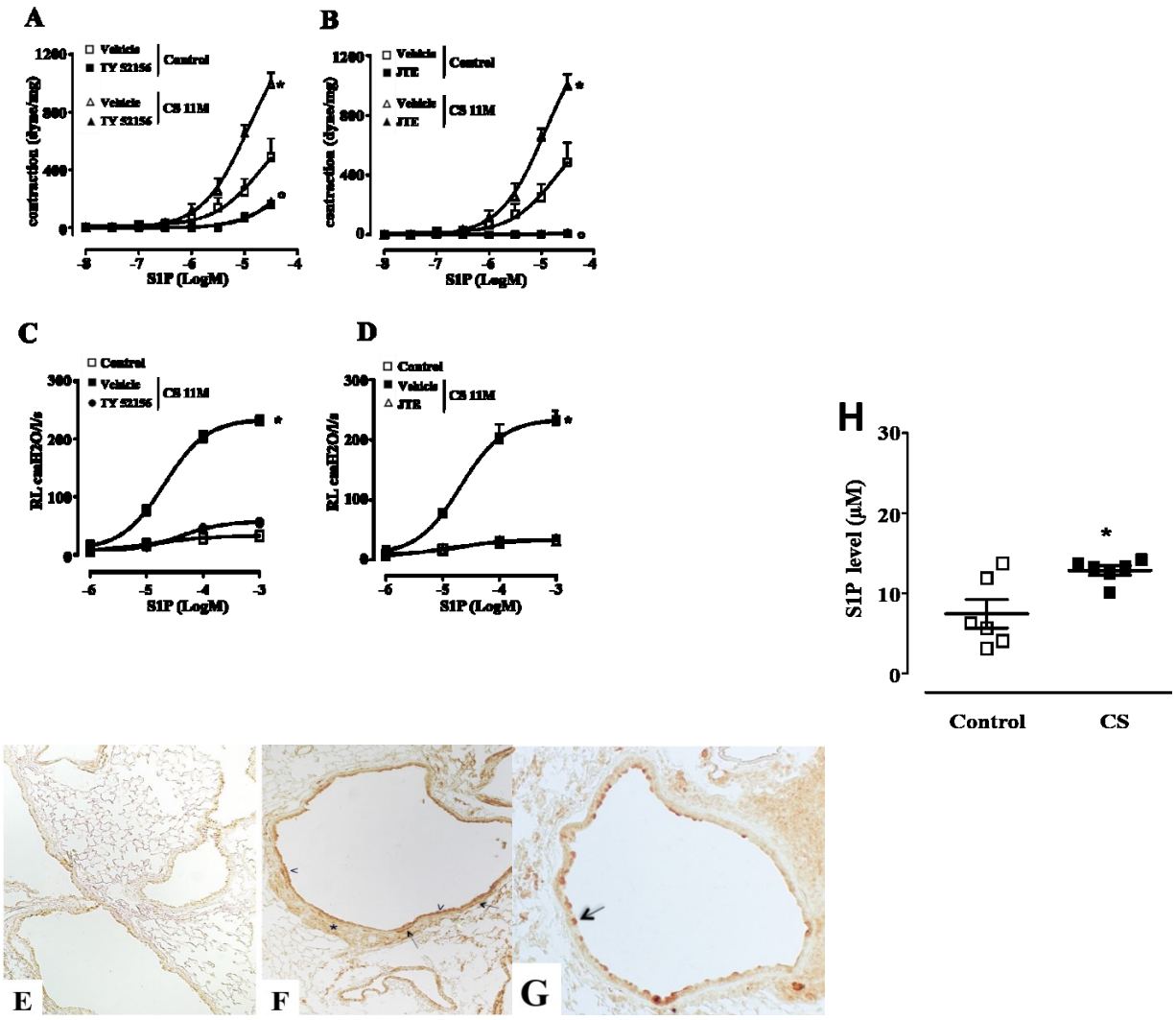

Figure 3.3.4: S1P2 and S1P3 are involved in S1P effects on the airway.

Isolated bronchi from control mice and mice exposed to cigarette smoke (CS) for 11 months were *in vitro* pre-treated with S1P3 antagonist (10µM) (A) or S1P3 antagonist JTE-013 (10µM) (B) before cumulative concentration-curve of S1P. Lung resistance to S1P was also measured after the administration of TY-52156 (C) or JTE-013 (D). (* $p<0.05$ vs. control vehicle, °$p<0.05$ vs CS vehicle, # $p<0.05$ vs control +TY52156 or JTE, two-way ANOVA with Bonferroni's post-test). Representative immunostaining images in smoking mice at 11 months for S1P2 (F) or S1P3(G) and control mice (E). Lung images were captured under light microscopy at 40X magnification. (H) Lungs from control mice and mice exposed to CS for 11 months were collected and homogenate with 1U/ml collagenase. Levels of S1P were determined with specific ELISA kit (* $p<0.05$ vs control; Student's t-test). Data are mean ± SEM, n=6 mice in each group.

3.4 Cross talk between S1P signaling and epithelial-mesenchymal transition (EMT) process

3.4.1 S1P is involved in the fibroproliferative process

Female BALB/c mice injected with S1P develop bronchial hyperresponsiveness (AHR) and lung hyperplasia in a time-dose dependent manner (Figure 3.4.1A). These effects are coupled with an increase in the lung of TGF β (Figure 3.4.1B), IL-33 (Figure 3.4.1C) and FGF-2 (Figure 3.4.1C) in a time-dependent manner. Interestingly, at 14 days after S1P challenge flow cytometry analysis on bronchi from S1P-treated mice displayed an increase in the expression of mesenchymal markers to epithelial one compared with control mice (Figure 3.4.1E). We have been exanimated two different markers: CD90, a mesenchymal marker and CD326 marker expressed on epithelial cell adhesion molecule. In connection with this data, fibroblasts isolated from the lung of S1P or vehicle-treated BALB/c mice showed an up-regulation of α-SMA expression after S1P exposure (Figure 3.4.1G). In addition, a significant increase occurs also in the proliferative rate in the cells from S1P treated mice compared to vehicle by using MTT assay (Figure 3.4.1.H).

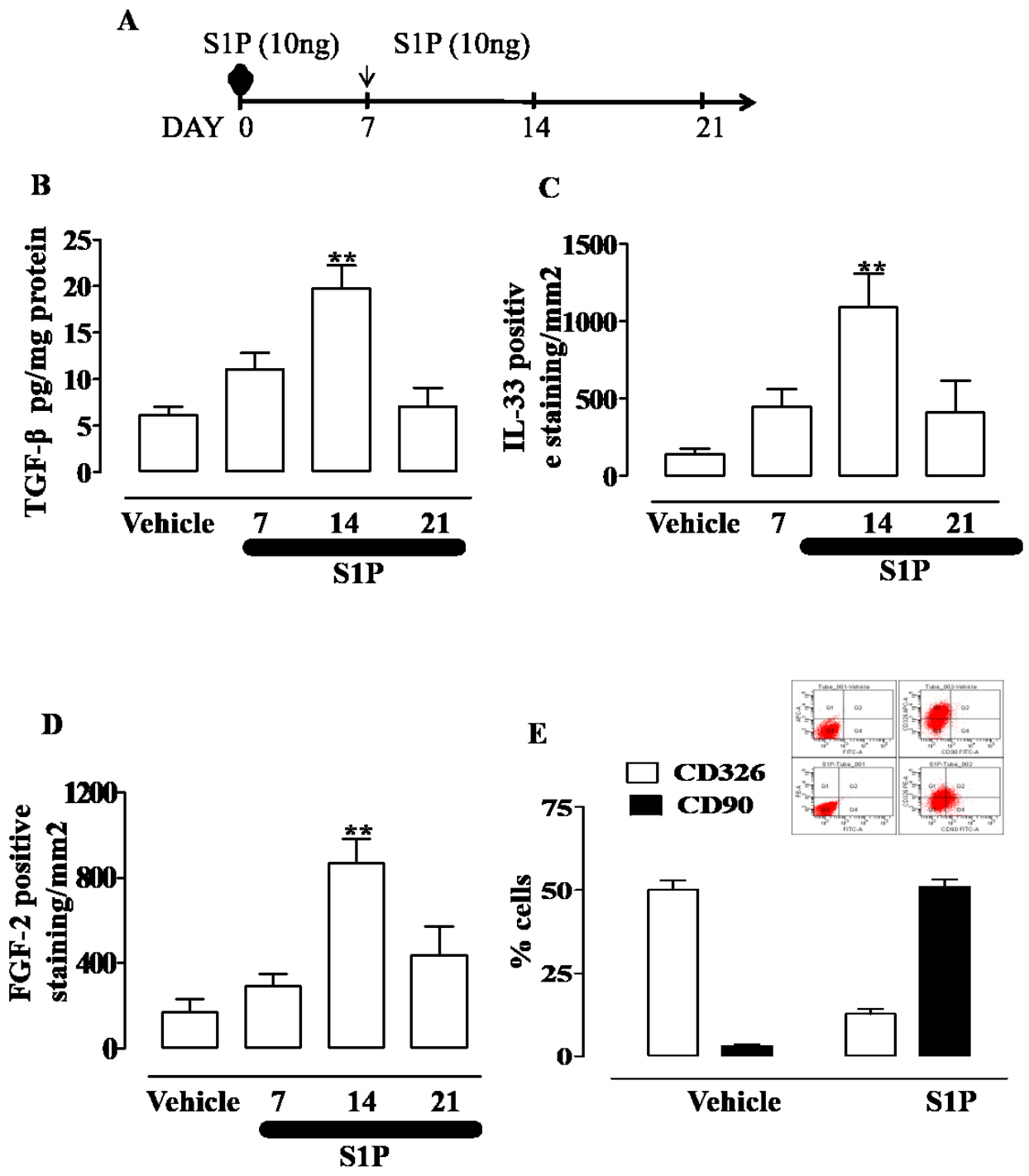
A
S1P (10ng)
S1P (10ng)
DAY 0
7
14
21
B
TGF-β pg/mg protein
25
20
15
10
5
0
**
Vehicle
7
14
21
S1P
C
IL-33 positive staining/mm2
1500
1000
500
0
**
Vehicle
7
14
21
S1P
D
FGF-2 positive staining/mm2
1200
800
400
0
**
Vehicle
7
14
21
S1P
E
CD326
CD90
% cells
75
50
25
0
Vehicle
S1P

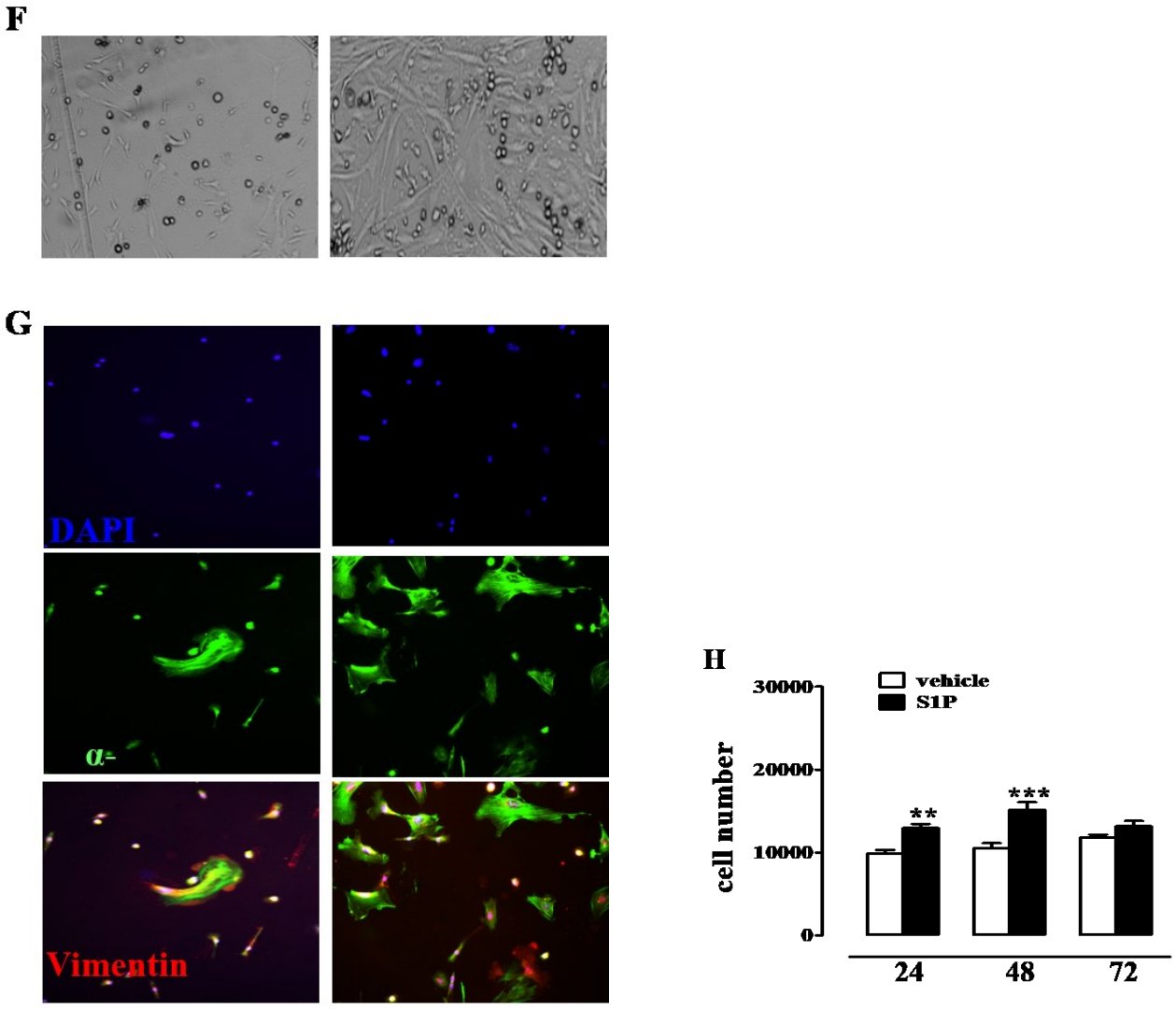

Figure 3.4.1: Systemic administration of S1P induces a fibroproliferative environment in the lung.

(A)Female BALB/c mice received subcutaneous administration of S1P (10ng) or vehicle (BSA 0.001%) at days 0 and 7. Mice were sacrificed at 7,14 and 21 days. (B) Lungs were collected and homogenate with 1U/ml collagenase. TGF β levels were measured by using specific ELISA (** $p<0.01$ vs. vehicle Student's t-test). Immunohistochemical quantification for IL-33 (C) and FGF-2 (D) on lung sections (** $p<0.01$ vs. vehicle Student's t-test). At 14 days, isolated bronchi from the vehicle and treated mice were used for flow cytometry analysis (E) of CD326 (epithelial marker) and CD90 (mesenchymal marker). (F) Morphology and proliferation of fibroblast isolated from lungs of vehicle and S1P treated mice at 14 days. (G) Immunofluorescence staining on isolated cells for fibroblast differentiation by using α-SMA and counterstain with DAPI. (H) Fibroblast proliferation was measured with MTT assay after 24, 48 AND 72h to S1P exposure. (**$p<0.01$ vs vehicle; ***<0.001 vs vehicle). Data are mean ± SEM, n=6 mice in each group.

3.4.2 S1P promotes epithelial-mesenchymal transition (EMT) in mouse airway.

The involvement of S1P in EMT process has been confirmed also from molecular studies. RT-PCR performed on bronchi harvested from both vehicle and S1P treated mice, at 14 days after S1P challenge, showed an increase in mRMA levels of type I (COL1A1) and type III (COL3A1) collagens as myofibroblast and EMT markers, respectively (Figure 3.4.2C-D). Also, the transcriptional regulators of EMT such as TWIST and SNAIL significantly increase at 14 days in S1P treated mice (Figure 3.4.2A-B). This improvement well linked to the development of cardinal features of severe asthma induced by S1P in mice.

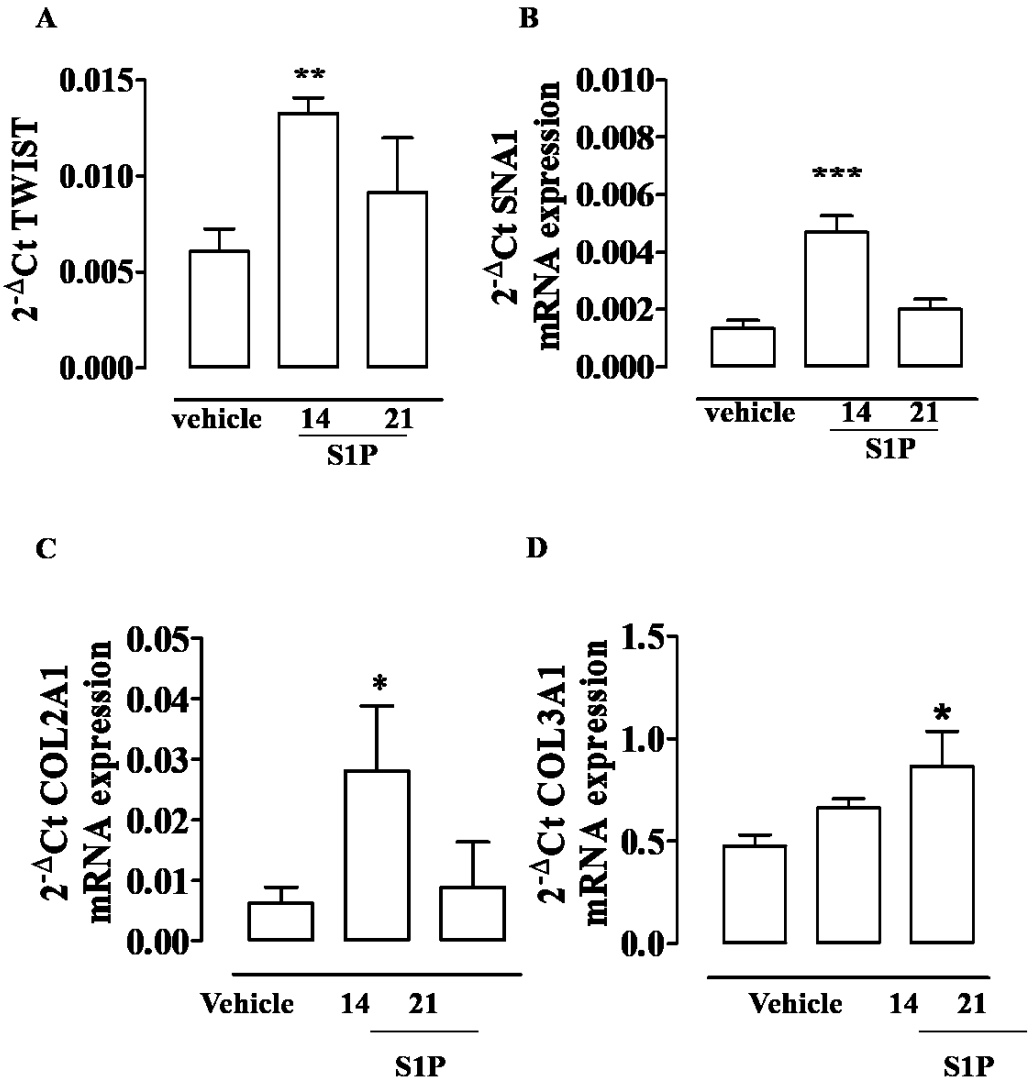

Figure 3.4.2: S1P promotes EMT in bronchi.

At 14 days, Bronchi harvested from mice treated with vehicle or S1P were used for molecular studies. mRNA expression levels of TWIST (A), SNAI 1 (B), COL2A1 (C) and COL3A1 (D) were measured by reverse-transcription polymerase chain reaction (qRT-PCR). Data are expressed as mean ± SEM and the results were normalized to glyceraldehyde-3-phosphate dehydrogenase (GAPDH) mRNA by using the $2^{-\Delta Ct}$ formula. (*p<0.05, **p<0.01 and ***p<0.001 *vs* vehicle). Data are mean ± SEM, n=6 mice in each group.

3.4.3 S1P shift epithelial-mesenchymal repertoire in mouse airway.

Further development was to analyzed other specific markers of both epithelial and mesenchymal cells on isolated bronchi from S1P treated mice. We observed a marked shift in epithelial markers to mesenchymal markers: vimentin, fibronectin 1 and α-SMA strongly increased in contrast to E-cadherin, cytokeratin, and ZO-1 that were reduced (Figure 3.4.3).

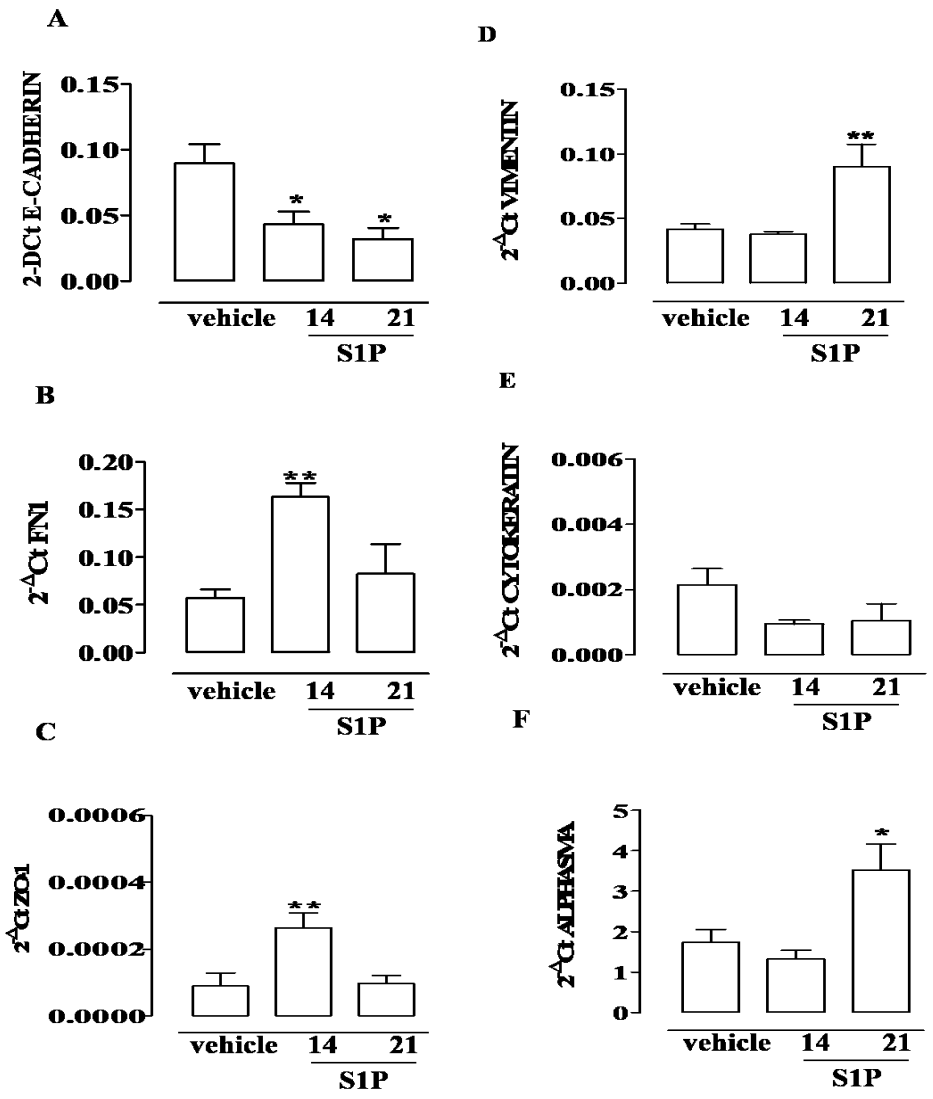

Figure 3.4.3: Shift from epithelial to mesenchymal morphology cells in the airway.

Main bronchi were harvested from mice treated with either the vehicle or S1P and sacrificed at 14 days. The markers changes were evaluated by qRT-PCR. mRNA expression levels of epithelial markers E-Cadherin (A), cytokeratin-1 (KRT1) (E) and ZOI-1 or mesenchymal vimentin (VIM) (D), fibronectin 1 (FN1) (B) and alpha-smooth muscle actin (α-SMA) (F) were measured. Data are expressed as mean ± SEM and the results were normalized to glyceraldehyde-3-phosphate dehydrogenase (GAPDH) mRNA by using the $2^{-\Delta Ct}$ formula (*p<0.05, **p<0.01 *vs* vehicle).

3.4.4 S1P promotes EMT activation in a TGF β-dependent manner in vitro model of epithelial cells

In vivo results suggest the ability of S1P to induce EMT. Next, we move on about *in vitro* studies in order to correlate the direct effect of S1P on epithelial cells. Starting with adenocarcinomic human alveolar basal epithelial cells (A549), we have demonstrated that A549 cells incubated with both S1P or TGF β shall obtain a fibroblast-like morphology characterized by elongated branched surrounding a central nucleus. When cells are cultured and incubated with LY2109761, an antagonist of the receptor of TGF β type I and II, the effects are reversed and restores the physiological pattern observed without any incubation (Figure 3.4.4A). Indeed, S1P increases the levels of mesenchymal marker CD90 and reduce the epithelial marker as CD326, in support with our *in vivo* data. Then, cell incubation with LY2109761 prior to TGFβ or S1P does not induce any effects (Figure 3.4.4B). Supplementary, immunofluorescence staining showed an up-regulation of vimentin and down-regulation of cytokeratin in both S1P or TGF β treated cells when compared to the control condition. Obviously, cells pre-treatment with LY2109761 prior to standard treatment reverse all previously observed effects (Figure 3.4.4C).

Overall these data indicate the direct action of S1P on epithelial cells in the epithelial-mesenchymal transition (EMT) process.

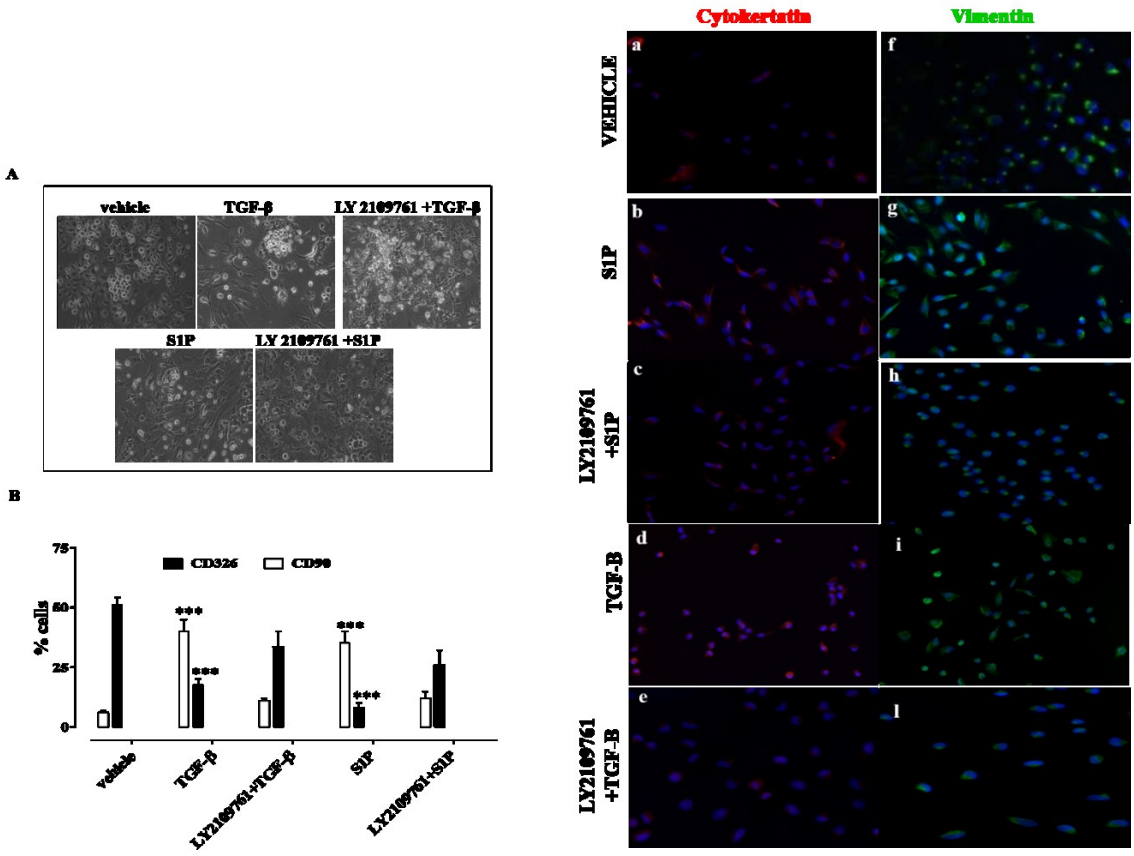

Figure 3.4.4: S1P-induced EMT *in vitro* is mediated by TGF-β.

(A) A549 cells were exposed to vehicle, TGF-β or S1P in the presence or absence of LY2109761 (antagonist of receptor type I and II of TGF-β) Morphological changes were assessed under light microscopy 20X. (B) Changes of CD326 (epithelial markers) and CD90 (mesenchymal markers) were evaluated utilizing flow cytometry. Data are expressed as mean ±SEM (***p<0.001 vs vehicle). (C) Immunofluorescence staining was made for the following markers: cytokeratin the epithelial marker (red fluorescence, left panels) and vimentin the mesenchymal markers (green fluorescence, right panels). Cells were photographed at 20X magnification.

3.4.5 TGF-β obligatory role in S1P-induced effects on airways.

In order to confirm the direct effect of S1P on EMT involves the TGF β signaling, we pretreated BALB/c mice with LY2109761 antagonist. Pharmacological treatment in this murine model S1P-induced bronchial hyperresponsiveness (AHR) is completely abrogated (Figure 3.4.5A) in addition to a reduction in mucus production detected by PAS staining and inhibition of cell infiltration by immunohistochemical analysis (Figure 3.4.5B). To consider whether the inhibitory action of LY2109761 on airway function translates into a modulation of EMT, flow cytometry analysis has been performed on main bronchi and clearly confirms the involvement of TGF β in the EMT action induced by S1P thought CD90 up-regulation and CD326 downregulation (Figure 3.4.5C).

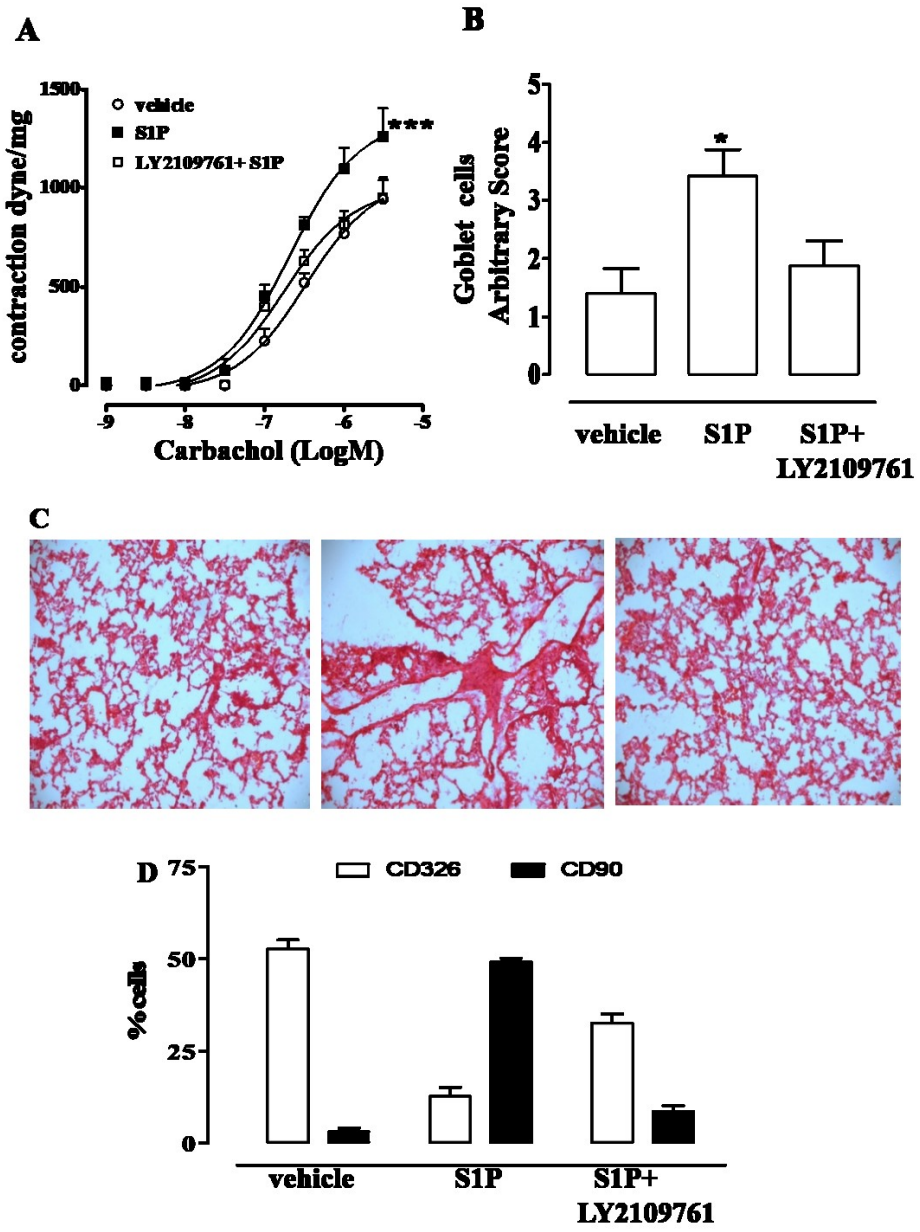

Figure 3.4.5: ***LY2109761 abrogates any effects induced by S1P on the airway.***

BALB/c mice were treated in vivo with vehicle, S1P or LY2109761 + S1P. (A) Bronchial reactivity to carbachol was assessed (*** P<0.001 vs vehicle, two-way ANOVA with Bonferroni's post-test). (B)The degree of inflammation was scored by using PAS staining**.** PAS-positive cryosections were analysed with scores 0 to 4 to describe low to severe lung inflammation as follows: 0: <5%; 1: 5 to 25%; 2: 25-50%; 3: 50-75%; 4: <75% positive staining/total lung area (*p<0.05 vs vehicle, Student's t-test). (C) Representative H&E staining on pulmonary sections of each treated mice group. (D) Flow cytometry analysis of CD326 (epithelial markers) and CD90 (mesenchymal markers) was performed on isolate bronchi (*** p<0.001 vs vehicle). Data are expressed as mean ±SEM n=6 mice in each group.

3.4.6 S1P drives EMT in OVA-sensitized mice

We already demonstrated that S1P signaling is involved in airway allergic TH2 response to different common allergens and, in particular, the S1P/SphK1/2 is involved in airway hyperresponsiveness in OVA-sensitised mice [123]. For this purpose, we decided to verify the link between S1P and EMT also in a common mouse model of allergic asthma obtained by exposure of mice to Ovalbumin. Allergen sensitization induced marked bronchoconstriction and the injection of Sphk1/2 inhibitor in OVA-treated mice reduced airway reactivity to carbachol (Figure 3.4.6A). Because EMT features are well characterized by the high levels of TGF β, we continued by evaluating the presence of TGF β by ELISA (Figure 3.4.6B) as well as the main markers of epithelial-mesenchymal transition in OVA-sensitized mice. Flow cytometry analysis performed on main bronchi clearly identify the upregulation of mesenchymal marker CD90 and downregulation of the epithelial marker CD326 in bronchi of OVA-sensitized mice (Figure 3.4.6C). Interestingly, we observed a significant reduction of CD90 and CD326 in the bronchi of OVA-sensitized mice treated with Sphk1/2 inhibitor. Sphk1/2 treatment reverses also OVA-induced fibroblast differentiation into myofibroblast as evident by light microscopy and determined by immunofluorescence analysis (Figure 3.4.6D). These data further confirm the role of S1P in EMT process, especially, the crosstalk S1P/SPK and TGF β pathway in epithelial plasticity.

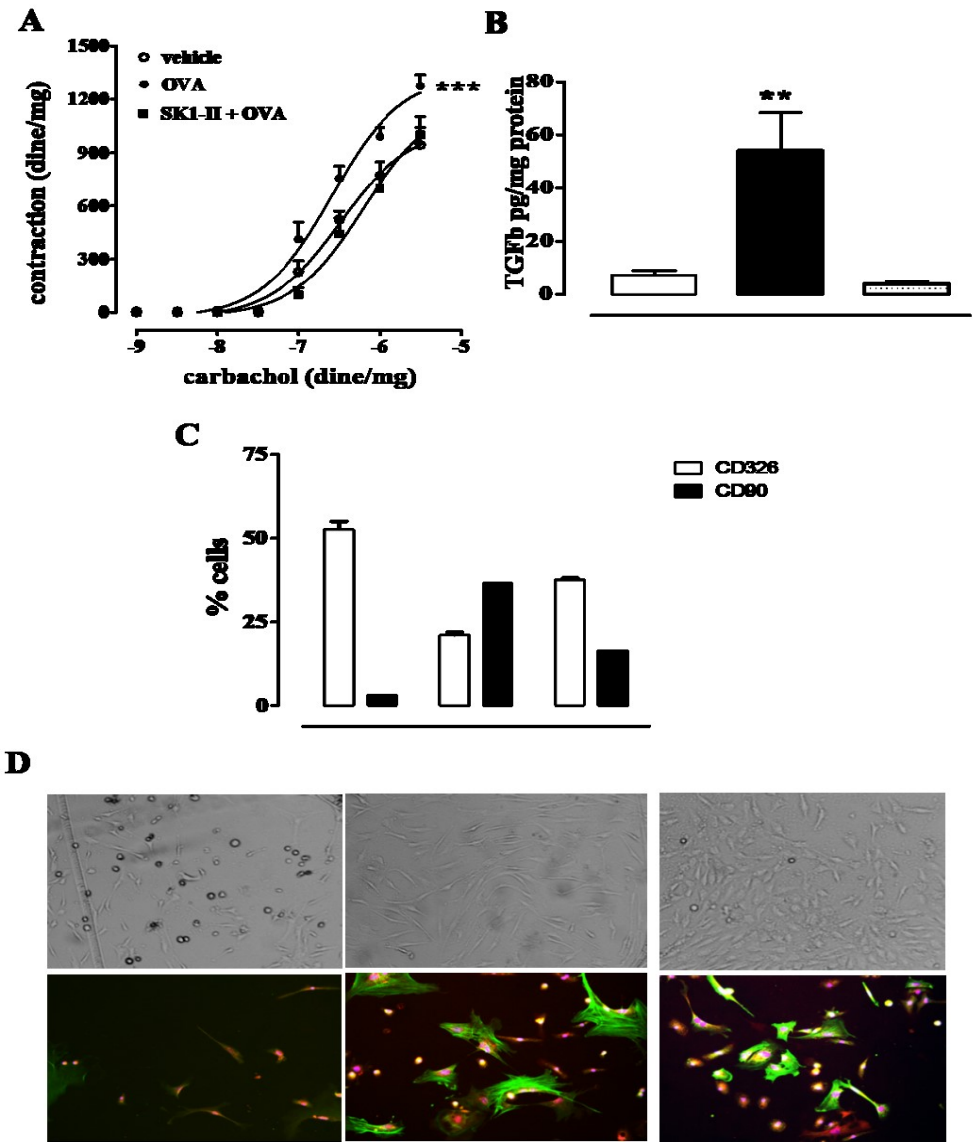

Figure 3.4.6: Inhibition of sphingosine kinases reverts changes in airway hyperreactivity, EMT and TGF β by Ovalbumin *in vivo.*

BALB/c mice were exposed to vehicle, OVA (10μg) or to SKI-II (sphingosine kinases inhibitor; 3mg/Kg) prior to OVA challenge. (A) Airway reactivity to carbachol was assessed on isolated bronchi (*** $p<0.001$ vs vehicle, two-way ANOVA with Bonferroni's post-test). (B) TGF-β levels were measured in lung homogenates by using specific ELISA (**$p<0.01$ vs vehicle, Student's t-test). (C) The epithelial marker CD326 and the mesenchymal marker CD90 were assessed in bronchi by using flow cytometry (* $p<0.05$ and **$p<0.01$ vs vehicle). (D) Pulmonary fibroblasts were harvested from each treated mouse and their differentiation was assessed by immunofluorescence analysis by using a monoclonal antibody against α-SMA. Data are expressed as mean ±SEM.

Chapter 4

Results

CHAPTER 4- RESULTS

Role of mast cells in sensitization mechanisms

4.1 Salvinorin A reduces bronchial hyperreactivity induced by OVA-sensitization in mouse

Salvinorin A is the principal active terpenoid molecule isolated from *Salvia divinorum* (Lamiaceae). Its action is mainly due to psychoactive and hallucinogen effects on the central nervous system. It has recently been demonstrated that *Salvinorin A* exerts some anti-inflammatory actions interfering, at least in part, on the inhibition of leukotrienes (LT) biosynthesis. Leukotrienes (LT) are predominantly known to promote inflammation in numerous inflammatory models *in vitro* and *in vivo*. Indeed, leukotrienes are considered crucial lipid mediators in allergic diseases such as asthma causing bronchoconstriction, inflammatory cell recruitment and liquid extravasation ending in edema. In collaboration with prof. Capasso, it was hypothesized whether *Salvinorin A* could positively modulate bronchial hyperresponsiveness and lung inflammation following OVA-sensitization in the mouse.

Female BALB/c mice were subcutaneously injected with 0.4 ml of a suspension containing OVA (100 µg/mouse) dissolved in Al(OH)3 gel (13 mg/ml in sterile saline) or vehicle (nonsensitized mice) at day 0 and 7. Salvinorin A (10mg/kg) or vehicle (DMS0 4% 0.5ml) were administered i.p. 30 min before each OVA challenging (Figure 4.1A). Bronchial reactivity to the cumulative concentration-response curve of carbachol in isolated organ Baths was performed on each treated mice group: vehicle, OVA or OVA+Salvinorin. Bronchi from OVA-sensitized mice showed a significant increase in Carbachol-induced contraction compared to the vehicle group. Pre-treatment with Salvinorin A ameliorates carbachol response and reported bronchial reactivity at the same values

observed in vehicle-treated mice (Figure 4.1B). Additionally, in perfect tune with functional studies, Salvinorin A reduces IL-13 lung levels (data not shown). Conversely, Salvinorin A does not affect by itself on pulmonary inflammation and does not affect IL-4 up-regulation and IgE plasma levels in OVA-sensitized mice (Figure 4.1C).

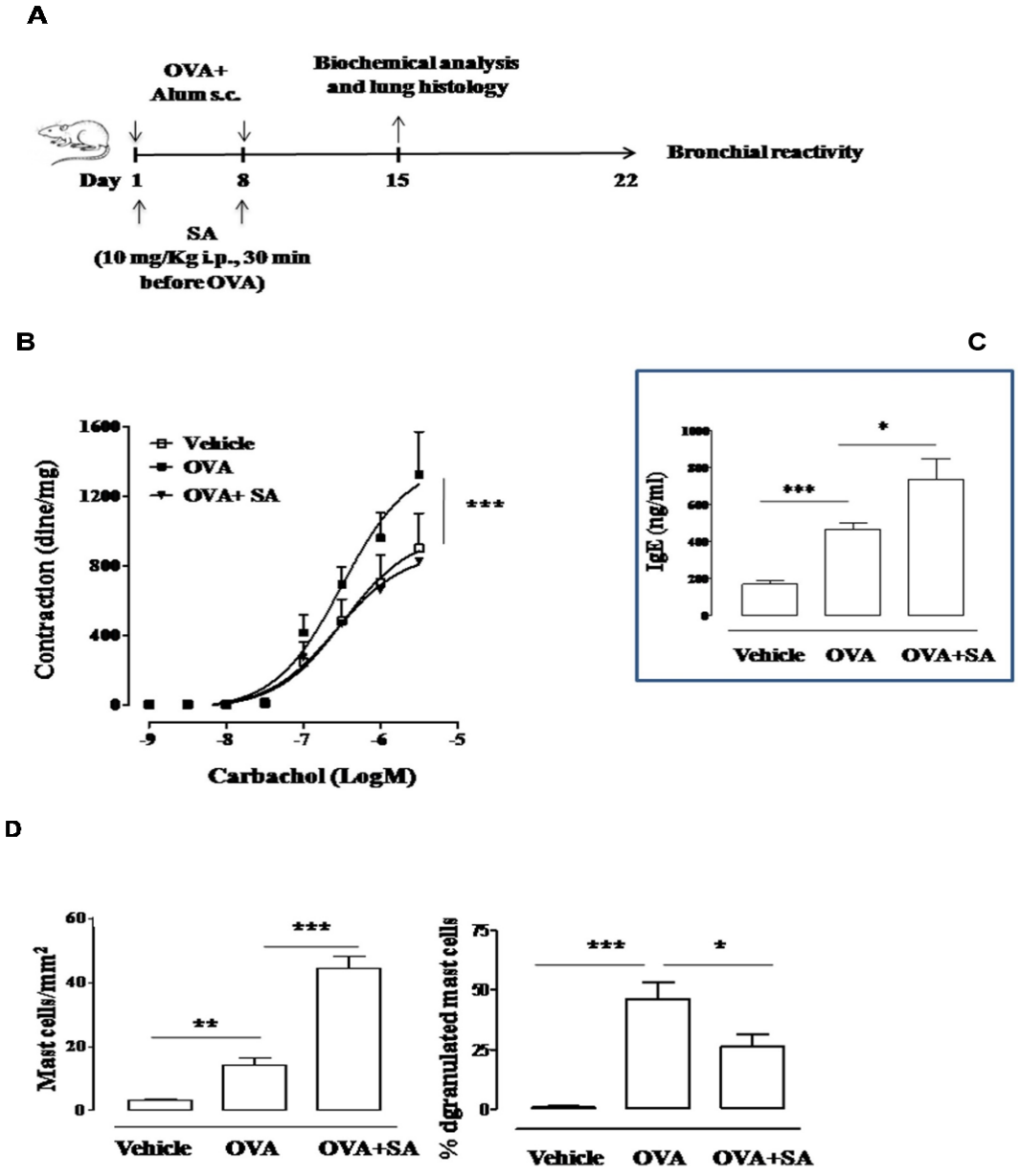

Figure 4.1: Effect of Salvinorin A on allergen-induced bronchial hyperreactivity.

(A)Schematic representation of experimental protocol. BALB/c mice received subcutaneous administration of OVA (100 µg) condensed with alum at day 0 and 8. Intraperitoneal administration of Salvinorin A or vehicle was performed 30min before each OVA challenge. (B) Measurement of bronchial reactivity to carbachol in isolated organ baths was evaluated 22 days after OVA injection (*** $p<0.001$ vs. control, two-way ANOVA with Bonferroni's post-test). (C) IgE plasma levels quantification by ELISA kit (* $p<0.05$, ***$p< 0.001$). (D) Quantification of toluidine staining and percentage of mast cell degranulation evaluated as the ratio between degranulated and non degranulated mast cells. Data are mean ± SEM, n=6 mice in each group

4.2 Palmitoylethanolamide (PEA) prevents airway dysfunction in OVA-sensitized mice

Palmitoylethanolamide (PEA) is an endogenous lipid mediator belong to the class of fatty acid ethanolamides as well as a natural lipid ingredient contained in food/dietary supplementation. Evidence suggests an involvement of PEA in mast recruitment and degranulation which are considered the principal orchestrator for airway hyperreactivity. We have already demonstrated that mast cell activation during allergen sensitization is responsible for bronchial reactivity[79]. Here, with prof. Izzo, we have further investigated the role of PEA in a well-established model of allergic asthma. Functional experiments using isolated organ baths were performed on isolated bronchi from OVA-sensitized mice treated with PEA (10mg/kg) or with the vehicle (saline, ETOH and tween-20, 8:1:1 v/v) 15 min before each OVA administration (Figure 4.2A). Bronchi harvested from OVA-treated mice showed increased reactivity to carbachol in comparison to vehicle-treated mice. In addition, hyperreactivity to carbachol was reverted by pre-treatment with PEA (Figure 4.2B). In another set of experiments, isolated bronchi were incubated with PEA and evaluate its action on a carbachol-induced contraction of both control and sensitized mice. In this case, PEA did not bring down the hyperresponsiveness to carbachol in OVA-treated mice suggesting that its role only correlates to the infiltration of immune cells during an allergic response and doesn't have a direct effect on smooth muscle cells responsible for bronchoconstriction (Figure 4.2 C). Similarly, PEA inhibits mast cell infiltration and cytokines expression in the lung but did not cause any change in plasma IgE levels (Figure 4.2 D). Indeed, toluidine staining on lung sections demonstrated a significant increase in mast cell recruitment in OVA-sensitised mice. PEA treatment prevented both mast cell recruitment and degranulation (Figure 4.2E). Sensitization caused also a significant increase in

IgE plasma levels that was not modified by PEA but prevented the increase in IL-13 and IL-4 pulmonary levels following sensitization.

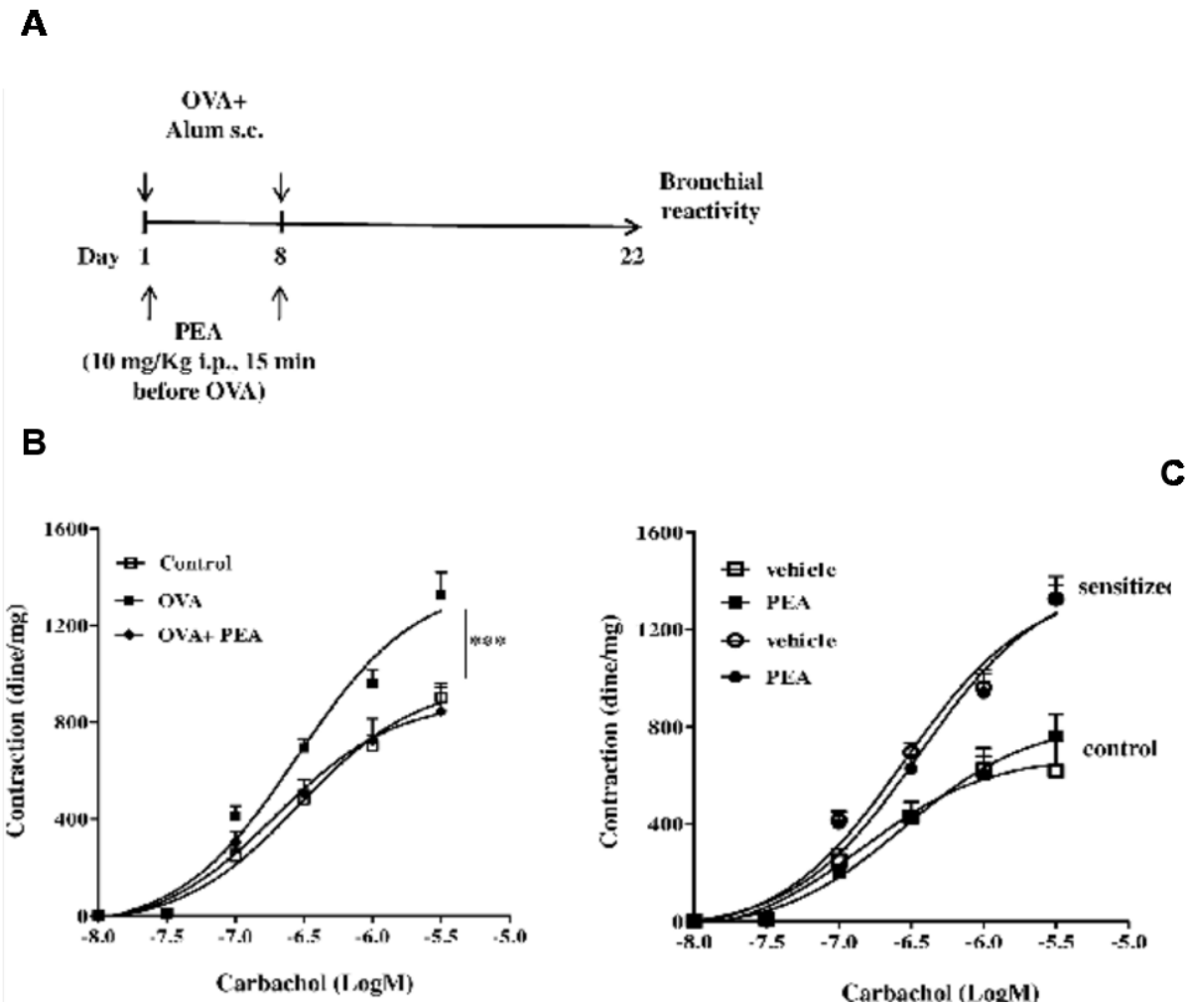

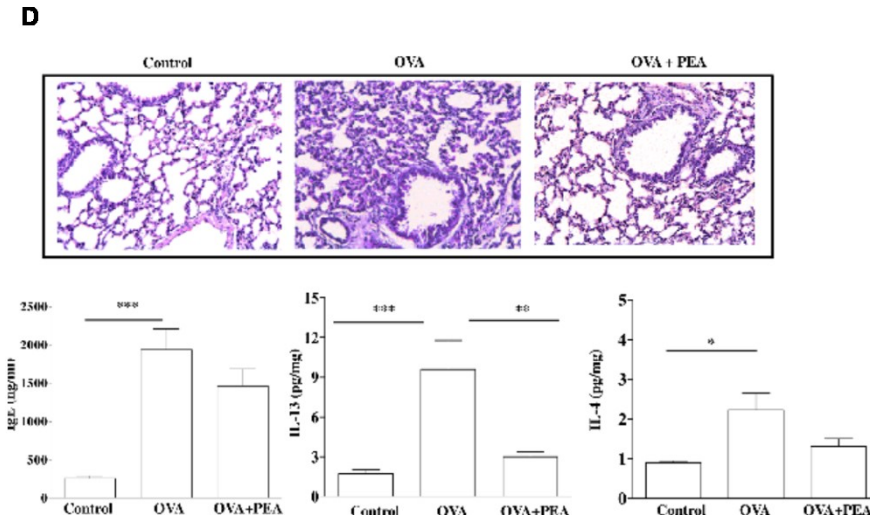

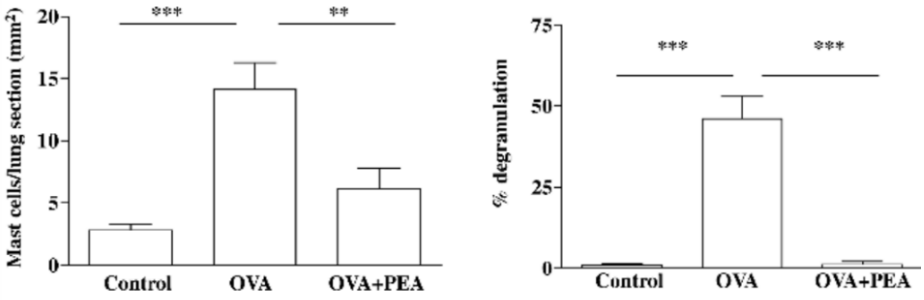

Figure 4.2: Effect of PEA on bronchial reactivity and lung inflammation in OVA-sensitized mice.

(A)Experimental protocol of sensitization and drug treatment. Mice were injected with subcutaneous administration of OVA (100 µg) adsorbed into aluminum hydroxide gel or vehicle on days 1 and 8. PEA was intraperitoneally administered 15 min before each OVA administration. (B) Measurement of bronchial reactivity to carbachol after 22 days of OVA sensitization (*** p<0.001 vs. control, two-way ANOVA with Bonferroni's post-test). (C) Direct administration of PEA (10^-5M) on isolated bronchi harvested from both control and OVA sensitized-mice. (D) IgE plasma levels, as well as IL-13 and IL-4 pulmonary levels, were quantified by specific ELISA kit (*p<0.05, ** p<0.01, *** p<0.001 vs. control or OVA, one way ANOVA with Bonferroni's post-test). (E) Quantification of toluidine staining and percentage of mast cell degranulation evaluated as a ratio between degranulated and non degranulated mast cells. Data are mean ± SEM, n=6 mice in each group

4.3 LT- dependent sex bias in AHR

Sex-difference with predominance in female versus male has been observed in most of the experimental animal model of asthma. Leukotrienes (LT) biosynthesis is implicated in allergic diseases participating over time to bronchoconstriction and lung inflammation leads to progressive asthma symptoms exacerbations. With prof Rossi, we have demonstrated the direct correlation with LT biosynthesis and sex-difference following allergen sensitization. This finding was translated into differences in bronchial reactivity, lung inflammation and mast cell recruitment/degranulation in female versus male. For this reason, pharmacological treatment with antagonist or inhibitor of leukotrienes metabolism protected female mice more efficiently than male mice. Bronchial reactivity in vitro to carbachol and lung inflammation using H&E staining were observed at different time points: 3 days, 8days, 14 days and 21 days after OVA-sensitization. For each time point, female mice are more prone to develop key asthma-like features than male as well as IgE levels in the plasma and pulmonary cytokine IL-13 and PGD2 correlate to mast cell degranulation (Figure 4.3). Also, we investigate trough bronchial reactivity to carbachol, the efficiency of different kinds of LT modifiers drugs in OVA-sensitized male and female BALB/c mice. Montelukast, Zileuton and MK886 significantly inhibited OVA-induced bronchial hyperreactivity in female but not in male animals (data not show).

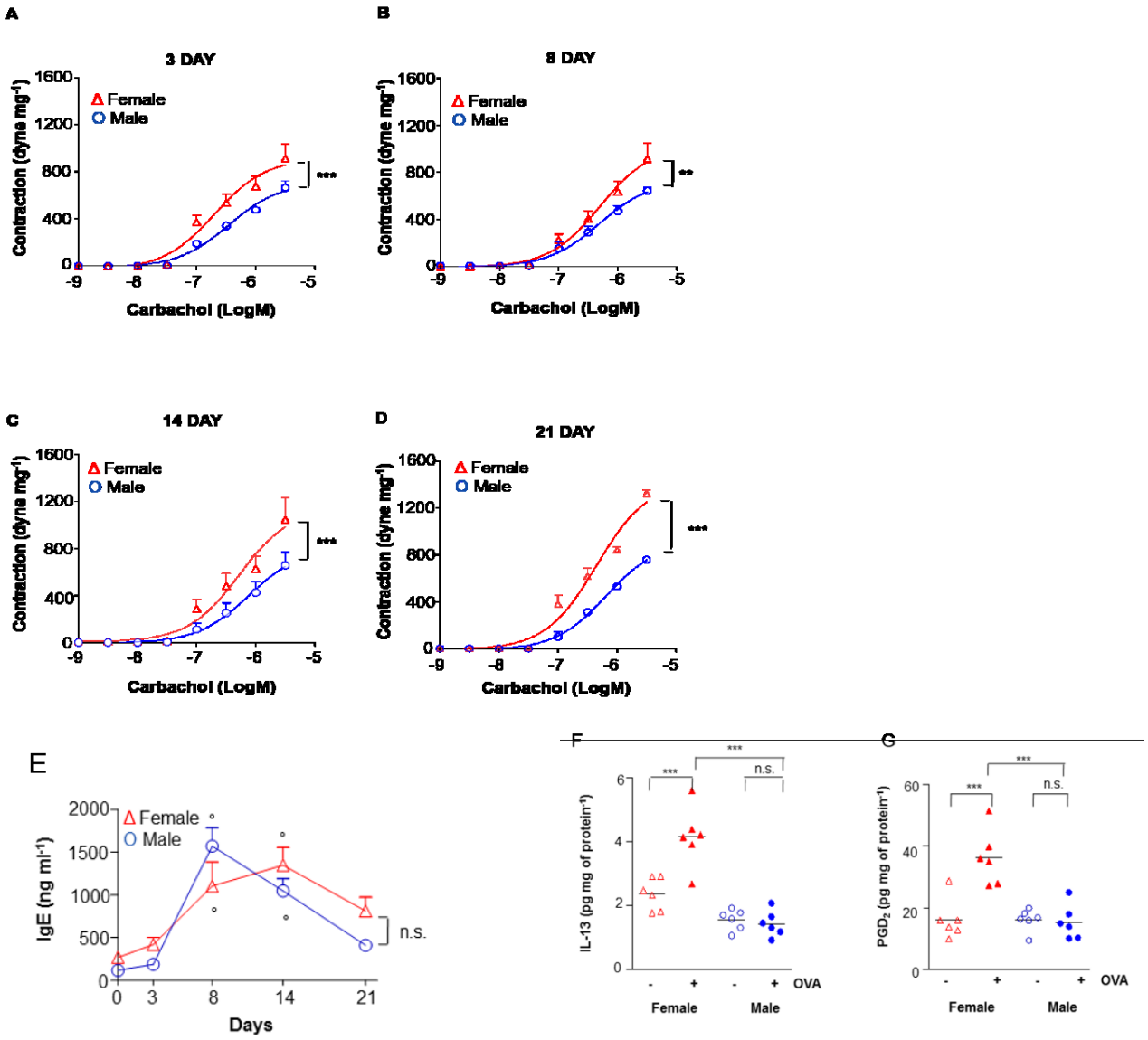

Figure 4.3: SEX difference in airway hyperreactivity, lung, and systemic inflammation during allergen sensitization.

Male and Female BALB/c received subcutaneous administration of Ovalbumin complexed with alum o days 0 and 7. Bronchial reactivity to carbachol was assessed in vitro after different time points: 3 days (A), 8 days (B), 14 days (C), 21 days (D) (**p<0.01, *** p<0.001 vs. male two-way ANOVA with Bonferroni's post-test). (E) IgE plasma levels and pulmonary IL-13 (F) and PGD2 (G) were measured at different time points by using specific ELIS kit (*** p<0.001, n.s., not significant (P> 0.05). One-way ANOVA plus Bonferroni's post-test). Data are mean ± SEM, n=6 mice in each group

Chapter 5

Results

Study of *De novo* sphingolipid biosynthesis and its cardioprotective functions in a mouse model of heart failure

Cardiovascular disease, including coronary artery disease (CAD), is the number one cause of death worldwide and hypercholesterolemia and hypertension are two major risk factors for coronary artery disease. ApoE$^{-/-}$ as well LDL $^{-/-}$ (receptor-knockout) mice have been extensively utilized to study atherosclerosis pathogenesis, but they develop these pathological conditions only when they fed with Western-type diet, resulting in high cholesterol levels >1400mg/dl compared to humans[124,125]. In addition, the principal limitation for this experimental animal model when mice, with a high-fat diet, develop atherosclerosis only in the aorta and aortic root but not in coronary artery vessels, the principal site where atherosclerosis plaque is formed in human[126]. Current animal models of atherosclerosis do not recapitulate coronary plaque rupture, myocardial infarction (MI) developing in humans. To overcome this inconvenient, transverse aortic constriction in ApoE$^{-/-}$ mice, on a regular chow diet, induce coronary lesions by combining hypercholesterolemia and high pressure[127]. In particular, atherosclerotic lesions develop only on right carotids and coronary artery which are exposed to high pressure induced by TAC surgery, and not in the vessel at low pressure as the aorta or left carotid. Here, we characterized the magnitude and the locations of coronary lesions and identified thrombotic events leading to myocardial infarction (MI) in ApoE$^{-/-}$ mice through the exposition of heart to high pressure by transverse aortic constriction (TAC) on chow diet (the combination of atherosclerosis and high pressure). Next, we investigate the potential role of NOGO-B protein as a negative regulator of sphingolipid biosynthesis in macrophages in the development of

coronary atherosclerosis, plaque stability, and cardiac function. We speculated on the idea that specific deletion of NOGO-B in macrophages (MΦNgKO) reduces coronary inflammation and atherogenesis in ApoE$^{-/-}$ post-TAC (MΦNgKO-ApoE$^{-/-}$) protecting the heart from CAD.

5.1 Characterization and distribution of coronary lesions in ApoE$^{-/-}$ mice after TAC

WT C57BL/6J male mice (11-14 weeks of age; 25-27g) were subjected to TAC or sham surgery. Minimally invasive TAC surgery was performed on ApoE$^{-/-}$ mice (25g) leading to a transthoracic pressure overload. Briefly, mice were anesthetized with a single injection of a cocktail of ketamine (100mg/kg) and xylazine (5mg/kg). After lateral thoracotomy at the second intercostal space, the thymus was opened, and the aortic arch was visualized with a dissecting scope (Zeiss Discovery V8Stereo). A 7.0 nylon ligature is placed between the innominate and left common carotid arteries with an overlapping 28-gauge needle, which was then rapidly removed. In sham-operated animals, the ligature was just tied loosely in the same space.

After TAC, different parameters were evaluated at different time point including the magnitude and presence of localization of coronary lesions, ECG analysis, and histology of the heart. At 8 weeks post-TAC histological analysis on the whole heart from the aortic valve (AV) to the apex was performed to identify the presence of coronary lesions, the degree of occlusion (Figure 5.1).

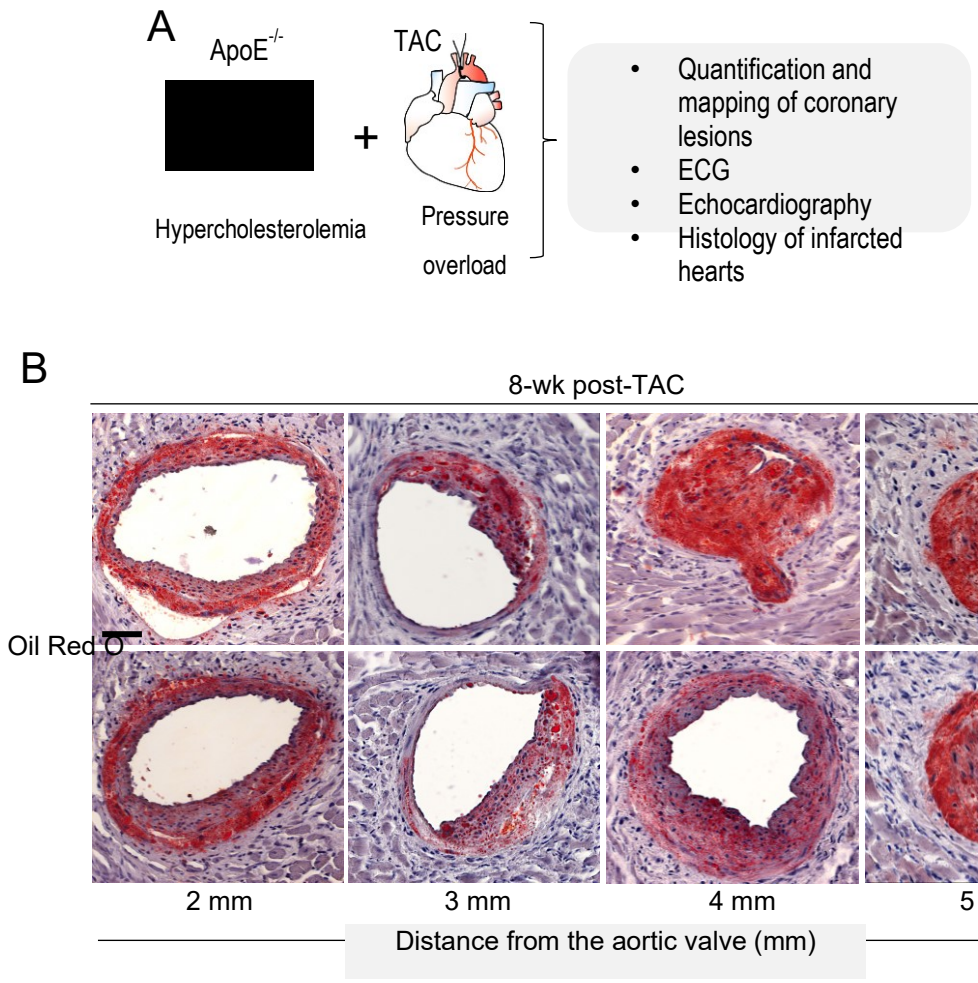

Figure 5.1: Characterization and distribution of coronary lesions in ApoE$^{-/-}$ mice after TAC.

(A)Experimental protocol scheme. Transverse aortic constriction (TAC) was made in male ApoE$^{-/-}$ mice (25 g) on chow diet following histological echocardiographic analysis at different time points. (B) Representative images of the coronary plaque in the LAD after 8 weeks post-TAC at a different distance from aortic valve (AV) showed different degrees of stenosis. (C)Quantification of LAD stenosis from di AV to te apex of 8-week TAC operated mice (n=10). (D) Lipid accumulation expressed as a percentage of plaque area to total area vessel (n=10)

5.2 Immunofluorescence staining for coronary lesions characterization

After 8 weeks post-TAC OIL-red O staining and immunofluorescence staining a whole heart from the aortic valve to the apex was performed to identify the presence and the quantification of coronary lesions. In early lesions, the accumulation of the lipids was limited to the intima or media, such as in humans with activation of smooth muscle cells. In contrast, the advanced coronary lesions presented a significant lipid accumulation in the lumen with different degrees of stenosis and macrophage infiltration (Figure 5.2).

A

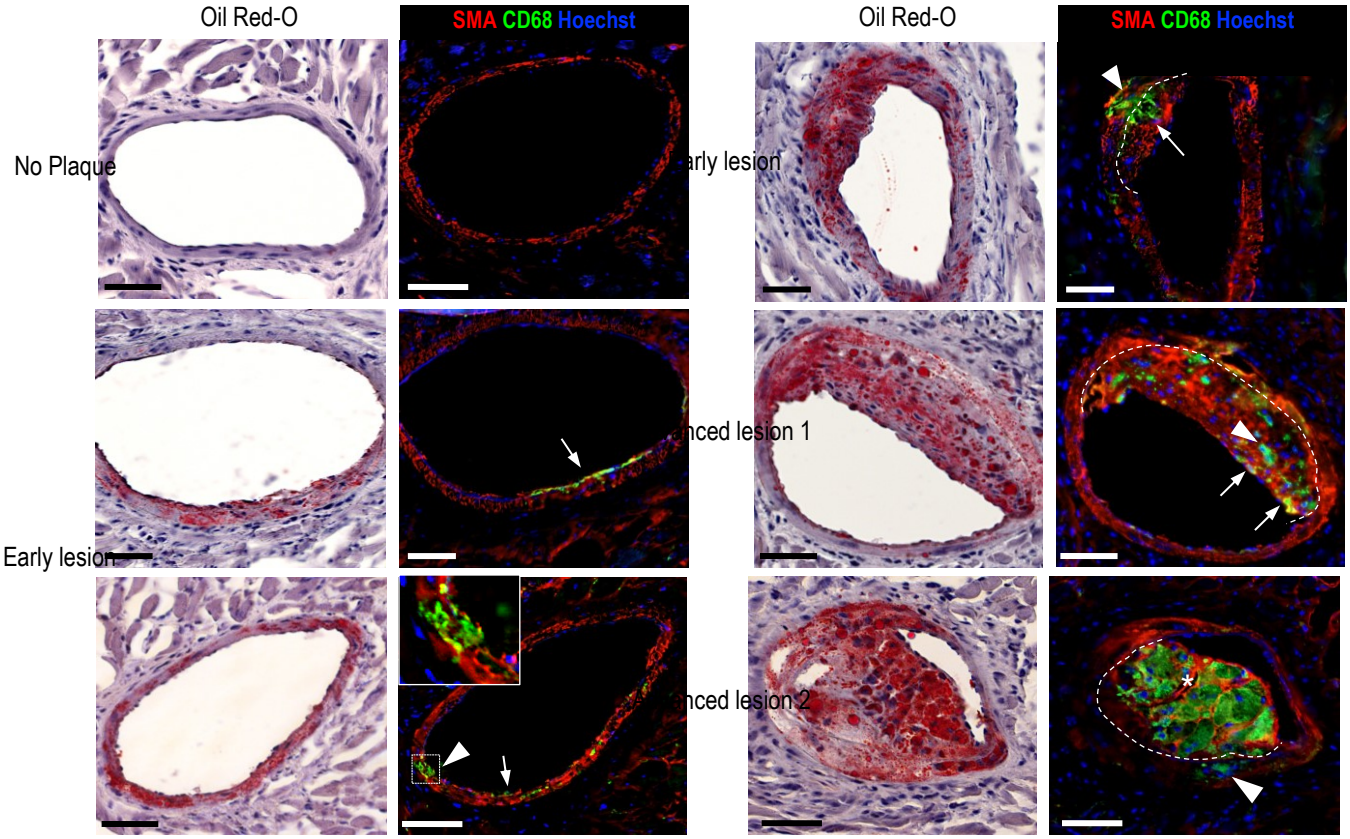

Figure 5.2: coronary lesions immunofluorescence.

(A)At 8 weeks after TAC, sequential myocardial sections were stained with Oil Red O (binding to lipids) and on the same sections was made immunofluorescence staining with αSMA (SMCs), CD68 (monocyte/macrophages), and Hoechst (nuclei). Oil Red O showed lipid accumulation in the vascular wall, including endothelial cells (ECs), SMCs, and macrophages, of early and advanced coronary lesions. Consecutive heart sections in immunofluorescence staining showed macrophage (green) infiltration into the intima and media of the coronary arteries Scale bar: 50 μm.

5.3 Effects of TAC on lipid deposition in carotid arteries and aortic valve (AV) in **MΦNgKO-ApoE$^{-/-}$ and control mice**.

After 10 weeks post-TAC, ApoE$^{-/-}$ but not MΦNgKO-ApoE$^{-/-}$ mice were sacrificed, the heart was excised and fixed with paraformaldehyde (PFA 4%) and embedded in OCT. In order to score and map the distribution of lipid accumulation in the coronary artery, I sectioned the whole heart and collecting 6x10 micron sections every 100 microns. Aortic valve (AV) and left and right carotids were stained with Oil red O. TAC induces remarkable atherosclerotic lesions in the high-pressure carotid artery and ascending aorta ApoE$^{-/-}$ but not MΦNgKO-ApoE$^{-/-}$ mice after 10 weeks post-TAC (Figure 5.3).

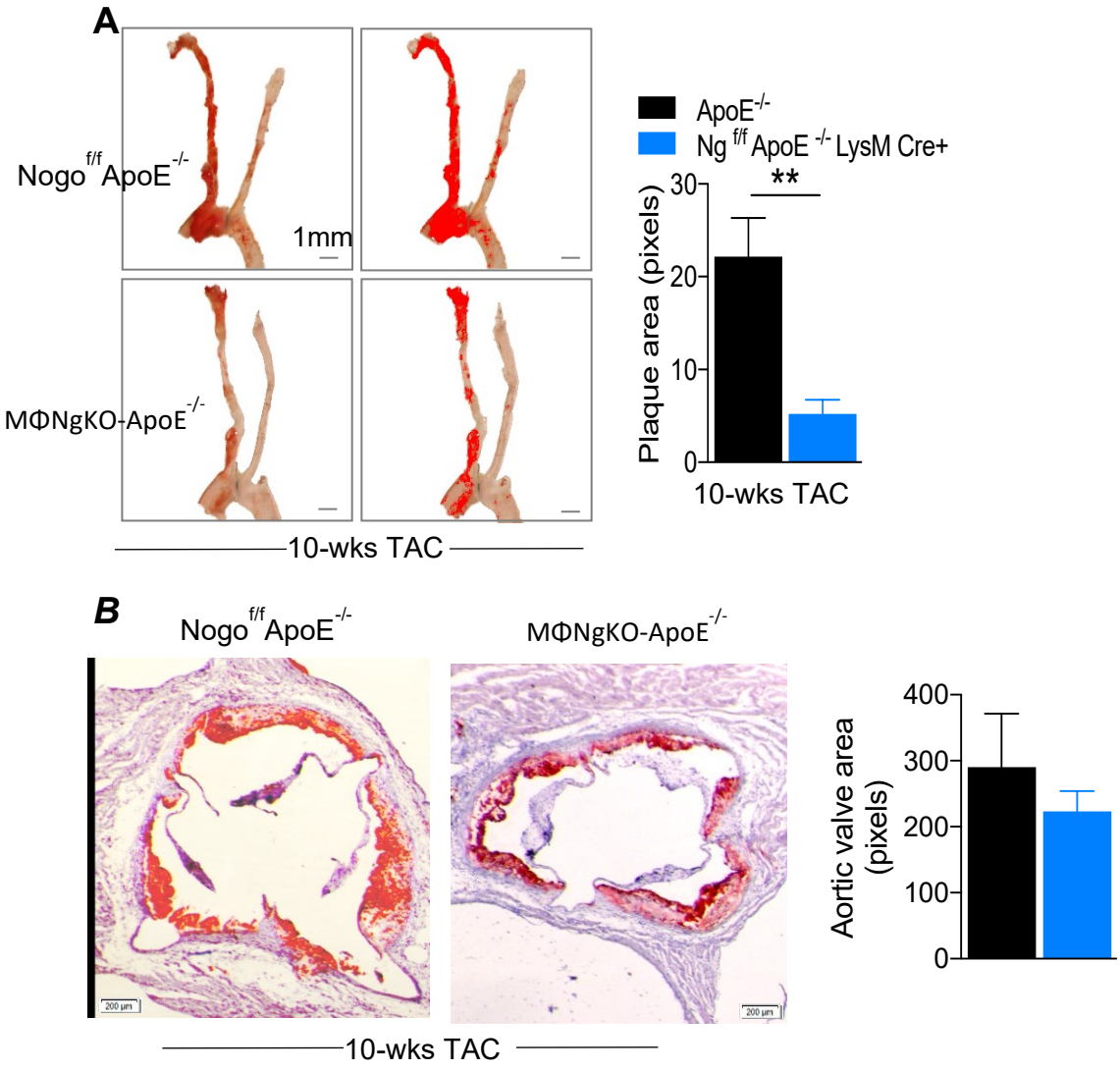

Figure 5.3: Oil red O staining quantification.

Quantification of lipid accumulation by Oil red O staining in left and right carotids (A) and aortic valves (B) in ApoE$^{-/-}$ and MΦNgKO-ApoE$^{-/-}$ after 10weeks post-TAC. Quantification of the atherosclerotic area (n=4 per each group). P<** by unpaired t-test.

Chapter 6

Discussion

Discussion

Asthma is a common chronic inflammatory respiratory disease that affects over 300 million people worldwide, resulting in a considerable impact on lifestyle, especially for their complications. It has been introduced in therapy many signs of progress and many new drugs, including monoclonal antibodies but they have still some limitations: a lot of patients, especially males, do not respond to conventional treatments such as corticosteroids or long term β-agonists. My research study is focused on exploring the new pharmacological tools that could be introduced in therapy. My first goal was to clarify the role of sphingosine-1-phosphate (S1P) in lung pathophysiology. The animal model that I used and finely characterized in my research study, represent an important tool to investigate the molecular and cellular mechanisms involving in S1P effects on airway function by using different experimental approaches trying to decrease the ongoing inflammation and reducing bronchial constriction. Reversible bronchoconstriction, lung inflammation, and mucus hyperproduction are the main hallmarks in the pathogenesis of allergic asthma. In Recent studies, sphingolipid metabolites and sphingosine-1-phosphate (S1P) are emerging as important signaling molecules in allergic disease especially asthma. Roviezzo et al. have previously demonstrated that S1P plays a critical role in pathological conditions regulating bronchial tone trough direct effects on smooth muscle cells via sphingosine kinases signaling. This hypothesis was confirmed by *in vitro* use of SPK inhibitor, D,L-threo-dihydrosphingosine (DTD), that abrogate the acetylcholine exacerbation contraction in OVA-sensitized bronchi[123]. In addition, systemic administration of S1P without additional adjuvant factors promotes in the mouse a disease mimicking asthma-like features such as bronchial hyperreactivity and pulmonary inflammation. These morphological and functional alterations were

associated with high circulating IgE plasma levels as well as an increase in Th2 pulmonary cytokines[78]. Furthermore, S1P is an endogenous mediator for mast cells (MCs) activation trough the crosslinking of the FcεRI on IgE. This engagement induces intracellular SPHKs activation, S1P production and subsequently the trans-activation of S1PR1 and S1PR2 receptors, resulting in enhanced cell functions. S1PR1 is involved in the MCs migration whereas S1PR2 contributes to the FcεRI- induced degranulation and the release of many inflammatory mediators such as histamine, PGD2, Cys-LTs, LTB4 and cytokines as IL-4, IL-13, IL-5, TGF-β, and TNF-α.[58,128,129].

Based on this evidence, I have evaluated the effect of Disodium Cromoglycate (DSCG), a common mast cell stabilizer widely used in human therapy, on S1P-induced asthma-likee features in the mouse. This pharmacological treatment completely inhibits airway hyperreactivity as well as lung inflammation, IgE plasma levels, and mucus production. The beneficial ability of DSCG to modulate mast cell activity is confirmed by the inhibition of PGD2, as a marker of mast cells activation[130]. S1P-induced asthma-like features are associated with a predominant Th2 bias and obligatory role of CD23/IgE signaling in mast cell recruitment/ activation. In order to look deeply into cellular mechanisms of positive DSCG effects in S1P-mediated asthma-like features, my attention has been focused on the CD23 receptor, the “low-affinity” receptor for IgE (FcεRII) responsible of IgE production[131]. Pre-treatment with DSCG (i.p. 50mg/Kg) inhibits pulmonary CD23 upregulation following S1P and, in particular, reduces expression of CD23 in both B and T cells with complementary attenuation of pulmonary inflammation such as low levels of circulating IgE, IL-13, and PGD2. The obtained results demonstrate the crucial involvement of CD23 signaling in the beneficial effects of DSCG. These data further confirm the clinical relevance of S1P in asthma pathogenesis. To note, all data concerning S1P airway effects

have been focused on its role in the development of adaptive immune cells. In addition to this phenomenon mainly found in severe and chronic asthma, the starting point of allergic response after exposure to ambient air pollution or other any pathogens, is still fully unclear. Emerging data suggest a key role for Toll-like-receptor (TLR4) in pathogen-induced immune innate response leading to activation and production of many innate molecules signaling cascade[132].Here, I have focused my attention on the involvement of innate response in S1P-induced allergic pulmonary inflammation. Emerging data suggest a key role for Toll-like-receptor (TLR4) in pathogen-induced immune innate response leading to asthma development[132]. Here I have assessed the effects of systemic administration of S1P in C3H/HeJ ($Tlr4^{Lps\text{-}d}$) mice. TLR4 defective mice are not inclined to develop airway hyperreactivity and lung inflammation following S1P exposure. Accordingly, exogenous administration of anti-TLR4 antibody in BALB/c mice abrogates all S1P effects in the lung. Thus, these data suggest an alternative and crucial role of S1P in innate immune response as sentinel mediator, together with TLR4, in the detection of the host. Interestingly, we found a physical association and combination between TLR4 and S1P1 receptors by immunofluorescence co-staining. Additionally, an increase of TLR4 positive cells occurs in the lung section when mice were treated with a co-administration of LPS+S1P. Immunoprecipitation and western blot analysis show an up-regulation of TLR4 expression in the main bronchi from mice treated with S1P compared to the vehicle. Altogether these data demonstrate that S1P triggers an innate immune response that in turn promotes a Th2 response responsible for asthma features manifestations. Since epithelial cells contribute to the innate response by promoting the release of inflammatory mediators such as a cytokine, I have also evaluated the role of the epithelium in our experimental model. Indeed, another important thing to consider in

asthma pathogenesis is the airway epithelium[133].After extensive and chronic airway inflammation, the structure of airway walls changes with irreversible reduction of airflow input/output and an accelerated decline in lung function. Fibroblasts are the major driver in airway remodeling but recent evidence supports the hypothesis of the epithelial-mesenchymal transition process or rather the trans-differentiation of epithelial cells into fibroblasts accompanied by pro-fibrotic cytokines such as TGF-β[134]or S1P[135,136]. For this purpose, in this set of experiments, the main bronchi harvested from S1P-treated mice show an increased expression of the mesenchymal and fibrosis markers and a reduction of the epithelial marker correlating EMT with S1P effects on airway and, of course, airway hyperreactivity (AHR). Also, we reproduced *in vitro* EMT by incubating airway epithelial cells with either TGF-β or S1P, and all the effects are reversed by pretreatment with LY2109761, a TGF-β antagonist. In perfect tune *in vivo* pre-treatment with LY2109761 inhibits bronchial hyperreactivity induced by S1P and reverses EMT as well. Also, in a common mouse model of asthma reproduced by exposure to Ovalbumin the sphingosine kinases inhibitor prevents EMT process. In conclusion, our findings confirm the direct correlation between S1P induced EMT and lung function by engaging TGF-β. Then, we wondered if airway S1P effects could be triggered also from other stimuli such as exposure to cigarette smoke. I measured the bronchial reactivity and pulmonary resistances in a well-established model of mild COPD. C57BL/6 mice were continuously exposed to cigarette smoke or room air (control mice) and sacrificed at different time points: 9, 10 and 11 months. Exposure to cigarette smoke leads to a progressive and increased bronchial hyperresponsiveness as well as the response to carbachol ending a plateau at 11 months. Pharmacological inhibition of the S1P pathway using non-selective inhibitors of sphingosine kinases or specific antagonists for S1P2 or S1P3

receptors abrogate the increased reactivity to carbachol following 11 months of cigarette smoke exposure reporting back the response to carbachol as control values. The involvement of the S1P pathway was confirmed by the increase in pulmonary S1P levels, too.

Considering the prominent role of mast cells in asthma pathogenesis, during my Ph.D. training I have also evaluated mast cells role in molecular mechanisms underlying allergen sensitization. Mast cells infiltrate the bronchial epithelium in asthma and act as effector cells in IgE-associated allergic disorders with immunoregulatory roles. This is of importance in disease pathogenesis for two reasons. First, mast cells are placed at the portal of entry of noxious stimuli such as aeroallergens, where they play an effector role in the ongoing immunologic response. Second, mast cell degranulation influences epithelial function. Indeed, mast cells adhere avidly to bronchial epithelial cells, and tryptase release stimulates airway epithelial activation. For this purpose, I have treated sensitized mice with Palmitoylethanolamide (PEA) and Salvinorin A, known for their ability to affect mast cell activation. Final data indicate that PEA as well as Salvinorin A significantly abrogate asthma features such as airway hyperreactivity. The beneficial actions of PEA and Salvinorin A in the airway have been demonstrated also by a significant reduction of IL-4 and IL-13 cytokine. In addition, both compounds do not affect sensitization mechanisms, but reduce the recruitment and degranulation of mast cells, confirming a critical role of mast cell in asthma symptoms manifestations. Literature data suggest that asthma has a higher incidence in females[137]. The prevalence and severity of asthma in women are frequently linked with hormonal fluctuations during the menstrual cycle. Indeed, asthma-related symptoms were related to hormonal changes and female patients develop a more prevalent hyper-responsiveness than male patients. The difference in the

gender associated with the incidence of asthma was assessed: Between the age of 4 and 14 years, asthma has more prevalent in males compared to females (11.5 vs. 9.9%). However, after puberty, asthma became more prevalent and severe in women[67]. Interestingly, after the menopause asthma becomes once again more severe in males. Additionally, sex dimorphism in asthma disease has been associated with different roles of sex hormones as well as leukotrienes (LT) synthesis on the immune response that drives sensitization[138]. In this context, I have also participated in a study demonstrating that a mast cell-dependent sex bias exists in allergen-induced airway hyperreactivity. During my last year of Ph.D. program at Weill Cornell Medical College, I have participated in a project focused on the contribution of S1P in coronary artery disease. Some murine models of atherosclerosis recapitulate several aspects of human disease, including high plasma cholesterol levels and lesion formation in the aortic root; however, these lesions rarely carried out to plaque rupture and MI. Furthermore, atherosclerosis is not observed in the coronary arteries, which is the major site of human plaque formation. Recently, transverse aortic constriction (TAC) was shown to induce coronary lesions in apolipoprotein E–deficient (ApoE-deficient) mice. In this context, my project has been centered on the characterization of development and progression of coronary lesions in $ApoE^{-/-}$ mice ending in myocardial events as a result of coronary plaque thrombosis and/or occlusion. Cumulatively, the results of these studies reveal that the TAC ApoE-deficient model recapitulates important aspects of human disease and indicates that this model has potential as an important tool for studying coronary lesion formation and rupture in human diseases. In addition, I investigated how the specific deletion of NOGO-B in macrophages (MΦNgKO) reduces coronary inflammation and atherogenesis in $ApoE^{-/-}$ mice (MΦNgKO-$ApoE^{-/-}$) after 10 weeks TAC.

Chapter 7

Bibliography

Bibliography

1. Hawthorne JN. A note on the life of J.L.W. Thudichum (1829-1901). *Biochem Soc Trans*. 1975;3(5):591. doi:10.1042/bst0030591

2. Abou-Ghali M, Stiban J. Regulation of ceramide channel formation and disassembly: Insights on the initiation of apoptosis. *Saudi J Biol Sci*. 2015;22(6):760-772. doi:10.1016/j.sjbs.2015.03.005

3. Fahy E, Subramaniam S, Brown HA, et al. A comprehensive classification system for lipids. *J Lipid Res*. 2005;46(5):839-861. doi:10.1194/jlr.E400004-JLR200

4. Kobayashi N, Kobayashi N, Yamaguchi A, Nishi T. Characterization of the ATP-dependent sphingosine 1-phosphate transporter in rat erythrocytes. *J Biol Chem*. 2009;284(32):21192-21200. doi:10.1074/jbc.M109.006163

5. Spiegel S, Maczis MA, Maceyka M, Milstien S. New insights into functions of the sphingosine-1-phosphate transporter SPNS2. *J Lipid Res*. 2019;60(3):484-489. doi:10.1194/jlr.S091959

6. Nicolson GL. The Fluid-Mosaic Model of Membrane Structure: still relevant to understanding the structure, function and dynamics of biological membranes after more than 40 years. *Biochim Biophys Acta*. 2014;1838(6):1451-1466. doi:10.1016/j.bbamem.2013.10.019

7. Futerman AH, Hannun YA. The complex life of simple sphingolipids. *EMBO Rep*. 2004;5(8):777-782. doi:10.1038/sj.embor.7400208

8. Hannun YA, Obeid LM. Principles of bioactive lipid signalling: lessons from sphingolipids. *Nat Rev Mol Cell Biol*. 2008;9(2):139-150. doi:10.1038/nrm2329

9. Hanada K, Hara T, Nishijima M, Kuge O, Dickson RC, Nagiec MM. A mammalian homolog of the yeast LCB1 encodes a component of serine palmitoyltransferase, the enzyme catalyzing the first step in sphingolipid synthesis. *J Biol Chem*. 1997;272(51):32108-32114. doi:10.1074/jbc.272.51.32108

10. Hanada K, Hara T, Nishijima M. Purification of the serine palmitoyltransferase complex responsible for sphingoid base synthesis by using affinity peptide chromatography techniques. *J Biol Chem*. 2000;275(12):8409-8415. doi:10.1074/jbc.275.12.8409

11. Hanada K, Hara T, Nishijima M. D-Serine inhibits serine palmitoyltransferase, the enzyme catalyzing the initial step of sphingolipid biosynthesis. *FEBS Lett*. 2000;474(1):63-65. doi:10.1016/s0014-5793(00)01579-9

12. Nagiec MM, Lester RL, Dickson RC. Sphingolipid synthesis: identification and characterization of mammalian cDNAs encoding the Lcb2 subunit of serine palmitoyltransferase. *Gene*. 1996;177(1-2):237-241. doi:10.1016/0378-1119(96)00309-5

13. Hornemann T, Richard S, Rütti MF, Wei Y, von Eckardstein A. Cloning and initial characterization of a new subunit for mammalian serine-palmitoyltransferase. *J Biol Chem*. 2006;281(49):37275-37281. doi:10.1074/jbc.M608066200

14. Adachi-Yamada T, Gotoh T, Sugimura I, et al. De novo synthesis of sphingolipids is required for cell survival by down-regulating c-Jun N-terminal kinase in Drosophila imaginal discs. *Mol Cell Biol*. 1999;19(10):7276-7286. doi:10.1128/mcb.19.10.7276

15. Hojjati MR, Li Z, Zhou H, et al. Effect of myriocin on plasma sphingolipid metabolism and atherosclerosis in apoE-deficient mice. *J Biol Chem*. 2005;280(11):10284-10289. doi:10.1074/jbc.M412348200

16. Hornemann T, Wei Y, von Eckardstein A. Is the mammalian serine palmitoyltransferase a high-molecular-mass complex? *Biochem J*. 2007;405(1):157-164. doi:10.1042/BJ20070025

17. Triola G, Fabrias G, Dragusin M, et al. Specificity of the dihydroceramide desaturase inhibitor N-[(1R,2S)-2-hydroxy-1-hydroxymethyl-2-(2-tridecyl-1-cyclopropenyl)ethyl]octanamide (GT11) in primary cultured cerebellar neurons. *Mol Pharmacol*. 2004;66(6):1671-1678. doi:10.1124/mol.104.003681

18. Wadsworth JM, Clarke DJ, McMahon SA, et al. The chemical basis of serine palmitoyltransferase inhibition by myriocin. *J Am Chem Soc*. 2013;135(38):14276-14285. doi:10.1021/ja4059876

19. Breslow DK, Collins SR, Bodenmiller B, et al. Orm family proteins mediate sphingolipid homeostasis. *Nature*. 2010;463(7284):1048-1053. doi:10.1038/nature08787

20. Harmon JM, Bacikova D, Gable K, et al. Topological and functional characterization of the ssSPTs, small activating subunits of serine palmitoyltransferase. *J Biol Chem*. 2013;288(14):10144-10153. doi:10.1074/jbc.M113.451526

21. Cai L, Oyeniran C, Biswas DD, et al. ORMDL proteins regulate ceramide levels during sterile inflammation. *J Lipid Res*. 2016;57(8):1412-1422. doi:10.1194/jlr.M065920

22. Davis DL, Gable K, Suemitsu J, Dunn TM, Wattenberg BW. The ORMDL/Orm-serine palmitoyltransferase (SPT) complex is directly regulated by ceramide: Reconstitution of SPT regulation in isolated membranes. *J Biol Chem*. 2019;294(13):5146-5156. doi:10.1074/jbc.RA118.007291

23. Sasset L, Zhang Y, Dunn TM, Di Lorenzo A. Sphingolipid De Novo Biosynthesis: A Rheostat of Cardiovascular Homeostasis. *Trends Endocrinol Metab*. 2016;27(11):807-819. doi:10.1016/j.tem.2016.07.005

24. Cantalupo A, Zhang Y, Kothiya M, et al. Nogo-B regulates endothelial sphingolipid homeostasis to control vascular function and blood pressure. *Nat Med*. 2015;21(9):1028-1037. doi:10.1038/nm.3934

25. Petrache I, Berdyshev EV. Ceramide Signaling and Metabolism in Pathophysiological States of the Lung. *Annu Rev Physiol*. 2016;78:463-480. doi:10.1146/annurev-physiol-021115-105221

26. Kitatani K, Idkowiak-Baldys J, Hannun YA. The sphingolipid salvage pathway in ceramide metabolism and signaling. *Cell Signal*. 2008;20(6):1010-1018. doi:10.1016/j.cellsig.2007.12.006

27. Maceyka M, Sankala H, Hait NC, et al. SphK1 and SphK2, sphingosine kinase isoenzymes with opposing functions in sphingolipid metabolism. *J Biol Chem*. 2005;280(44):37118-37129. doi:10.1074/jbc.M502207200

28. Weigert A, von Knethen A, Thomas D, et al. Sphingosine kinase 2 is a negative regulator of inflammatory macrophage activation. *Biochim Biophys Acta Mol Cell Biol Lipids*. 2019;1864(9):1235-1246. doi:10.1016/j.bbalip.2019.05.008

29. Stahelin RV, Hwang JH, Kim J-H, et al. The mechanism of membrane targeting of human sphingosine kinase 1. *J Biol Chem*. 2005;280(52):43030-43038. doi:10.1074/jbc.M507574200

30. Hait NC, Bellamy A, Milstien S, Kordula T, Spiegel S. Sphingosine kinase type 2 activation by ERK-mediated phosphorylation. *J Biol Chem*. 2007;282(16):12058-12065. doi:10.1074/jbc.M609559200

31. Song D-D, Zhou J-H, Sheng R. Regulation and function of sphingosine kinase 2 in diseases. *Histol Histopathol*. 2018;33(5):433-445. doi:10.14670/HH-11-939

32. Czubowicz K, Jęśko H, Wencel P, Lukiw WJ, Strosznajder RP. The Role of Ceramide and Sphingosine-1-Phosphate in Alzheimer's Disease and Other Neurodegenerative Disorders. *Mol Neurobiol*. 2019;56(8):5436-5455. doi:10.1007/s12035-018-1448-3

33. Kluk MJ, Hla T. Signaling of sphingosine-1-phosphate via the S1P/EDG-family of G-protein-coupled receptors. *Biochim Biophys Acta*. 2002;1582(1-3):72-80. doi:10.1016/s1388-1981(02)00139-7

34. Sanchez T, Hla T. Structural and functional characteristics of S1P receptors. *J Cell Biochem*. 2004;92(5):913-922. doi:10.1002/jcb.20127

35. Taha TA, Argraves KM, Obeid LM. Sphingosine-1-phosphate receptors: receptor specificity versus functional redundancy. *Biochim Biophys Acta*. 2004;1682(1-3):48-55. doi:10.1016/j.bbalip.2004.01.006

36. Zhou J, Saba JD. Identification of the first mammalian sphingosine phosphate lyase gene and its functional expression in yeast. *Biochem Biophys Res Commun*. 1998;242(3):502-507. doi:10.1006/bbrc.1997.7993

37. Lanterman MM, Saba JD. Characterization of sphingosine kinase (SK) activity in Saccharomyces cerevisiae and isolation of SK-deficient mutants. *Biochem J*. 1998;332 (Pt 2):525-531. doi:10.1042/bj3320525

38. Sato K, Malchinkhuu E, Horiuchi Y, et al. Critical role of ABCA1 transporter in sphingosine 1-phosphate release from astrocytes. *J Neurochem*. 2007;103(6):2610-2619. doi:10.1111/j.1471-4159.2007.04958.x

39. Mitra P, Oskeritzian CA, Payne SG, Beaven MA, Milstien S, Spiegel S. Role of ABCC1 in export of sphingosine-1-phosphate from mast cells. *Proc Natl Acad Sci USA*. 2006;103(44):16394-16399. doi:10.1073/pnas.0603734103

40. Kawahara A, Nishi T, Hisano Y, Fukui H, Yamaguchi A, Mochizuki N. The sphingolipid transporter spns2 functions in migration of zebrafish myocardial precursors. *Science*. 2009;323(5913):524-527. doi:10.1126/science.1167449

41. Yatomi Y, Yamamura S, Ruan F, Igarashi Y. Sphingosine 1-phosphate induces platelet activation through an extracellular action and shares a platelet surface receptor with lysophosphatidic acid. *J Biol Chem*. 1997;272(8):5291-5297. doi:10.1074/jbc.272.8.5291

42. Hänel P, Andréani P, Gräler MH. Erythrocytes store and release sphingosine 1-phosphate in blood. *FASEB J*. 2007;21(4):1202-1209. doi:10.1096/fj.06-7433com

43. Spiegel S, Milstien S. The outs and the ins of sphingosine-1-phosphate in immunity. *Nat Rev Immunol*. 2011;11(6):403-415. doi:10.1038/nri2974

44. Liu Y, Wada R, Yamashita T, et al. Edg-1, the G protein-coupled receptor for sphingosine-1-phosphate, is essential for vascular maturation. *J Clin Invest*. 2000;106(8):951-961. doi:10.1172/JCI10905

45. Ishii I, Ye X, Friedman B, et al. Marked perinatal lethality and cellular signaling deficits in mice null for the two sphingosine 1-phosphate (S1P) receptors, S1P(2)/LP(B2)/EDG-5 and S1P(3)/LP(B3)/EDG-3. *J Biol Chem*. 2002;277(28):25152-25159. doi:10.1074/jbc.M200137200

46. Allende ML, Bektas M, Lee BG, et al. Sphingosine-1-phosphate lyase deficiency produces a pro-inflammatory response while impairing neutrophil trafficking. *J Biol Chem*. 2011;286(9):7348-7358. doi:10.1074/jbc.M110.171819

47. Peters SLM, Alewijnse AE. Sphingosine-1-phosphate signaling in the cardiovascular system. *Curr Opin Pharmacol*. 2007;7(2):186-192. doi:10.1016/j.coph.2006.09.008

48. Igarashi J, Michel T. Sphingosine-1-phosphate and modulation of vascular tone. *Cardiovasc Res*. 2009;82(2):212-220. doi:10.1093/cvr/cvp064

49. Sphingolipid metabolism and drug resistance in ovarian cancer. doi:doi ： 10.20517/cdr.2018.06

50. Chi H. Sphingosine-1-phosphate and immune regulation: trafficking and beyond. *Trends Pharmacol Sci*. 2011;32(1):16-24. doi:10.1016/j.tips.2010.11.002

51. Rivera J, Proia RL, Olivera A. The alliance of sphingosine-1-phosphate and its receptors in immunity. *Nat Rev Immunol*. 2008;8(10):753-763. doi:10.1038/nri2400

52. Schwab SR, Cyster JG. Finding a way out: lymphocyte egress from lymphoid organs. *Nat Immunol*. 2007;8(12):1295-1301. doi:10.1038/ni1545

53. Cohen JA, Chun J. Mechanisms of fingolimod's efficacy and adverse effects in multiple sclerosis. *Ann Neurol*. 2011;69(5):759-777. doi:10.1002/ana.22426

54. Olivera A, Urtz N, Mizugishi K, et al. IgE-dependent activation of sphingosine kinases 1 and 2 and secretion of sphingosine 1-phosphate requires Fyn kinase and contributes to mast cell responses. *J Biol Chem*. 2006;281(5):2515-2525. doi:10.1074/jbc.M508931200

55. Olivera A, Mizugishi K, Tikhonova A, et al. The sphingosine kinase-sphingosine-1-phosphate axis is a determinant of mast cell function and anaphylaxis. *Immunity*. 2007;26(3):287-297. doi:10.1016/j.immuni.2007.02.008

56. Sun X, Ma S-F, Wade MS, et al. Functional variants of the sphingosine-1-phosphate receptor 1 gene associate with asthma susceptibility. *J Allergy Clin Immunol*. 2010;126(2):241-249, 249.e1-3. doi:10.1016/j.jaci.2010.04.036

57. Nishiuma T, Nishimura Y, Okada T, et al. Inhalation of sphingosine kinase inhibitor attenuates airway inflammation in asthmatic mouse model. *Am J Physiol Lung Cell Mol Physiol*. 2008;294(6):L1085-1093. doi:10.1152/ajplung.00445.2007

58. Jolly PS, Bektas M, Olivera A, et al. Transactivation of sphingosine-1-phosphate receptors by FcepsilonRI triggering is required for normal mast cell degranulation and chemotaxis. *J Exp Med*. 2004;199(7):959-970. doi:10.1084/jem.20030680

59. Roviezzo F, Del Galdo F, Abbate G, et al. Human eosinophil chemotaxis and selective in vivo recruitment by sphingosine 1-phosphate. *Proc Natl Acad Sci U S A*. 2004;101(30):11170-11175. doi:10.1073/pnas.0401439101

60. Ballesteros-Martinez C, Mendez-Barbero N, Montalvo-Yuste A, et al. Endothelial Regulator of Calcineurin 1 Promotes Barrier Integrity and Modulates Histamine-Induced Barrier Dysfunction in Anaphylaxis. *Front Immunol*. 2017;8:1323. doi:10.3389/fimmu.2017.01323

61. Sanchez T, Skoura A, Wu MT, Casserly B, Harrington EO, Hla T. Induction of vascular permeability by the sphingosine-1-phosphate receptor-2 (S1P2R) and its downstream effectors ROCK and PTEN. *Arterioscler Thromb Vasc Biol*. 2007;27(6):1312-1318. doi:10.1161/ATVBAHA.107.143735

62. Tauseef M, Kini V, Knezevic N, et al. Activation of sphingosine kinase-1 reverses the increase in lung vascular permeability through sphingosine-1-phosphate receptor signaling in endothelial cells. *Circ Res*. 2008;103(10):1164-1172. doi:10.1161/01.RES.0000338501.84810.51

63. Sammani S, Moreno-Vinasco L, Mirzapoiazova T, et al. Differential effects of sphingosine 1-phosphate receptors on airway and vascular barrier function in the murine lung. *Am J Respir Cell Mol Biol*. 2010;43(4):394-402. doi:10.1165/rcmb.2009-0223OC

64. Puneet P, Yap CT, Wong L, et al. SphK1 regulates proinflammatory responses associated with endotoxin and polymicrobial sepsis. *Science*. 2010;328(5983):1290-1294. doi:10.1126/science.1188635

65. Maceyka M, Spiegel S. Sphingolipid metabolites in inflammatory disease. *Nature*. 2014;510(7503):58-67. doi:10.1038/nature13475

66. Spiegel S, Milstien S. Sphingosine-1-phosphate: an enigmatic signalling lipid. *Nat Rev Mol Cell Biol*. 2003;4(5):397-407. doi:10.1038/nrm1103

67. Shah R, Newcomb DC. Sex Bias in Asthma Prevalence and Pathogenesis. *Front Immunol*. 2018;9:2997. doi:10.3389/fimmu.2018.02997

68. Mims JW. Asthma: definitions and pathophysiology. *Int Forum Allergy Rhinol*. 2015;5 Suppl 1:S2-6. doi:10.1002/alr.21609

69. Robinson D, Humbert M, Buhl R, et al. Revisiting Type 2-high and Type 2-low airway inflammation in asthma: current knowledge and therapeutic implications. *Clin Exp Allergy*. 2017;47(2):161-175. doi:10.1111/cea.12880

70. Schatz M, Rosenwasser L. The allergic asthma phenotype. *J Allergy Clin Immunol Pract*. 2014;2(6):645-648; quiz 649. doi:10.1016/j.jaip.2014.09.004

71. Licona-Limón P, Kim LK, Palm NW, Flavell RA. TH2, allergy and group 2 innate lymphoid cells. *Nat Immunol*. 2013;14(6):536-542. doi:10.1038/ni.2617

72. Sousa AR, Poston RN, Lane SJ, Nakhosteen JA, Lee TH. Detection of GM-CSF in asthmatic bronchial epithelium and decrease by inhaled corticosteroids. *Am Rev Respir Dis*. 1993;147(6 Pt 1):1557-1561. doi:10.1164/ajrccm/147.6_Pt_1.1557

73. Woolley KL, Adelroth E, Woolley MJ, Ellis R, Jordana M, O'Byrne PM. Granulocyte-macrophage colony-stimulating factor, eosinophils and eosinophil cationic protein in subjects with and without mild, stable, atopic asthma. *Eur Respir J*. 1994;7(9):1576-1584. doi:10.1183/09031936.94.07091576

74. Ammit AJ, Hastie AT, Edsall LC, et al. Sphingosine 1-phosphate modulates human airway smooth muscle cell functions that promote inflammation and airway remodeling in asthma. *FASEB J*. 2001;15(7):1212-1214. doi:10.1096/fj.00-0742fje

75. Pfaff M, Powaga N, Akinci S, et al. Activation of the SPHK/S1P signalling pathway is coupled to muscarinic receptor-dependent regulation of peripheral airways. *Respir Res*. 2005;6(1):48. doi:10.1186/1465-9921-6-48

76. Kume H, Takeda N, Oguma T, et al. Sphingosine 1-phosphate causes airway hyper-reactivity by rho-mediated myosin phosphatase inactivation. *J Pharmacol Exp Ther*. 2007;320(2):766-773. doi:10.1124/jpet.106.110718

77. Giuseppe cirino fiorentina roviezzo. Sphingosine-1-phosphate/sphingosine kinase pathway is involved in mouse airway hyperresponsiveness. *Am J Respir Cell Mol Biol*. 36:757–762.

78. Giuseppe cirino fiorentina roviezzo. Systemic administration of sphingosine-1-phosphate increases bronchial hyperresponsiveness in the mouse. *Am J Respir Cell Mol Biol*. 2010;42 572-577.

79. Roviezzo F, Sorrentino R, Bertolino A, et al. S1P-induced airway smooth muscle hyperresponsiveness and lung inflammation in vivo: molecular and cellular mechanisms. *Br J Pharmacol*. 2015;172(7):1882-1893. doi:10.1111/bph.13033

80. Bradding P, Brightling C. Mast cell infiltration of airway smooth muscle in asthma. *Respir Med*. 2007;101(5):1045; author reply 1046-1047. doi:10.1016/j.rmed.2007.01.004

81. Postma DS, Kerstjens HA. Characteristics of airway hyperresponsiveness in asthma and chronic obstructive pulmonary disease. *Am J Respir Crit Care Med*. 1998;158(5 Pt 3):S187-192. doi:10.1164/ajrccm.158.supplement_2.13tac170

82. Blease K, Lukacs NW, Hogaboam CM, Kunkel SL. Chemokines and their role in airway hyper-reactivity. *Respir Res*. 2000;1(1):54-61. doi:10.1186/rr13

83. Blease K, Lukacs NW, Hogaboam CM, Kunkel SL. Chemokines and their role in airway hyper-reactivity. *Respir Res*. 2000;1(1):54-61. doi:10.1186/rr13

84. Aronsson D, Tufvesson E, Ankerst J, Bjermer L. Allergic rhinitis with hyper-responsiveness differ from asthma in degree of peripheral obstruction during metacholine challenge test. *Clin Physiol Funct Imaging*. 2008;28(2):81-85. doi:10.1111/j.1475-097X.2007.00772.x

85. Yeganeh B, Xia C, Movassagh H, et al. Emerging mediators of airway smooth muscle dysfunction in asthma. *Pulm Pharmacol Ther*. 2013;26(1):105-111. doi:10.1016/j.pupt.2012.06.011

86. Taub DD, Oppenheim JJ. Chemokines, inflammation and the immune system. *Ther Immunol*. 1994;1(4):229-246.

87. Zlotnik A, Morales J, Hedrick JA. Recent advances in chemokines and chemokine receptors. *Crit Rev Immunol*. 1999;19(1):1-47.

88. Strieter RM, Kunkel SL, Showell HJ, et al. Endothelial cell gene expression of a neutrophil chemotactic factor by TNF-alpha, LPS, and IL-1 beta. *Science*. 1989;243(4897):1467-1469. doi:10.1126/science.2648570

89. Chung KF, Patel HJ, Fadlon EJ, et al. Induction of eotaxin expression and release from human airway smooth muscle cells by IL-1beta and TNFalpha: effects of IL-10 and corticosteroids. *Br J Pharmacol*. 1999;127(5):1145-1150. doi:10.1038/sj.bjp.0702660

90. Cottin V. Eosinophilic Lung Diseases. *Clin Chest Med*. 2016;37(3):535-556. doi:10.1016/j.ccm.2016.04.015

91. Bentley AM, Menz G, Storz C, et al. Identification of T lymphocytes, macrophages, and activated eosinophils in the bronchial mucosa in intrinsic asthma. Relationship to symptoms and bronchial responsiveness. *Am Rev Respir Dis*. 1992;146(2):500-506. doi:10.1164/ajrccm/146.2.500

92. Wardlaw AJ, Dunnette S, Gleich GJ, Collins JV, Kay AB. Eosinophils and mast cells in bronchoalveolar lavage in subjects with mild asthma. Relationship to bronchial hyperreactivity. *Am Rev Respir Dis*. 1988;137(1):62-69. doi:10.1164/ajrccm/137.1.62

93. Schulman ES. The role of mast cells in inflammatory responses in the lung. *Crit Rev Immunol*. 1993;13(1):35-70.

94. Schulman ES. The role of mast cell derived mediators in airway hyperresponsiveness. *Chest*. 1986;90(4):578-583. doi:10.1378/chest.90.4.578

95. Ebina M, Takahashi T, Chiba T, Motomiya M. Cellular hypertrophy and hyperplasia of airway smooth muscles underlying bronchial asthma. A 3-D morphometric study. *Am Rev Respir Dis*. 1993;148(3):720-726. doi:10.1164/ajrccm/148.3.720

96. Yang J, Tian B, Brasier AR. Targeting Chromatin Remodeling in Inflammation and Fibrosis. *Adv Protein Chem Struct Biol*. 2017;107:1-36. doi:10.1016/bs.apcsb.2016.11.001

97. Haberberger RV, Tabeling C, Runciman S, et al. Role of sphingosine kinase 1 in allergen-induced pulmonary vascular remodeling and hyperresponsiveness. *J Allergy Clin Immunol*. 2009;124(5):933-941.e1-9. doi:10.1016/j.jaci.2009.06.034

98. Tsai H-C, Han MH. Sphingosine-1-Phosphate (S1P) and S1P Signaling Pathway: Therapeutic Targets in Autoimmunity and Inflammation. *Drugs*. 2016;76(11):1067-1079. doi:10.1007/s40265-016-0603-2

99. Feng Z, Zhou H, Ma S, et al. FTY720 attenuates intestinal injury and suppresses inflammation in experimental necrotizing enterocolitis via modulating CXCL5/CXCR2 axis. *Biochem Biophys Res Commun*. 2018;505(4):1032-1037. doi:10.1016/j.bbrc.2018.10.013

100. Berdyshev EV, Gorshkova I, Skobeleva A, et al. FTY720 inhibits ceramide synthases and up-regulates dihydrosphingosine 1-phosphate formation in human lung endothelial cells. *J Biol Chem*. 2009;284(9):5467-5477. doi:10.1074/jbc.M805186200

101. Pavord ID, Green RH, Haldar P. Chapter 39 - Diagnosis and Management of Asthma in Adults. In: Spiro SG, Silvestri GA, Agustí A, eds. *Clinical Respiratory Medicine (Fourth Edition)*. Philadelphia: W.B. Saunders; 2012:501-520. doi:10.1016/B978-1-4557-0792-8.00039-8

102. Writing Group Members, Mozaffarian D, Benjamin EJ, et al. Heart Disease and Stroke Statistics-2016 Update: A Report From the American Heart Association. *Circulation*. 2016;133(4):e38-360. doi:10.1161/CIR.0000000000000350

103. Yatsuya H, Matsunaga M, Li Y, Ota A. Risk Factor of Cardiovascular Disease Among Older Individuals. *J Atheroscler Thromb*. 2017;24(3):258-261. doi:10.5551/jat.ED064

104. Falk E. Pathogenesis of atherosclerosis. *J Am Coll Cardiol*. 2006;47(8 Suppl):C7-12. doi:10.1016/j.jacc.2005.09.068

105. Camici PG, d'Amati G, Rimoldi O. Coronary microvascular dysfunction: mechanisms and functional assessment. *Nat Rev Cardiol*. 2015;12(1):48-62. doi:10.1038/nrcardio.2014.160

106. Badimon L, Vilahur G. Thrombosis formation on atherosclerotic lesions and plaque rupture. *J Intern Med*. 2014;276(6):618-632. doi:10.1111/joim.12296

107. Iqbal J, Walsh MT, Hammad SM, Hussain MM. Sphingolipids and Lipoproteins in Health and Metabolic Disorders. *Trends Endocrinol Metab*. 2017;28(7):506-518. doi:10.1016/j.tem.2017.03.005

108. Zhang DX, Fryer RM, Hsu AK, et al. Production and metabolism of ceramide in normal and ischemic-reperfused myocardium of rats. *Basic Res Cardiol*. 2001;96(3):267-274. doi:10.1007/s003950170057

109. Russo I, Femminò S, Barale C, et al. Cardioprotective Properties of Human Platelets Are Lost in Uncontrolled Diabetes Mellitus: A Study in Isolated Rat Hearts. *Front Physiol*. 2018;9:875. doi:10.3389/fphys.2018.00875

110. Zhang Y, Huang Y, Cantalupo A, et al. Endothelial Nogo-B regulates sphingolipid biosynthesis to promote pathological cardiac hypertrophy during chronic pressure overload. *JCI Insight*. 2016;1(5). doi:10.1172/jci.insight.85484

111. Tono T, Tsujimura T, Koshimizu U, Kasugai T, Isozaki K, Nishikawa S. c-kit gene was not transcribed in cultured mast cells of mast cell-deficient Wsh/Wsh mice that have a normal number of erythrocytes and a normal c-kit coding region. *Blood 1992, 80(6):1448-53*.

112. Berrozpe G, Timokhina I, Yukl S, Tajima Y, Ono M. The Wsh, W57, and Ph Kit expression mutations define tissue-specific control elements located between -23 and -154 kb upstream of Kit. *Blood 1999, 94(8):2658-66*.

113. Glode LM, Scher I, Osborne B, Rosenstreich DL. Cellular mechanism of endotoxin unresponsiveness in C3H/HeJ mice. *J Immunol*. 1976;116(2):454-461.

114. Carvalho M, Benjamim C, Santos F, Ferreira S, Cunha F. Effect of mast cells depletion on the failure of neutrophil migration during sepsis. *Eur J Pharmacol*. 2005;525(1-3):161-169. doi:10.1016/j.ejphar.2005.09.049

115. Guida G, Riccio AM. Immune induction of airway remodeling. *Semin Immunol*. 2019;46:101346. doi:10.1016/j.smim.2019.101346

116. Flechsig P, Dadrich M, Bickelhaupt S, et al. LY2109761 attenuates radiation-induced pulmonary murine fibrosis via reversal of TGF-β and BMP-associated proinflammatory and proangiogenic signals. *Clin Cancer Res*. 2012;18(13):3616-3627. doi:10.1158/1078-0432.CCR-11-2855

117. Yingling JM, Blanchard KL, Sawyer JS. Development of TGF-beta signalling inhibitors for cancer therapy. *Nat Rev Drug Discov*. 2004;3(12):1011-1022. doi:10.1038/nrd1580

118. Daubeuf F, Frossard N. Eosinophils and the ovalbumin mouse model of asthma. *Methods Mol Biol*. 2014;1178:283-293. doi:10.1007/978-1-4939-1016-8_24

119. Cavarra E, Bartalesi B, Lucattelli M, et al. Effects of cigarette smoke in mice with different levels of alpha(1)-proteinase inhibitor and sensitivity to oxidants. *Am J Respir Crit Care Med*. 2001;164(5):886-890. doi:10.1164/ajrccm.164.5.2010032

120. De Cunto G, Bartalesi B, Cavarra E, Balzano E, Lungarella G, Lucattelli M. Ongoing Lung Inflammation and Disease Progression in Mice after Smoking Cessation: Beneficial Effects of Formyl-Peptide Receptor Blockade. *Am J Pathol*. 2018;188(10):2195-2206. doi:10.1016/j.ajpath.2018.06.010

121. Huppé CA, Blais Lecours P, Lechasseur A, et al. A sphingosine-1-phosphate receptor 1 agonist inhibits tertiary lymphoid tissue reactivation and hypersensitivity in the lung. *Mucosal Immunol*. 2018;11(1):112-119. doi:10.1038/mi.2017.37

122. Teijaro JR, Walsh KB, Cahalan S, et al. Endothelial cells are central orchestrators of cytokine amplification during influenza virus infection. *Cell*. 2011;146(6):980-991. doi:10.1016/j.cell.2011.08.015

123. Roviezzo F, Di Lorenzo A, Bucci M, et al. Sphingosine-1-phosphate/sphingosine kinase pathway is involved in mouse airway hyperresponsiveness. *Am J Respir Cell Mol Biol*. 2007;36(6):757-762. doi:10.1165/rcmb.2006-0383OC

124. Nakashima Y, Plump AS, Raines EW, Breslow JL, Ross R. ApoE-deficient mice develop lesions of all phases of atherosclerosis throughout the arterial tree. *Arterioscler Thromb*. 1994;14(1):133-140. doi:10.1161/01.atv.14.1.133

125. Animal models of atherosclerosis. - PubMed - NCBI. https://www.ncbi.nlm.nih.gov/pubmed/22383700. Accessed January 24, 2020.

126. Bentzon JF, Falk E. Atherosclerotic lesions in mouse and man: is it the same disease? *Curr Opin Lipidol*. 2010;21(5):434-440. doi:10.1097/MOL.0b013e32833ded6a

127. Liu D, Lei L, Desir M, et al. Smooth Muscle Hypoxia-Inducible Factor 1α Links Intravascular Pressure and Atherosclerosis--Brief Report. *Arterioscler Thromb Vasc Biol*. 2016;36(3):442-445. doi:10.1161/ATVBAHA.115.306861

128. Saluja R, Kumar A, Jain M, Goel SK, Jain A. Role of Sphingosine-1-Phosphate in Mast Cell Functions and Asthma and Its Regulation by Non-Coding RNA. *Front Immunol*. 2017;8:587. doi:10.3389/fimmu.2017.00587

129. Oskeritzian CA, Price MM, Hait NC, et al. Essential roles of sphingosine-1-phosphate receptor 2 in human mast cell activation, anaphylaxis, and pulmonary edema. *J Exp Med*. 2010;207(3):465-474. doi:10.1084/jem.20091513

130. Nittner-Marszalska M, Cichocka-Jarosz E, Sanak M, et al. 9α,11β-PGF2, a Prostaglandin D2 Metabolite, as a Marker of Mast Cell Activation in Bee Venom-Allergic Patients. *Arch Immunol Ther Exp (Warsz)*. 2015;63(4):317-325. doi:10.1007/s00005-015-0334-1

131. Gould HJ, Sutton BJ. IgE in allergy and asthma today. *Nat Rev Immunol*. 2008;8(3):205-217. doi:10.1038/nri2273

132. Bauer RN, Diaz-Sanchez D, Jaspers I. Effects of air pollutants on innate immunity: the role of Toll-like receptors and nucleotide-binding oligomerization domain-like receptors. *J Allergy Clin Immunol*. 2012;129(1):14-24; quiz 25-26. doi:10.1016/j.jaci.2011.11.004

133. Holgate ST. The airway epithelium is central to the pathogenesis of asthma. *Allergol Int*. 2008;57(1):1-10. doi:10.2332/allergolint.R-07-154

134. Willis BC, Liebler JM, Luby-Phelps K, et al. Induction of epithelial-mesenchymal transition in alveolar epithelial cells by transforming growth factor-beta1: potential role in idiopathic pulmonary fibrosis. *Am J Pathol*. 2005;166(5):1321-1332. doi:10.1016/s0002-9440(10)62351-6

135. Milara J, Navarro R, Juan G, et al. Sphingosine-1-phosphate is increased in patients with idiopathic pulmonary fibrosis and mediates epithelial to mesenchymal transition. *Thorax*. 2012;67(2):147-156. doi:10.1136/thoraxjnl-2011-200026

136. Huang LS, Natarajan V. Sphingolipids in pulmonary fibrosis. *Adv Biol Regul*. 2015;57:55-63. doi:10.1016/j.jbior.2014.09.008

137. Fuseini H, Newcomb DC. Mechanisms Driving Gender Differences in Asthma. *Curr Allergy Asthma Rep*. 2017;17(3):19. doi:10.1007/s11882-017-0686-1

138. Trinh HKT, Suh D-H, Nguyen TVT, Choi Y, Park H-S, Shin YS. Characterization of cysteinyl leukotriene-related receptors and their interactions in a mouse model of asthma. *Prostaglandins Leukot Essent Fatty Acids*. 2019;141:17-23. doi:10.1016/j.plefa.2018.12.002